



ΠΟΛΥΤΕΧΝΕΙΟ ΚΡΗΤΗΣ
TECHNICAL UNIVERSITY OF CRETE

DIPLOMA THESIS

In partial fulfillment of the requirements for the degree of
DIPLOMA IN ELECTRICAL & COMPUTER ENGINEERING

By

Poulea Efstathia

Whole Brain Parcellation via Resting-State fMRI Data Analysis

Committee:

Professor Liavas Athanasios (Supervisor)

Professor Zervakis Mixalis

Professor Christopoulos Dionysios

Chania, November 2023

Abstract

Functional magnetic resonance imaging (fMRI) is a noninvasive method which provides significant insight into brain functionality. It is a technique which measures and maps brain activity by detecting changes associated with blood flow. The most common form of fMRI measures the blood-oxygen-level dependent (BOLD) signal, which is created by changes in blood flow in the brain. Furthermore, it is being used in many studies to understand how the brain works. Since brain activity is intrinsic, any brain region will have spontaneous fluctuations in BOLD signal. Thus, even at rest, the BOLD signal reflects systematic fluctuations in the regional brain activity. It is widely believed that resting-state networks are the cause of these systematic fluctuations. So, there is a common brain parcellation across subjects, based on functionality.

In this thesis, we study a method which computes a common (over many subjects) brain parcellation, with no prior knowledge on the properties of the parcels. At first, we present the proposed method which computes the common spatial subspace via Generalized Canonical Correlation Analysis (gCCA). Then, we test this approach on real data for healthy and non-healthy subjects and we compare the results.

Table of Contents

List of Tables	4
Acknowledgments	5
1 Introduction	6
1.1 Background & Related work	6
1.2 Contribution	7
1.3 Outline	7
2 Background & Related work	8
2.1 The fMRI method	8
2.2 The MRI method and Bold Imaging	9
2.3 MRI signal sensitivity in brain activity	10
2.4 Modeling the BOLD response	11
2.5 Structural & Anatomical MRI	12
3 Brain Anatomy	14
3.1 Brain Activity	14
3.2 Materials of the brain	15
4 Multiple Sclerosis	17
4.1 The symptoms of multiple sclerosis	17
4.2 MS diagnosis	18
4.3 The types of multiple sclerosis	18
4.4 Causes of multiple sclerosis	19
4.5 The early signs of MS	20
4.6 The risk factors for MS	20
4.7 Treatments for multiple sclerosis	20
5 Systemic Lupus Erythematosus	22
5.1 Causes of SLE	22
5.2 The signs and the symptoms	22
5.3 SLE diagnosis	22
5.4 The treatment of SLE	23
5.5 SLE dangers	23

6	Implementation	24
6.1	Brain Parcellation	24
6.1.1	Estimating Common Spatial Subspace via gCCA	25
6.1.2	Estimating the numbers of clusters	25
6.1.3	Estimation of the common spatial factor A and temporal components S_k	26
7	Experimental Results	31
7.1	Experimental Results	31
7.2	Brain maps for control subjects	31
7.3	Brain maps for MS subjects	47
7.4	Brain maps for SLE subjects	62
7.5	Number of voxels comparison	76
7.6	Comparison clusters of MS with the largest cluster 19 of control subjects.	83
7.7	Comparison clusters of SLE with the largest cluster 19 of control subjects.	85
7.8	Comparison clusters of SLE with the cluster 27 of control subjects.	87
7.9	Comparison clusters of SLE with the cluster 22 of control subjects.	89
7.10	Comparison clusters of SLE with the cluster 7 of control subjects.	90
7.11	Comparison the clusters of control and MS subjects.	91
7.12	Comparison the clusters of control and SLE subjects.	93
8	Appendices	95
8.1	Histograms of energy of each material	95
	List of Abbreviations	102
	Bibliography	103

List of Tables

7.1	This table represents the clusters of the control patients and the number of voxels on the side according to descent classification.	32
7.2	The clusters of MS subjects having sorted from the largest number of voxels to the smallest (descent).	47
7.3	The clusters of SLE subjects and the number of voxels on the side according to descent classification.	62
7.4	The clusters of the control subjects having sorted from the smallest number of voxels to the largest (ascent).	77
7.5	The clusters of MS subjects having sorted from the smallest number of voxels to the largest (ascent).	77
7.6	The clusters of the control subjects having sorted from the smallest number of voxels to the largest (ascent).	78
7.7	The clusters of SLE subjects having sorted from the smallest number of voxels to the largest (ascent).	78
7.8	In the table above we matched the number of clusters from MS subjects with the largest cluster of control patients. The limit is that the number of voxels must be greater than 1000.	83
7.9	In the table above we matched the number of clusters from SLE subjects with the largest cluster of control patients. The limit is that the number of voxels must be greater than 1000 which was the threshold.	85
7.10	In the table above we matched the number of clusters from SLE Subjects with the cluster 27 of control subjects.	87
7.11	In the table above we matched the number of clusters from SLE subjects with the cluster 22 of control subjects.	89
7.12	In the table above we matched the number of clusters from SLE subjects with the cluster 7 of control subjects.	90
7.13	Comparison table of number of clusters of control subjects and (MS) subjects and display of their common voxels.	91
7.14	Descent classification table of the clusters of control subjects.	91
7.15	Comparison table of number of clusters of control subjects and (SLE) subjects and display of their common voxels.	93
7.16	Descent classification table of the clusters of control subjects.	93

Acknowledgments

I would like to show my gratitude and appreciation to my supervisor professor Athanasios Liavas for his continuous support and enlightenment in the conduction of my Diploma Thesis. His professional knowledge and progressive ideas have broaden my mind and expanded my opportunities in the upcoming working and educational challenges.

Next, I would like to mention how grateful I am to my colleague Margarita-Antonia Psychountaki, for providing me all the important information. She was an essential support during the implementation of my Thesis and i wish her all the best in her new career.

Finally, I would like to thank my friends and my family for their continuous support. They provided me with all the important values to continuously chase my dreams and ambitions and achieve my goals and my dreams. They have always persuaded me to set my standards and goals as high as possible so as to excel upon every aspect of my life.

CHAPTER. 1

Introduction

Functional Magnetic Imaging (fMRI) is a class of imaging methods developed in order to demonstrate regional time-varying changes in brain metabolism. These metabolic changes can be consequent to task-induced cognitive state changes or the result of unregulated processes in the resting brain. Since its inception in 1990, fMRI has been used in an exceptionally large number of studies in the cognitive neuroscience, clinical, psychiatry and psychology. However, the popularity of fMRI derives from its widespread availability, non-invasive nature, relatively low cost, and spatial resolution.

The fMRI data that are collected when the subject is resting are commonly used by neuroscientists in order to analyze and interpret human brain activity. A question which is worth researching is if there are any similarities in subjects' brain activity when they are resting. In this thesis, we examine this problem by studying the methodology and comparing brain activity of healthy and non-healthy subjects. Firstly, authors in [1] find a common brain parcellation over different subjects. These parcels do not overlap each other and no prior knowledge on their properties is required. Specifically, the proposed method uses subjects' common spatial subspace, \mathbf{G} , via Generalized Canonical Correlation Analysis (gCCA). Then, they solve a semi-orthogonal non-negative matrix factorization problem to obtain the common spatial factor \mathbf{A} from \mathbf{G} , such that $\mathbf{A}^T \mathbf{A} = \mathbf{I}$ and $\mathbf{A} \geq \mathbf{0}$. Because of its properties, \mathbf{A} practically defines the regions which are included in each parcel.

1.1 Background & Related work

At fist, the Generalized Canonical Correlation Analysis (gCCA) is commonly used in fMRI studies for a common spatial component over subjects to be found. In addition, there is an extensive overview of fMRI clustering methods and the problem of data driven brain parcellation in reference [2] which refers to task fMRI data. Another solution and approach

of the problem is presented in [3] in which the problem is solved only for cortex areas.

1.2 Contribution

First and foremost we examine the problem of the brain parcellation by studying the method which is proposed in [1]. We studied the preprocessing steps, which are applied to raw fMRI data so that the fMRI data can be used for analyzing. In addition, we were able to comprehend which problems could be solved by pre-processing steps, how these problems are modeled and how they can be resolved in order to be reassured that the initial assumptions of [1] are not violated because of the data preprocessing. We investigated the behavior of the algorithms used in the paper [1], on synthetic and real data. We made some experiments using two different synthetic data formats in order to model them as close as it was possible to real data. For the synthetic data we examined the behavior of the rank criterion based on the number of parcels. We have also tried different types of algorithms until we calculate A, some of them are presented below. The second algorithm is the method which is suggested by the authors [1]. We also studied the rank criterion for the real data as well. In this case it was not clear which number of cluster should be used. Furthermore, we used a threshold based on the behavior of the criterion for synthetic data and we also applied trimming to exclude outlier values in order to have a clearer insight. In conclusion, we decided to examine the brain parcellation only for parcel number 27. We implement this procedure for two different types of data for healthy and non-healthy subjects. Finally, we made the application and we can compare the results.

1.3 Outline

Chapter 1 contains the introduction, the subject of this thesis and some general information about fMRI method. Chapter 2 provides some detailed information about fMRI and MRI method and more specific the usage of this method, how it works and some details and information about the diagram BOLD. Chapter 3 includes information about the anatomy of the brain and how it is combined with the MRI procedure. Chapter 4 presents information about the Multiple Sclerosis (MS), disease such as symptoms and the treatment. Chapter 5 presents information about the Systemic Lupus Erythematosus (SLE), disease such as symptoms and the treatment. Chapter 6 contains all the procedure of the implementation and the methods that we used in this thesis either on healthy or non-healthy subjects. Chapter 7 includes the experimental results and the brain maps for each disease. Finally, Chapter 8 includes the appendices and some related work that we did before the brain maps.

CHAPTER. 2

Background & Related work

2.1 The fMRI method

Functional Magnetic resonance imaging (fMRI) is a noninvasive method, which studies brain function and dominates brain mapping research. More specifically, it is a technique which uses magnetic resonance to measure the small changes in blood oxygenation and flow that occur with brain activity. Furthermore, it may be used to examine the brain's functional anatomy, evaluate the effects of stroke or other disease, or to guide brain treatment. The fMRI may detect abnormalities within the brain that cannot be found with other imaging techniques. The most important form of fMRI is measures the blood oxygen-level-dependent (BOLD) signal. The magnitude of BOLD signal is an indirect measure of neuronal activity and is a composite which reflects changes in regional cerebral blood flow, volume and oxygenation. The basic concept is that an increase in local neuronal activity stimulates both higher energy and increases blood flow. According to Ashby [4], the information which is provided by fMRI is useful for studying neural and cognitive architecture, but not for answering questions about process. The resultant indirect determination of brain function is typically represented as a statistical map which reflects regional activity. The information transfer between neurons with a demanding process which requires an increased flow of oxygenated blood. The result of this procedure is a map showing which brain regions responded to some particular manipulation mental or perceptual functions. Thus the thing that lies in the fMRI technique is the temporal resolution because of a five second lag between the initial neural activity and the image. Also because its poor temporal resolution sometimes may not truly represent moment-to-moment the brain activity.

2.2 The MRI method and Bold Imaging

Magnetic resonance imaging (MRI) is a medical imaging technique which forms picture of the anatomy and the physiological processes of the body. Most MRI machines are large, tube-shaped magnets. Moreover, the MRI can be used for examining the activity of the brain under specific activities (functional MRI-fMRI). The biggest advantage of MRI is that uses no radiation. The magnetic resonance (MR) scanner uses superconducting electromagnets to produce a static, uniform magnetic field of high strength. Many years ago, the standard field strength which was used in fMRI research was 1.5 Tesla (T). Some research centers have scanners approximately stronger than 10 units of Tesla (T).

Furthermore, MRI is the most sensitive imaging method and it examines the structure of the brain and the spinal cord. It works by exciting the tissue hydrogen protons, which in turn emit electromagnetic signals back to the MRI machine. The MRI machine also detects their intensity and translates it into gray-scale MRI image.

However, trying to subscribe MRI sequences we refer to the shade of grey of tissues or fluid by using the intensity. When we observe a T-weighted image the white color refers to high signal intensity, the grey colour refers to intermediate signal intensity and the black colour refers to a low signal intensity. We have two categories of images T1-weighted and T2-weighted as it referred in [5]. The first is one of the basic pulse sequences in MRI and demonstrates differences in the T1 relaxation times of tissues. A T1-weighted image relies upon the longitudinal relaxation of a tissue's net magnetization vector. Basically, spins aligned in an external field (B_0) are put into the transverse plane by a radio frequency (RF) pulse. They then slide back toward the original equilibrium of (B_0). Not all tissues return back to equilibrium in the same amount of time, and a tissue's T1 reflects the amount of time taken for its proton's spins to realign with the main magnetic field (B_0). T1-weighting tends to have short echo time (TE) which refers to the time between the application and the radio frequency excitation pulse and the peak of the signal induced in the coil. It is measured in milliseconds (ms). Furthermore it has also short repetition time (TR) which refers to the time between an excitation pulse and the next pulse. It determines how much longitudinal magnetization recovers between each pulse and it measures also in milliseconds (ms).

One of the most important steps is the relaxation which is described by turning off the RF pulses, the nucleus relaxes to its original equilibrium alignment. Two separating processes take place during relaxation: T1 relaxation and T2 relaxation. The T1 relaxation is the

process which measures how quickly the net magnetization recovers to its initial maximum value parallel to B_0 . The amount of time required to obtain 63% of the initial longitudinal magnetization is known as the T1 relaxation time. Transversal plane events are described by the T2 and T2* relaxation. When a pulse is turned off the nucleus dephases, because of inhomogeneities of the main magnetic field (T2* decays) and spin-spin interactions (T2 decays). These inhomogeneities may be the result of intrinsic defects in the magnet itself or from susceptibility-induced field distortions produced by the tissue or the other materials placed within the field. T2 relaxation time is defined as the time needed to dephase up to 37% of the original value. When the nucleus relaxes to its original equilibrium alignment, energy is released (transition from lower to higher energy levels), which is detected by the coils as the raw MR signal. The software that controls all the magnetic fields is typically called the pulse sequence. The pulse is run on the main computer by which the scanner is controlled. In most fMRI experiments, the stimuli which are presented to the subject are generated by a second computer which also records the subjects behavioral responses. Both computers have to be synchronized, in a way that the onset of each stimulus presentation occurs at a precisely controlled moment during image acquisition. Furthermore, two types of pulse sequences are commonly used, depending on whether the goal is structural or functional imaging. The structural MR is normally used to measure the density of water molecules, which differs for example in bone, gray matter, cerebrospinal fluid and tumors. The vast majority of functional MRI experiments measure the blood oxygen-level dependent (BOLD) signal.

2.3 MRI signal sensitivity in brain activity

The MR signal change is an indirect effect related to the changes in blood flow that follow the changes in the brain neural activity.

The first effect is that oxygen-rich blood and oxygen-poor blood have different magnetic properties related to the hemoglobin that binds oxygen in blood. This has a small effect on the MR signal, so that if the blood is more oxygenated the signal is slightly stronger.

The second effect relates to an unexpected physiological phenomenon. For some reasons we can observe that neural activity triggers a much larger change in blood flow than in oxygen metabolism, and this leads to the blood more oxygenated when neural activity increases. This somewhat paradoxical blood oxygenation level dependent (BOLD) effect is the basis for fMRI.

However, the BOLD signal cannot separate feedback and feed forward active networks in a region, the slowness of the vascular response means the final signal is the summed version of the whole region's blood flow is not discontinuous as the processing proceeds. Also, both inhibitory and excitatory input to a neuron from other neurons sum and contribute to the BOLD signal. Within a neuron these two inputs that dilate blood vessels, and attention.

More recent characterization of the BOLD signal has used optogenetic techniques in rodents to precisely control neuronal firing while simultaneously monitoring the BOLD response using high field magnets. These techniques suggest that neuronal firing is well correlated with the measured BOLD signal including approximately linear summation of the BOLD signal over closely spaced bursts of neuronal firing. Linear summation is an assumption of commonly used event-related fMRI designs.

2.4 Modeling the BOLD response

It is important to simulate a model as far as the neural activity and the diagram BOLD is concerned by observing them. Most fMRI applications make the assumption that this transformation from neural activation to BOLD response can be modeled as a linear and time-invariant system. We characterize a system as linear and time-variant if and only if the superposition principle is satisfied. By making this assumption, we are able to determine the BOLD response to any neural activation from a simple experiment. The only thing that we have to do is to determine the impulse response function $h(t)$, which in case of fMRI is known as hemodynamic response (HRF). So, if we know $h(t)$ for any neural activation $N(t)$, we are able to calculate the BOLD response $B(t)$ by using the following:

$$B(t) = \int_0^t N(t)h(t-t)dt \quad (2.1)$$

The role of the HRF is very important for the analysis of the fMRI data. The most common to determine HRF is the use of a specific mathematical function, based on how we expect the HRF to look like. The gamma function or the difference of two gamma functions are the most commonly used functions for determining HRF.

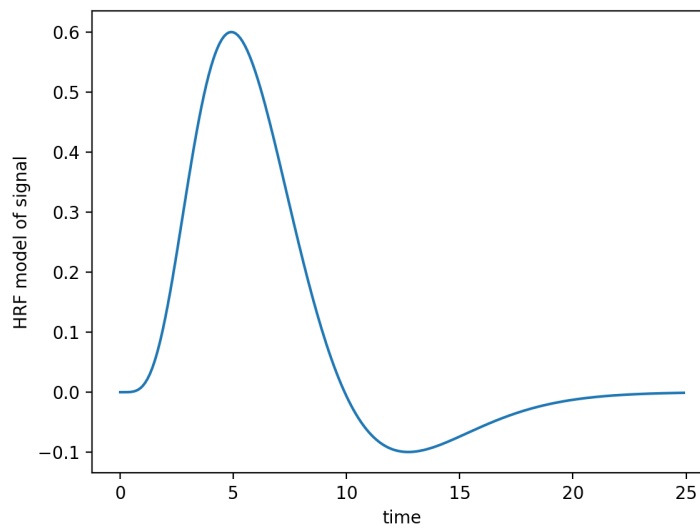


Figure 2.1. The simulation of the hemodynamic response function (HRF) by using SPM12 to create and illustrate it.

2.5 Structural & Anatomical MRI

As it has been mentioned in [6] structural MRI provides information which concern brain activity to complement functional MRI in different ways. Since brain function depends to some extent on the integrity of brain structure, measures that characterize the underlying tissue integrity allow either to examine the impact of tissue loss or damage on functional signs.

Many pulse sequences are available, emphasizing different aspects of normal and abnormal brain tissue. By modifying sequence parameters such as repetition time (TR) and echo time (TE), for example, anatomical images can emphasize contrast between gray and white matter (e.g. T1-weighted with short TR and short TE) or between brain tissue and cerebrospinal fluid (e.g. T2-weighted with long TR and long TE).

Some information from structural MRI can be used to describe the shape, the size, and the integrity of gray and white matter structures in the brain territory. Furthermore, the morphometric techniques measure either the volume or the shape of gray matter structures, such as subcortical nuclei or hippocampus, and the volume, thickness, or surface area of the cerebral neocortex. The volume of normal and abnormal white matter also can allow inference of macrostructural white matter integrity, providing indications of inflammation, edema and demyelination complementary microstructural studies using imaging diffusion

imaging can help to provide a more comprehensive picture of white matter integrity.

Thus, if we want to combine these three different types, the structural MRI, the functional MRI and the diffusion imaging we can characterize normal and abnormal brain function, supporting biomarker studies of neurodegenerative or psychiatric disorders to determine risk, progression and therapeutic effectiveness.

CHAPTER. 3

Brain Anatomy

3.1 Brain Activity

The brain is an essential organ that regulates memories, thoughts, emotions, motor skills and all other processes involved in the body. Brain MRI examination should follow a systematic approach starting from a midline and going laterally. Thus, the brain MRI analysis shall start from the ventricles, going to the surrounding subcortical structures, brain lobes, cerebral cortex, to the meninges and skull. We would like to analyze below some of the most important parts of the brain and how they look like in the MRI.

Cerebrum

It is the biggest part of the brain. The cerebrum or the front part of the brain consists of the right and left hemispheres. Its main functions include the initiation and co-ordination of movement, reasoning, problem-solving, emotions, learning, touch, vision and hearing. In addition the memory lives in the cerebrum, both the short-term memory (constitutes an act which was presented in the recent past) and the long-term memory (constitutes an act which was presented in the old past). Scientists think as it referred in [7] that the right half helps you think about abstract things like music, colors and shapes. However, the left half is said to be more analytical, helping you with math, logic and speech. Scientists do know for sure that the right half of the cerebrum controls the left side of your body and respectively for the right side.

Cerebellum

The cerebellum lies below the occipital lobe of the brain, occupying the posterior cranial fossa. It is at the back of the brain, below the cerebrum and it is very small as it referred in [7] but also an important part of the whole brain. It consists of the right and left hemispheres that are interconnected by a midline area called the vermis. Furthermore, it controls balance and movement and so because of it we can stand upright, keep our balance and move around.

Brainstem

The brainstem is the middle part of the brain and sits beneath the cerebrum and in front of the cerebellum. It is very small as it referred in [7] but so important because it makes the connection between the rest of the brain and the spinal cord which runs down the neck and back. The brain stem is in charge of all the functions your body needs to stay alive. Its main functions include relaying sensory information, like pain, eye and mouth movement, involuntary muscle movements, respirations, hunger, consciousness and cardiac function.

Hypothalamus

This part is like your brain's inner thermostat. The hypothalamus knows what temperature your body should be as it referred in [7]. For example if your body is too hot, the hypothalamus tells it to sweat whereas if is too cold it gets you shivering. Both these reactions are attempts to get your body's temperature back where it needs to be namely in 37°C or 98.7°F.

3.2 Materials of the brain

The human brain consists of six materials which we will analyze them below.

The grey matter refers to unmyelinated neurons and other cells of the central nervous system. It is present in the brainstem and cerebellum and present throughout the spinal cord. In living tissue, grey matter actually has a very light grey colour with yellowish or pinkish hues, which come from capillary blood and neuronal cell bodies.

The white matter is the tissue through which messages pass between different areas of grey matter within the central nervous system. It is white because of the fatty substance (myelin) that surrounds the nerve fibers (axons).

The cerebrospinal fluid (CSF) is a clear fluid that surrounds the brain and spinal cord. It

cushions the brain and spinal cord from injury and also serves as a nutrient delivery and waste removal system for the brain.

The bone is so important because it protects the brain. There are eight bones in the brain. The front bone forms the forehead. Two parietal bones form the upper sides of the skull, whole two temporal bones form the lower sides.

The soft tissue occupies about 3-4 pounds of the brain floating in fluid within the skull. Under the skull there are three layers of membrane that cover and protect the brain. The brain tissue is soft and therefore can be squeezed, pulled and stretched.

The background (air) is the last part of the brain materials. In many occasions it has been cuted of in order to make the pictures more clear.

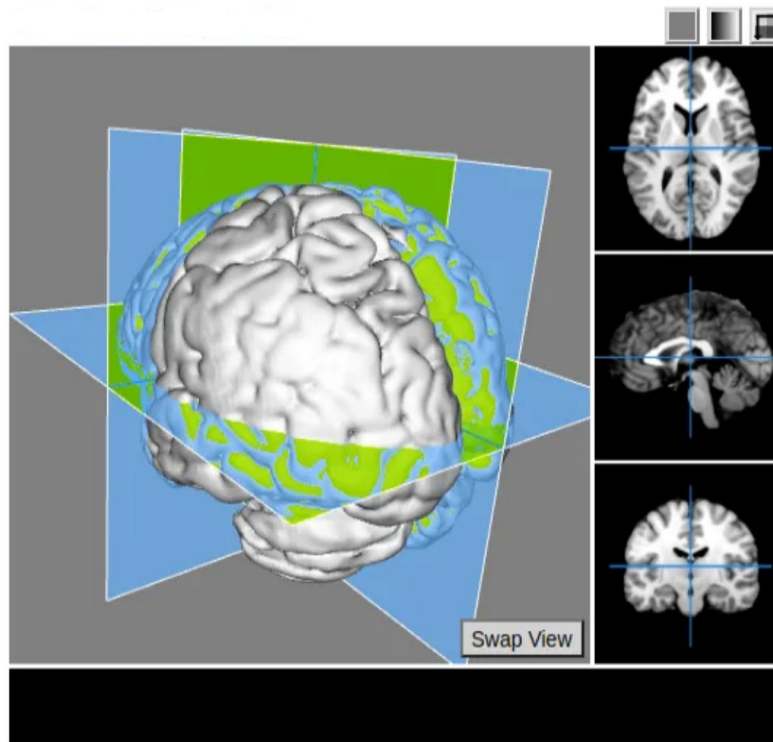


Figure 3.1. The 3-D display of the brain of a control subject using the papaya program.

CHAPTER. 4

Multiple Sclerosis

Multiple sclerosis (MS) is a chronic condition involving the central nervous system (CNS). In this disease as it is referred in [8] the immune system attacks to myelin (white matter) of the brain which is the protective layer around nerve fibers. MS causes inflammation and temporary lesions. It can also lead to lasting lesions caused by scar tissue which can make it hard for your brain to send signals to the rest of your body. The main parts that are affected are the brain stem, the cerebellum which coordinates movement and controls balance, the spinal cord, the optic nerves and the white matter material in some regions of the brain. Unfortunately there is no cure for multiple sclerosis (MS) but it is possible to manage symptoms.

4.1 The symptoms of multiple sclerosis

Some of the most common symptoms that are associated with this disease are referred below.

- Fatigue
- Difficulty waking
- Vision problems, such as blurred vision
- Problems in controlling the bladder
- Numbness or tingling in different parts of the body
- Muscle stiffness and spasms in the whole body
- Problems with balance and co-ordination

Depending on the type of MS you have, your symptoms may come and go in phases or get steadily worse over time (progress).

4.2 MS diagnosis

If you diagnosed with MS disease it is obligatory to consult a neurologist and need to perform not only neurological exams but also some other tests in order to examine that you have this disease.

Diagnostic testing may include the following:

- **MRI scan.** Using a contrast dye with the MRI allows your doctor to detect active and inactive lesions throughout your brain and spinal cord.
- **Optical coherence tomography (OCT).** It is a test, a picture is taken of the nerve layers in the back of your eye to check for thinning around the optic nerve.
- **Spinal tap (lumbar puncture).** Your doctor may order a spinal tap to find abnormalities in your spinal fluid. This test can help rule out infectious diseases. It can also be used to look for oligoclonal bands (OCBs) , which can be used to diagnose MS.
- **Blood tests.** Your doctor can order blood tests to help eliminate the possibility of other conditions that have similar symptoms.
- **Visual evoked potentials (VEP) test.** This test requires the stimulation of nerve pathways to analyze electrical activity in your brain .

4.3 The types of multiple sclerosis

The four categories defined by the NMSS (National Multiple Sclerosis Society) are now relied upon by the medical community at large and create a common language for diagnosing and treating MS. As it mentioned in [8] the categories' classifications are based on how far the disease has progressed in each patient.

Clinically Isolated Syndrome (CIS)

As it is mentioned in [9] the CIS is a pre-MS condition involving one episode lasting at least 24 hours. These symptoms are caused by inflammation and demyelination in the central nervous system. Although, this episode is characteristic of MS, it is not enough to prompt a diagnosis. When CIS is accompanied by lesions on a brain MRI (magnetic resonance imaging) that are similar to those seen in MS, the person has a high likelihood of a second episode of neurologic symptoms and diagnosis of relapsing-remitting MS. When CIS is not accompanied by MS-like lesions on a brain MRI, the person has a much

lower likelihood of developing MS. If there is more than one lesion or positive oligoclonal band (OCB) in your spinal fluid at the time of a spinal tap, you are more likely to receive a diagnosis of RRMS. If these lesions are not present or your spinal fluid doesn't show OCBs, you are less likely to receive an MS diagnosis.

Relapsing-remitting MS (RRMS)

Relapsing-remitting MS (RRMS) is the most common disease course and involves clear relapses of disease activity followed by remissions. It attacks of new or increasing neurologic symptoms. During remission periods, all symptoms are mild or absent, and there is mild to moderate disease progression. RRMS can be characterized as either active or not active, as well as worsening or not worsening. The RRMS is the most common form of MS at onset and accounts for about 85 percent of all cases.

Primary progressive (PPMS)

If you have primary progressive MS (PPMS), neurological function becomes progressively worse from the onset of your symptoms.

Secondary progressive MS (SPMS)

Secondary progressive MS (SPMS) occurs when RRMS transitions into the progressive form. You may still have noticeable relapses in addition to disability or gradual worsening of function.

4.4 Causes of multiple sclerosis

The protective layer of myelin around some of the nerve fibers of your brain, optic nerve, and spinal cord become damaged. It is thought that the damage as it is mentioned in [8] is the result of an immune system attack. Researchers think there could be an environmental trigger, such as a virus or toxin, that sets off the immune system attack. As your immune system attacks myelin, it causes demyelination. This can go into remission as new layers for myelin form, but chronic inflammation can lead to scar tissue, which can result in lasting neurological impairment.

4.5 The early signs of MS

Multiple sclerosis can develop all at once, or the symptoms can be so mild that you easily dismiss them. Three of the most common early symptoms of MS are:

- Numbness and tingling that affects the arms, legs or one side of your face. These sensations are similar to the pins-and-needles feeling you get when your foot falls asleep. However, they occur without a trigger.
- Uneven balance and weak legs. You may find yourself tripping easily while walking or doing some other type of physical activity.
- Double vision, blurry vision in one eye, or partial vision loss. These can be early indicators of MS. You may also have eye pain.

4.6 The risk factors for MS

The exact cause of the multiple sclerosis is still unknown. However, there are several risk factors for developing MS. These risk factors include:

- having a close relative with MS
- obesity
- certain infections
- smoking
- certain autoimmune disorders like for example rheumatoid arthritis.

4.7 Treatments for multiple sclerosis

There is currently no cure for MS, but a number of treatments can help control the condition. The treatment you need will depend on the specific symptoms and difficulties you have. It may include:

- treating relapses with short courses of steroid medicine to speed up recovery
- specific treatments for individual MS symptoms
- treatment to reduce the number of relapses using medicines called disease-modifying therapies

Disease-modifying therapies may also help to slow or reduce the overall worsening of disability in people with a type of MS called relapsing remitting MS, and in those with a type called secondary progressive MS who have relapses. Unfortunately, there is currently no treatment that can slow the progress of a type of MS called primary progressive MS, or secondary progressive MS in absence of relapses.

CHAPTER. 5

Systemic Lupus Erythematosus

Systemic lupus erythematosus (SLE) is the most common type of lupus. As it is mentioned in [10], SLE is an autoimmune disease in which the immune system of the body attacks its own tissues and organs. This is a chronic disease that causes inflammation in connective tissues, such as cartilage and the lining of blood vessels, which provide strength and flexibility to structures throughout the body. The signs and symptoms of SLE vary among affected individuals and can involve many organs and systems, including the skin, joints, kidneys, lungs, central nervous system, including forming (hematopoietic) system.

5.1 Causes of SLE

The cause of SLE is not clearly known. It may be linked to genetic, environmental and hormonal factors. This disease is more common in women than men and it may occur at any age. However, it appears most often in young women between the ages of 15 and 44.

5.2 The signs and the symptoms

People with SLE experience a variety of symptoms that include fatigue, skin rashes, fevers, and pain or swelling in the joints. Other symptoms can include sun sensitivity, oral ulcers, arthritis, lung problems, heart problems, kidney problems, seizures, psychosis and blood and immunological abnormalities.

5.3 SLE diagnosis

Systemic lupus erythematosus diagnosed, as it is referred in [11] by a health care provider using symptom assessments, physical examination, X-rays, and lab tests. This disease may be difficult to diagnose because its early signs and symptoms are not specific and they are look like with some from other diseases. SLE may also be misdiagnosed if

only a blood test is used for diagnosis. Rheumatologists sometimes use specific criteria to classify the disease of SLE.

5.4 The treatment of SLE

Treating SLE often requires a team approach because of the number of organs that can be affected. These disease may occur with other autoimmune conditions that require additional treatments.

5.5 SLE dangers

Causes of premature death associated with SLE are mainly active disease, organ failure, infection, or cardiovascular disease from accelerated atherosclerosis. Generally as it is mentioned in [12] people with SLE have episodes in which sometimes the condition gets worse and other times gets better. Overall, SLE can attack and damage the major organs of the body and can be life-threatening.

CHAPTER. 6

Implementation

6.1 Brain Parcellation

This chapter is focused on the presentation of a whole-brain parcellation methodology, which is introduced at [1]. The methodology which is performed on the resting state data and it has to extract a common brain parcellation to all of the healthy and non-healthy subjects, into non-overlapping clusters without any prior knowledge about clusters. As we mentioned before the mathematical explanations are given in [1] and all the equations and the examples too. For example there exists a common brain parcellation for all subjects, resting state data for each subject k can be modeled as follows:

$$X_k = AS_k + E_k \quad \text{for } k = 1, \dots, K \quad (6.1)$$

where

- K is the number of the subjects.
- X_k is the fMRI pre-processed data of k^{th} subject. More especially, $X_k \in \mathbb{R}^{N \times M}$ where N is the number of voxels, and M is the number of time points with $N \gg M$.
- $\mathbf{A} \in \mathbb{R}_+^{N \times M}$ with $R < M$ and $A^T A = I_R$. It denotes the common spatial component related with the spontaneous fMRI activity. Namely, each column of \mathbf{A} represents one of the R clusters. To be more specific, the non zero elements of each column indicate the voxels which belong to this cluster.
- $S_k \in \mathbb{R}^{N \times M}$, each column of S_k indicates the temporal component of each cluster, which is associated with the spontaneous fMRI activity. The term S_k may be different across subjects.
- $E_k \in \mathbb{R}^{N \times M}$, represents the unmodeled fMRI signal of k^{th} subject and it can be considered as (strong) additive noise. The terms E_k are assumed as statistically independent from each other.

6.1.1 Estimating Common Spatial Subspace via gCCA

Canonical Correlation Analysis (CCA) is a method which estimates a linear common subspace of two sets of random variables. Generalization of CCA (gCCA) estimates a linear common subspace of more than two random vectors. It is a well-studied subject [13], [14]. Our model which is analyzed assumes that subjects share common information, and estimates the common spatial subspace over all subjects via the MAX-VAR formulation of GCCA. The MAX-VAR formulation is modeled as follows:

$$\underset{\{Q\}_{i=1}^I, G}{\text{minimize}} \sum_{i=1}^I \|X_i Q_i - G\|_F^2$$

where I is the number of subjects, $X_i \in \mathbb{R}^{N \times M}$ $N \times M$ is the data of i^{th} subject, $Q_i \in \mathbb{R}^{M \times R}$ corresponds to the R canonical components of X_i , $G \in \mathbb{R}^{N \times R}$ corresponds to a common latent representation of our data.

6.1.2 Estimating the numbers of clusters

In the previous sections, we assume that the real number of clusters (which is equivalent to the common subspace dimension) R is known, but that seldom happens. However, by using the data, we can estimate the number of clusters. A way to do this is by dividing our data set into two sets. By using the gCCA method we can estimate the column space of these sets and after that, we can apply a criterion function, that uses the distance between the column spaces of two sets, to come to a conclusion about the number of clusters. Let us consider that data are noiseless and we divide our data set of K elements to two sets $\{S_1, S_2\}$ randomly. So if we assume that R is the real number of clusters and estimate the column space of two sets then we will have $col(G_{opt, 1}) = col(G_{opt, 2})$. However, if the real data set is not so in this case the two column spaces will not be equal. We compute their gap, which is defined as:

$$\rho_{g,2}(Y_1, Y_2) = \|P_{Y_1} - P_{Y_2}\|_2 = \sin(\theta_1)$$

where

- P_{Y_1} is the projection matrix of Y_1
- P_{Y_2} is the projection matrix of Y_2
- and θ_1 is the largest canonical angle between Y_1 and Y_2 .

In the sequel, we assume that

$$\|E_k\| = O(\epsilon)$$

for $k = 1, \dots, K$ with ϵ a small positive number. So first we have to examine three cases:

1. $R_{est} = R$

In this case, the gCCA method returns two orthonormal bases whose vectors span approximately the same subspace and so the gap will be $O(\epsilon)$.

2. $R_{est} > R$

In this case the gCCA method except for the R -dimensional common spatial subspace attempts to model "common noise". However, since we assume that the E_k are statistically independent among subjects and $N \gg M$, we have no reason to believe that there is common noise subspace, thus we expect that the gap will be close to 1.

3. $R_{est} < R$

In this case, we underestimate the dimension of common spatial subspace and we expect that the gap value will range from $O(\epsilon)$ to 1, because each gCCA will randomly estimate a "subspace" of the spatial subspace.

As we can see, the gap criterion can be useful for the estimation of the number of clusters. We choose to utilize the some number of clusters in order to be able to compare the results.

6.1.3 Estimation of the common spatial factor \mathbf{A} and temporal components S_k

We have already estimated the common spatial subspace G_{opt} and so we have an estimation of the column subspace of common spatial factor \mathbf{A} . Now, we want to obtain from the orthonormal basis G_{opt} the common spatial factor \mathbf{A} . We know that the in the noiseless case the G_{opt} can be expressed as:

$$\mathbf{G}_{opt} = \mathbf{A}\mathbf{B}^T$$

where $B \in \mathbb{R}^{R \times R}$. However, there is noise, so will try to solve the following semi-Orthogonal Nonnegative Factorization (s-ONMF) problem in order to estimate factor \mathbf{A} .

$$\underset{\mathbf{A}, S_k}{\text{minimize}} \frac{1}{2} \|G_{opt} - AB^T\|_F^2$$

However, penalty methods are a certain class of algorithms for solving constrained optimization problems. These methods try to approximate a constrained optimization problem with an unconstrained one and then apply standard search techniques to obtain solutions. The approximation is achieved by adding a term to the objective function that prescribes a high cost for violation of constraints.

Penalty method for semi-Orthogonal Nonnegative Matrix Factorization (s-ONMF)

It is a two-step iterative optimization process. More specifically, we consider random initial matrices A_0, B_0 . In each iteration, we estimate the matrix \mathbf{A} by solving the previous problem using a projected gradient method and considering that the matrix \mathbf{B} is fixed and after that, we consider that the matrix \mathbf{A} is fixed.

Algorithm 1 Penalty method for s-ONMF algorithm

```

1: procedure PENALTY METHOD( $G_{opt}, c_k$ )
2:   Initialize:
      $A_0, B_0, k = 0$ 
3:   while terminating condition is FALSE do
4:      $A_k = \text{Projected Gradient}(A_{k-1}, B_{k-1}, G_{opt}, c_k)$ 
5:      $B_k = (A_k^T A_k)^{-1} A_k^T G_{opt}$ 
6:      $k = k + 1$ 
7:   end while
8:   return  $A_k$ 
9: end procedure

```

Accelerated penalty method for semi-Orthogonal Nonnegative Matrix Factorization (s-ONMF)

In this section, we modify the cost as it is proposed in [15]. The constraint $A^T A = I$ can be divided into two parts. The first part includes the constraints $a_i^T a_i = 1$, which is not important, because we can scale the columns of A and B without increasing the error. The second part is the constraints with form $a_i^T a_j = 0$ for any $i \neq j$. So the problem can be as expressed with the algorithms which are shown below.

Algorithm 2 Penalty Gradient for A estimation

```

1: procedure PENALTY METHOD( $A_0, B, G_{opt}, c_k$ )
2:   Initialize:
3:      $k = 0$ 
4:   while terminating condition is FALSE do
5:     Compute  $\nabla F(A_{k-1})$ 
6:      $a_k = \frac{1}{\lambda_{max}(B^T B) + 2c_k(3\lambda_{max}(A_{k-1}^T A_{k-1})^{\frac{1}{2}} I_R)}$ 
7:      $A_k = \max(0, A_{k-1} - a_k \nabla F(A_{k-1}))$ 
8:      $k = k + 1$ 
9:   end while
10:  return  $A_k$ 
11: end procedure

```

We solve a sequence of subproblems, which have the form of the previous problem as we have already described. In each iteration, we increase the value of penalty constant c_k and solve the corresponding subproblem. In the first iteration we consider that initial points for the problem are random matrices, for the rest iterations the initial points will be the solutions of previous subproblem. The subproblem is solved by using alternating least squares. It is a two-step iterative optimization process. More specifically, in each iteration we estimate the matrix A by using a projected gradient method and considering that the matrix B is fixed and after that we estimate the problem considering that the matrix A is fixed. The corresponding algorithms are described below.

Algorithm 3 Accelerated Penalty Method for s-ONMF algorithm

```

1: procedure ACCELERATED PENALTY METHOD( $G_{opt}, A_0, B_0, c_k, \alpha$ )
2:   while terminating condition is FALSE do
3:     while terminating condition is FALSE do
4:        $A_k = \text{NesterovProjectedGradient}(A_{k-1}, B_{k-1}, G_{opt}, c_k, \alpha)$ 
5:       normalization of matrix  $A_k$ 
6:        $B_k = (A_k^T A_k)^{-1} G_{opt}^T A_k$ 
7:        $k = k + 1$ 
8:     end while
9:      $c_k = a * c_k$ 
10:     $k = 0$ 
11:     $A_0 = A_k$ 
12:     $B_0 = B_k$ 
13:  end while
14:  return  $A_k$ 
15: end procedure

```

Algorithm 4 Nesterov Accelerated Projected Gradient for A estimation

```

1: procedure NESTEROV PROJECTED GRADIENT( $A_0, B, G_{opt}, c_k, \alpha_0$ )
2:  Initialize:
3:     $k = 1, X_0 = A_0$ 
4:     $q = \frac{\lambda_{max}(BB^T \otimes I_N + c_k Q \otimes I_N)}{\lambda_{min}(BB^T \otimes I_N + c_k Q \otimes I_N)}$ 
5:  while terminating condition is FALSE do
6:    Compute  $\nabla F(A_{k-1})$ 
7:     $a_k = \frac{1}{\lambda_{max}(BB^T \otimes I_N + c_k Q)}$ 
8:     $X_k = \max(0, A_{k-1} - \alpha_k \nabla F(A_{k-1}))$ 
9:    Compute  $\alpha_k \in (0, 1)$  as the solution of equation:  $\alpha_k^2(1 - \alpha_k)\alpha_{k-1}^2 - q\alpha_k = 0$ 
10:    $\beta_{k-1} = \frac{\alpha_{k-1}(1 - \alpha_{k-1})}{\alpha_{k-1}^2 + \alpha_k}$ 
11:    $A_k = X_k + \beta_{k-1}(X_k - X_{k-1})$ 
12:    $k = k + 1$ 
13: end while
14: return  $A_k$ 
15: end procedure

```

Estimation of the temporal components S_k

Finally after the estimation of the common subspace factor \mathbf{A} , we can estimate the temporal components \mathbf{S}_k , for $k = 1, \dots, K$. Each of the term \mathbf{S}_k is the solution of the least square problem:

$$\underset{\mathbf{A}, S_k}{\text{minimize}} \frac{1}{2} \|\mathbf{X}_k - \mathbf{A}S_k^T\|_F^2$$

where \mathbf{A} is fixed and equal to the \mathbf{A}_{est} , which is the solution of the factorization problem.

So we will have:

$$S_k = (\mathbf{A}_k^T \mathbf{A}_k)^{-1} \mathbf{A}_k^T X_k$$

.

CHAPTER. 7

Experimental Results

7.1 Experimental Results

In this chapter we will describe the experimental results upon executing the different experiments in the brain. We will analyze the brain maps between healthy and non-healthy subjects. Next we will see the histograms with the subtracted mean of the control and MS (multiple sclerosis) patients for all the materials.

7.2 Brain maps for control subjects

First we explain the definition of the voxel. The fMRI machines divide the brain into three-dimensional areas called voxels, each approximately five cubic millimeters in size. The activity of the brain at any instant can be recorded using a three-dimensional grid of 60 x 60 x 30 voxels. Also we divide the brain in 27 clusters and each cluster contains a different number of voxels. The number of voxels in each cluster is related with the patient (if is healthy or non-healthy).

We created some brain maps for each of the 27 clusters we study in healthy and non-healthy subjects. The clusters related to brain histograms are shown in the images below. The clusters are presented in ascending order by the number of voxels. First we display the control subjects.

Cluster of control subjects	Number of voxels
19	28245
27	20290
22	17039
7	13626
8	11279
10	10781
2	10514
9	10302
14	10264
24	10183
6	9826
23	7343
5	7308
20	6614
11	6101
17	5987
21	5530
4	5282
16	4412
3	4230
25	3971
1	3971
15	3595
26	2442
18	2392
13	2264
12	2201

Table 7.1. This table represents the clusters of the control patients and the number of voxels on the side according to descent classification.

1. **Cluster 19** consists of 28245 voxels which correspond to 12.5006% of the whole brain (background, soft tissue, bone are excluded).

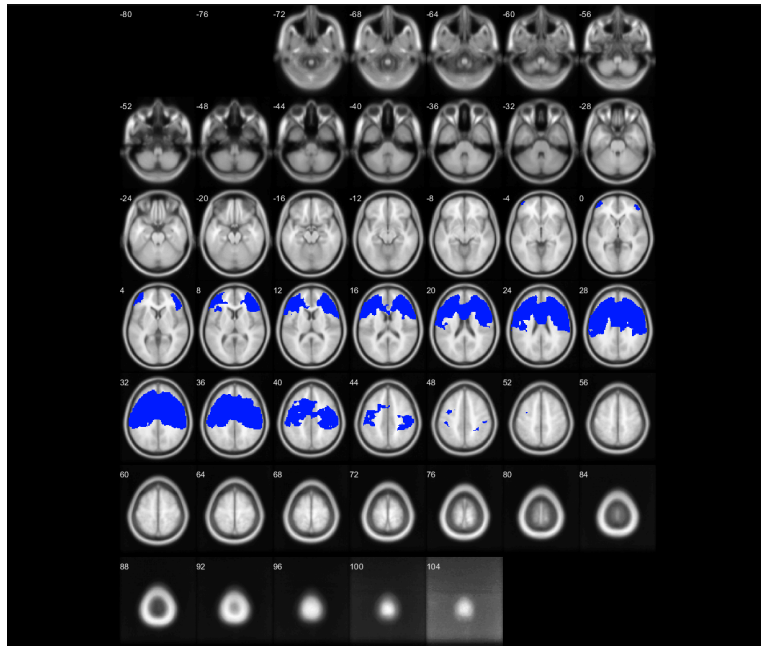


Figure 7.1. Blue areas indicate the voxels which belong to cluster 19 of the control subjects.

2. **Cluster 27** consists of 20290 voxels which correspond to 8.9799% of the whole brain (background, soft tissue, bone are excluded).

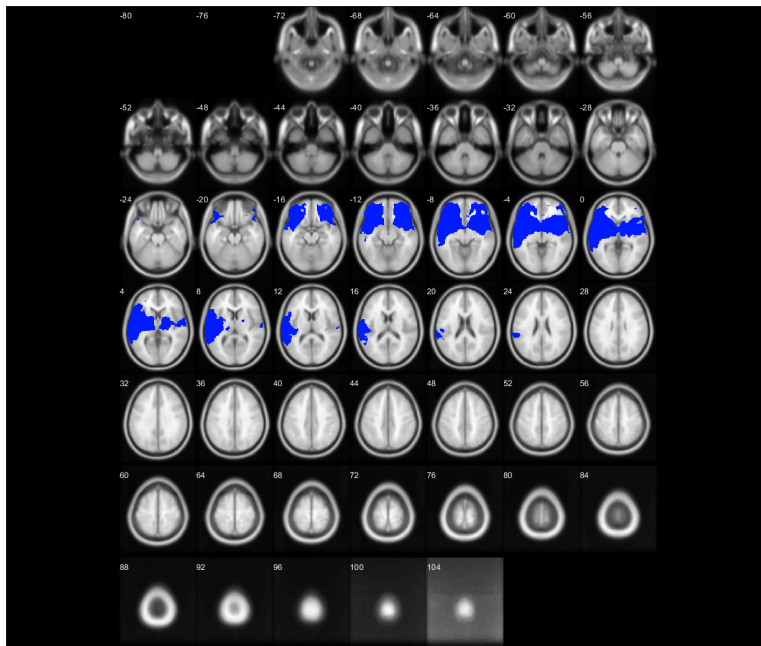


Figure 7.2. Blue areas indicate the voxels which belong to cluster 27 of the control subjects.

3. Cluster 22 consists of 17039 voxels which correspond to 7.5411% of the whole brain (background, soft tissue, bone are excluded).

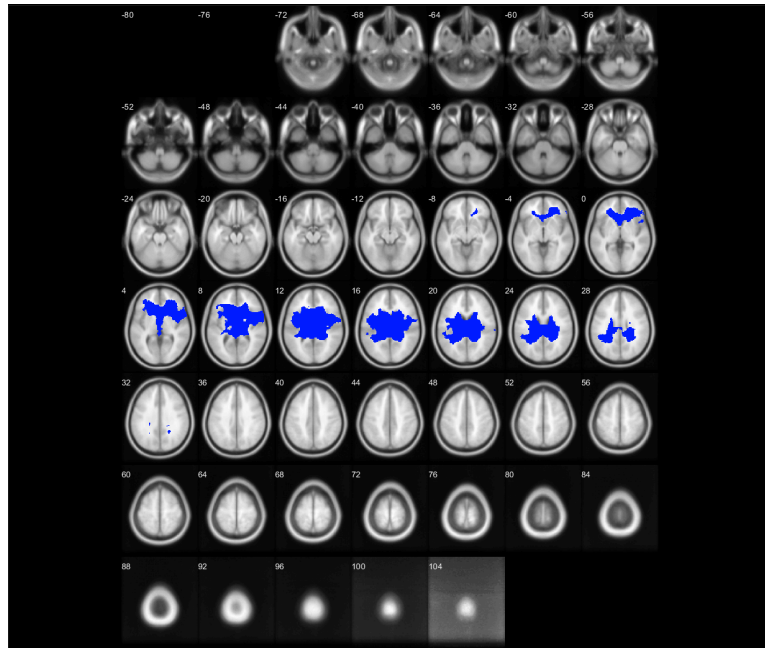


Figure 7.3. Blue areas indicate the voxels which belong to cluster 22 of the control subjects.

4. Cluster 7 consists of 13626 voxels which correspond to 6.0305% of the whole brain (background, soft tissue, bone are excluded).

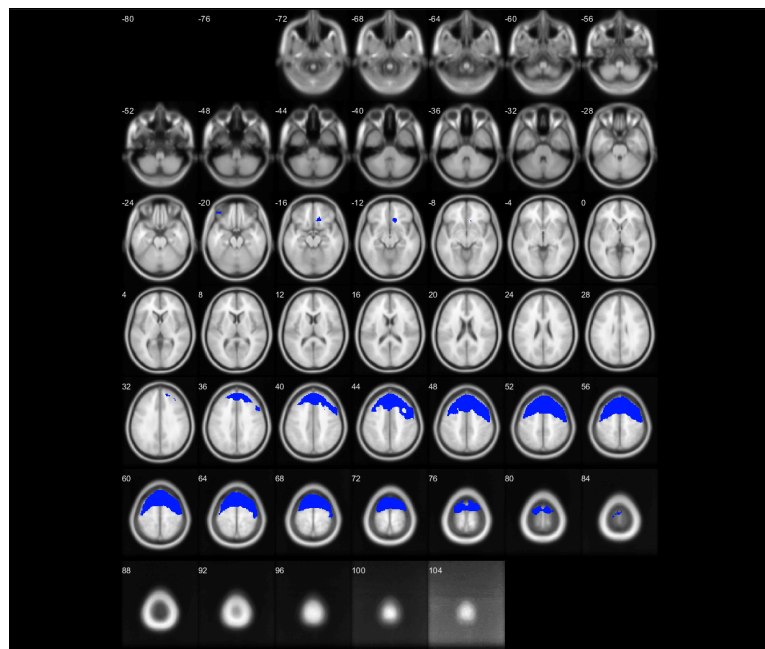


Figure 7.4. Blue areas indicate the voxels which belong to cluster 7 of the control subjects.

5. Cluster 8 consists of 11279 voxels which correspond to 4.9918% of the whole brain (background, soft tissue, bone are excluded).

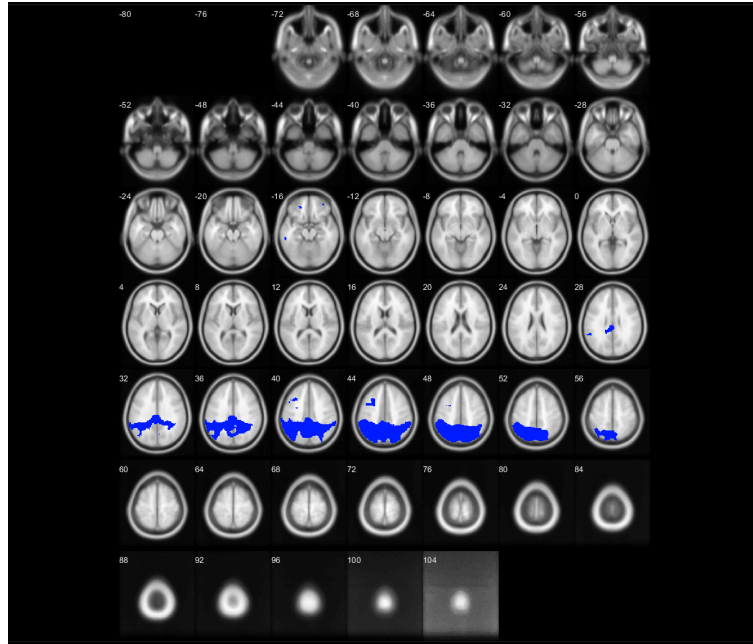


Figure 7.5. Blue areas indicate the voxels which belong to cluster 8 of the control subjects.

6. Cluster 10 consists of 10781 voxels which correspond to 4.7714% of the whole brain (background, soft tissue, bone are excluded).

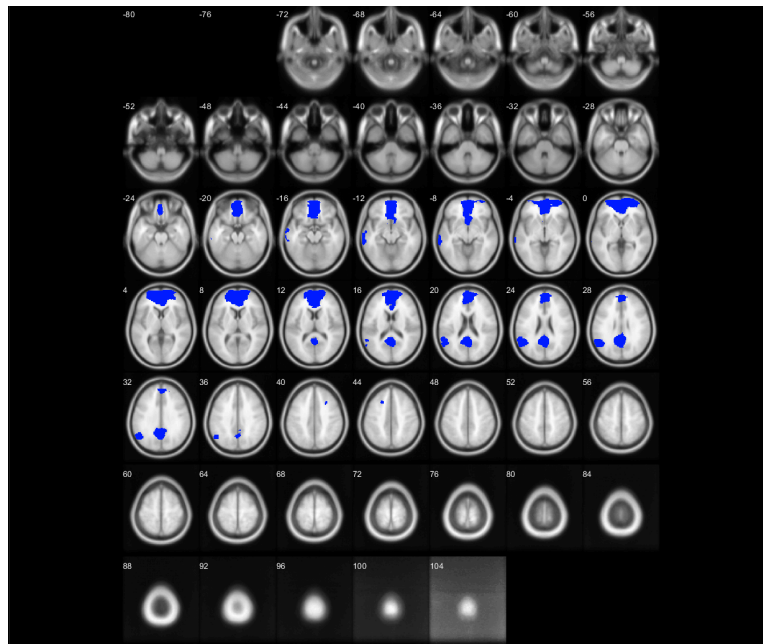


Figure 7.6. Blue areas indicate the voxels which belong to cluster 10 of the control subjects.

7. **Cluster 2** consists of 10514 voxels which correspond to 4.6532% of the whole brain (background, soft tissue, bone are excluded).

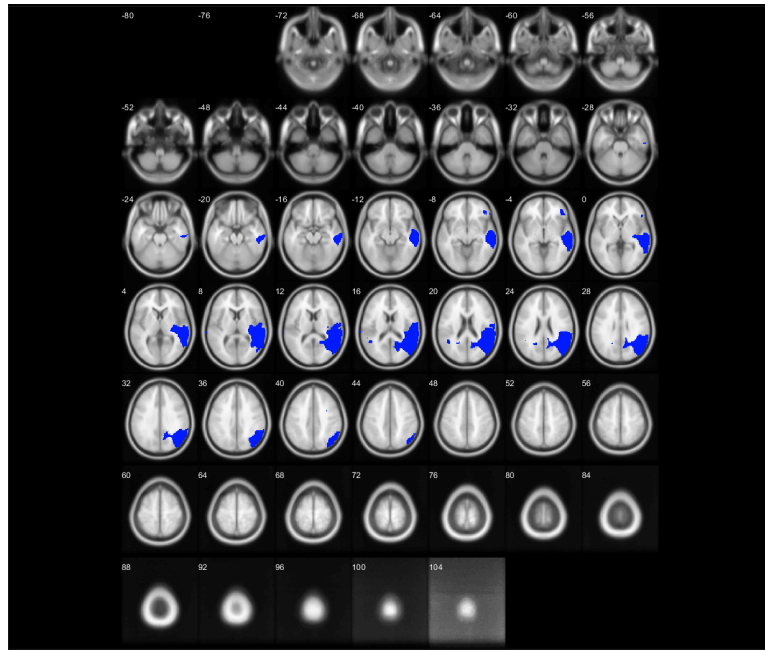


Figure 7.7. Blue areas indicate the voxels which belong to cluster 2 of the control subjects.

8. **Cluster 9** consists of 10302 voxels which correspond to 4.5594% of the whole brain (background, soft tissue, bone are excluded).

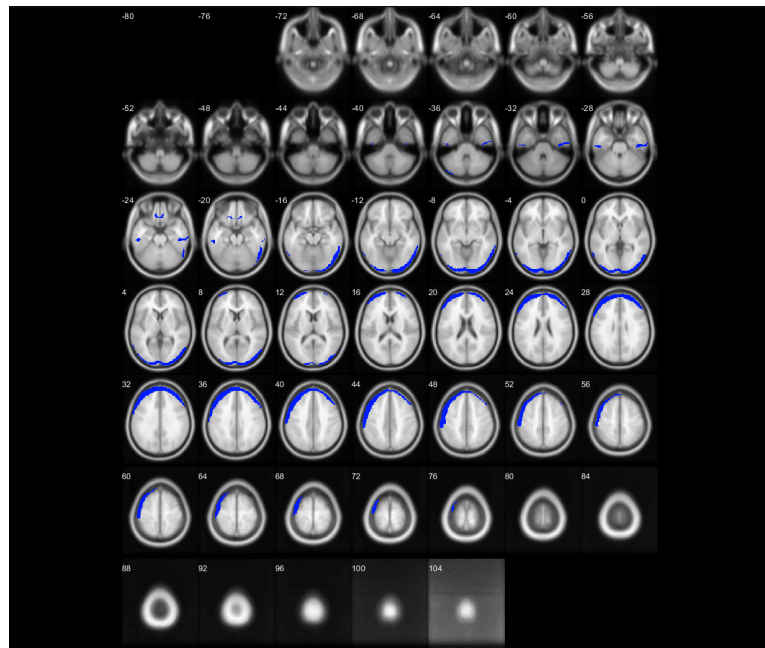


Figure 7.8. Blue areas indicate the voxels which belong to cluster 9 of the control subjects.

9. Cluster 14 consists of 10264 voxels which correspond to 4.5426% of the whole brain (background, soft tissue, bone are excluded).

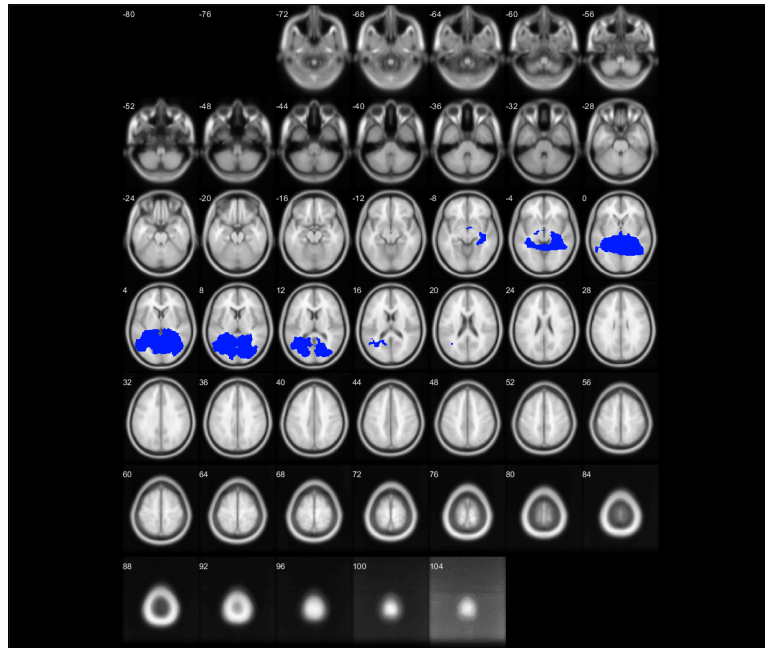


Figure 7.9. Blue areas indicate the voxels which belong to cluster 14 of the control subjects.

10. Cluster 24 consists of 10183 voxels which correspond to 4.5067% of the whole brain (background, soft tissue, bone are excluded).

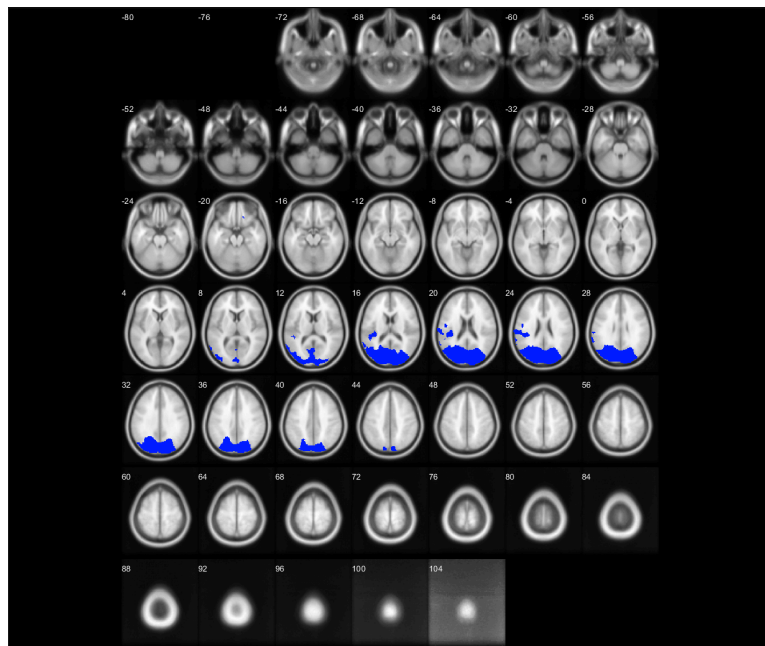


Figure 7.10. Blue areas indicate the voxels which belong to cluster 24 of the control subjects.

11. Cluster 6 consists of 9826 voxels which correspond to 4.3487% of the whole brain (background, soft tissue, bone are excluded).

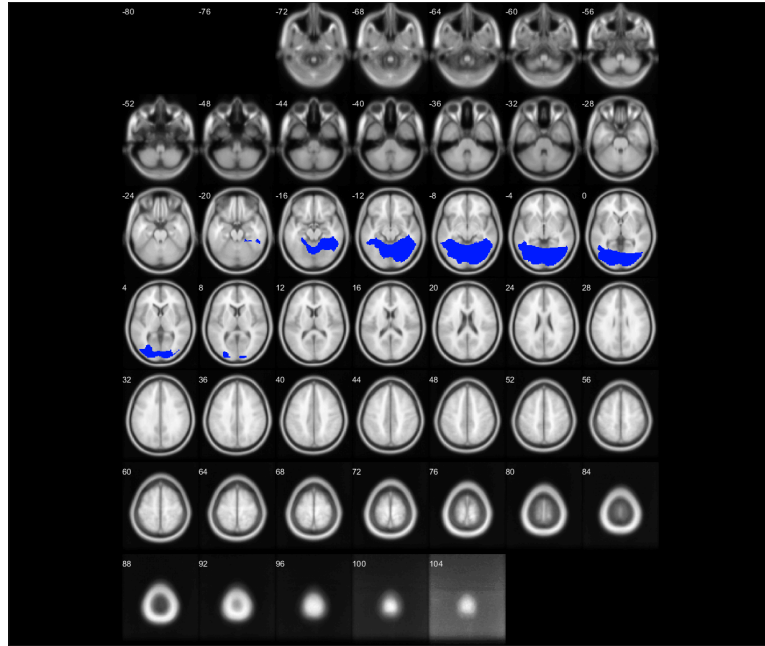


Figure 7.11. Blue areas indicate the voxels which belong to cluster 6 of the control subjects.

12. Cluster 23 Cluster 23 consists of 7343 voxels which correspond to 3.2498% of the whole brain (background, soft tissue, bone are excluded).

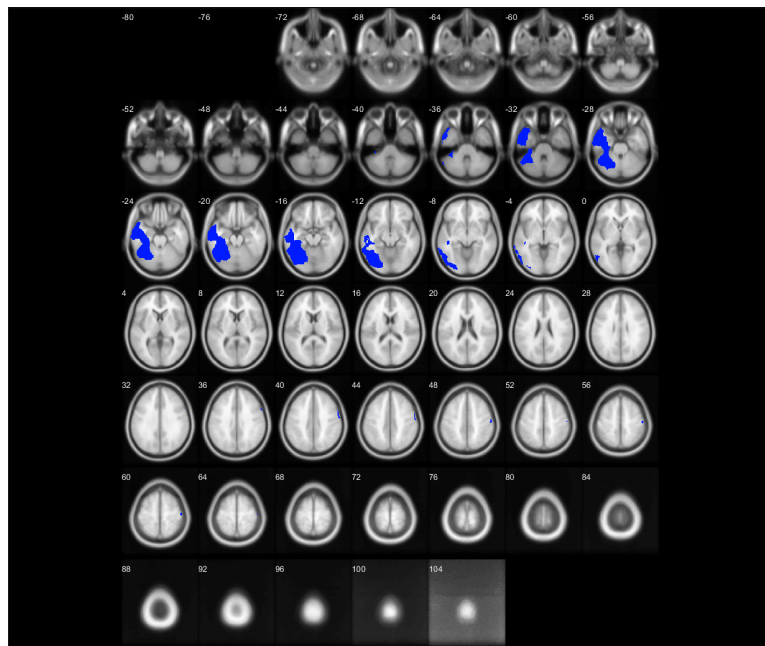


Figure 7.12. Blue areas indicate the voxels which belong to cluster 23 of the control subjects.

13. Cluster 5 consists of 7308 voxels which correspond to 3.2343% of the whole brain (background, soft tissue, bone are excluded).

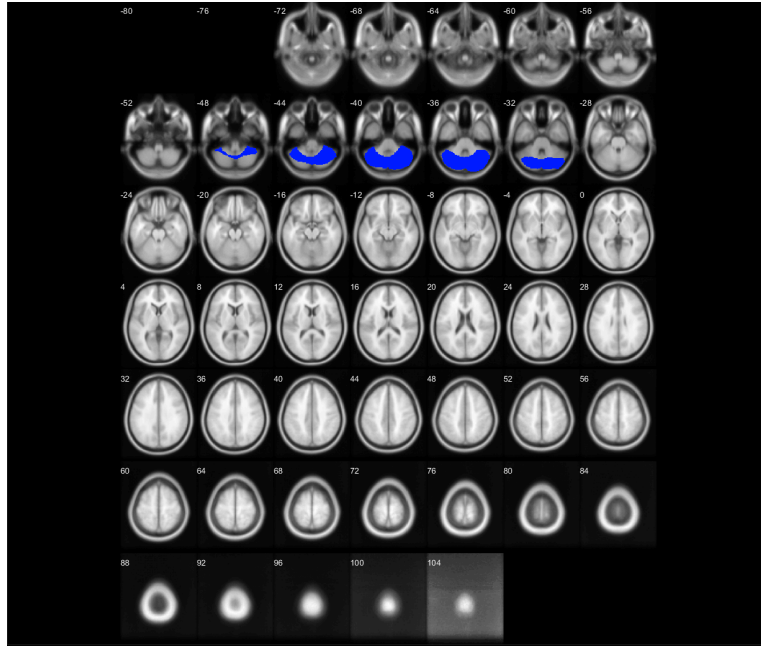


Figure 7.13. Blue areas indicate the voxels which belong to cluster 5 of the control subjects.

14. Cluster 20 consists of 6614 voxels which correspond to 2.9272% of the whole brain (background, soft tissue, bone are excluded).

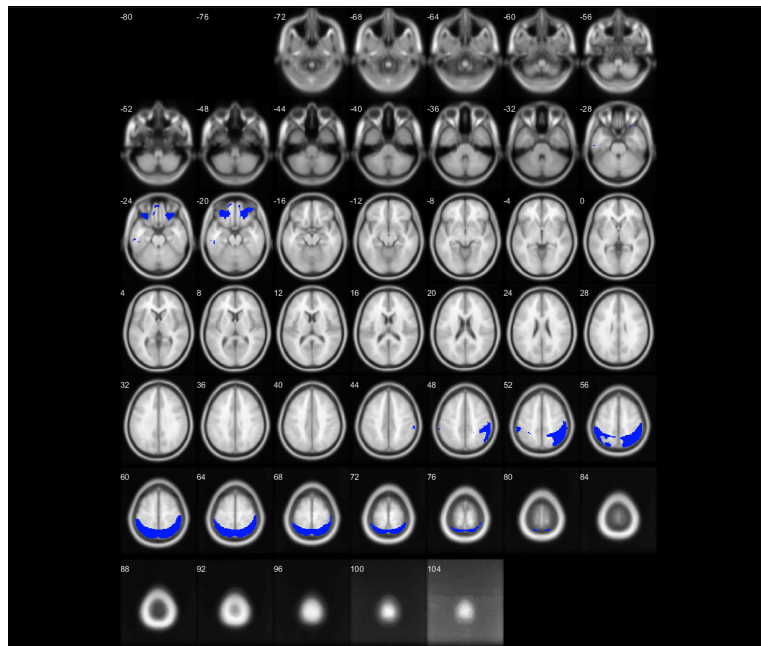


Figure 7.14. Blue areas indicate the voxels which belong to cluster 20 of the control subjects.

15. Cluster 11 consists of 10302 voxels which correspond to 2.7001% of the whole brain (background, soft tissue, bone are excluded).

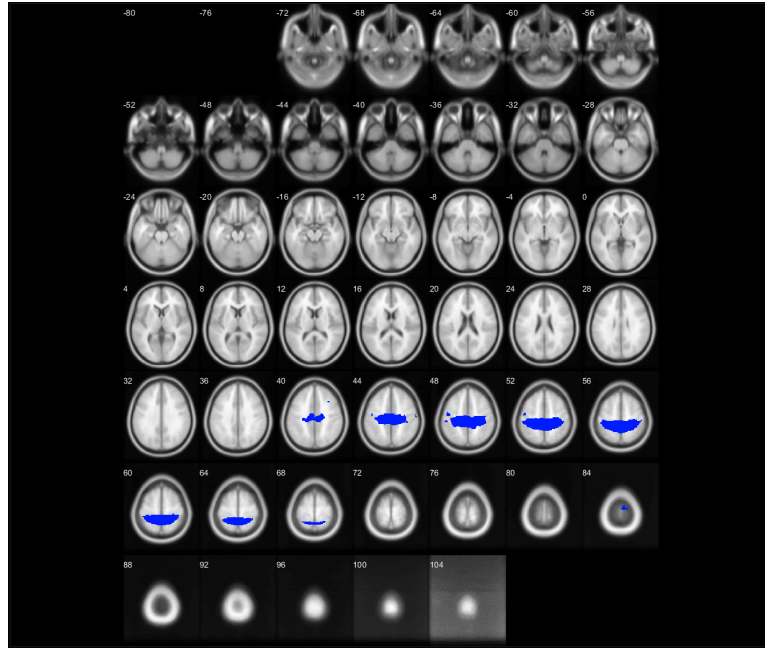


Figure 7.15. Blue areas indicate the voxels which belong to cluster 11 of the control subjects.

16. Cluster 17 consists of 5987 voxels which correspond to 2.6497% of the whole brain (background, soft tissue, bone are excluded).

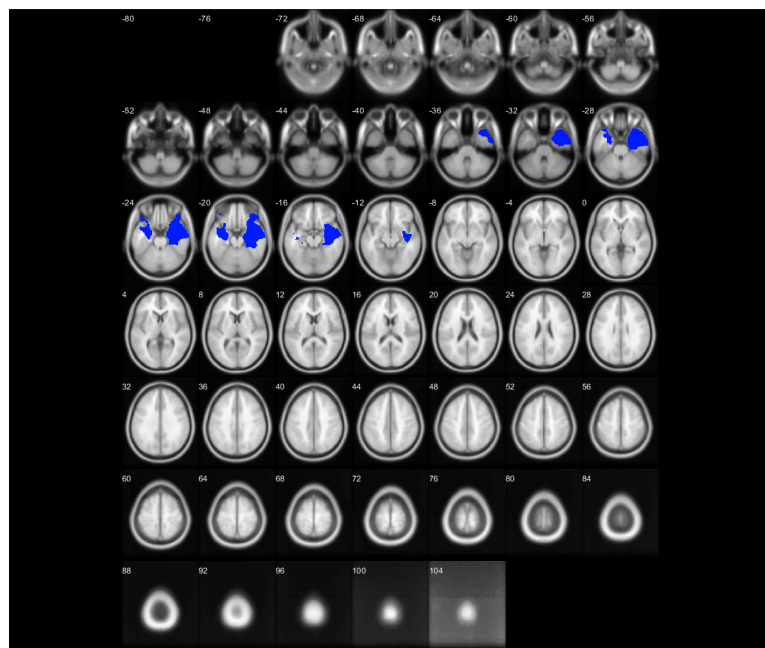


Figure 7.16. Blue areas indicate the voxels which belong to cluster 17 of the control subjects.

17. Cluster 21 consists of 5530 voxels which correspond to 2.4474% of the whole brain (background, soft tissue, bone are excluded).

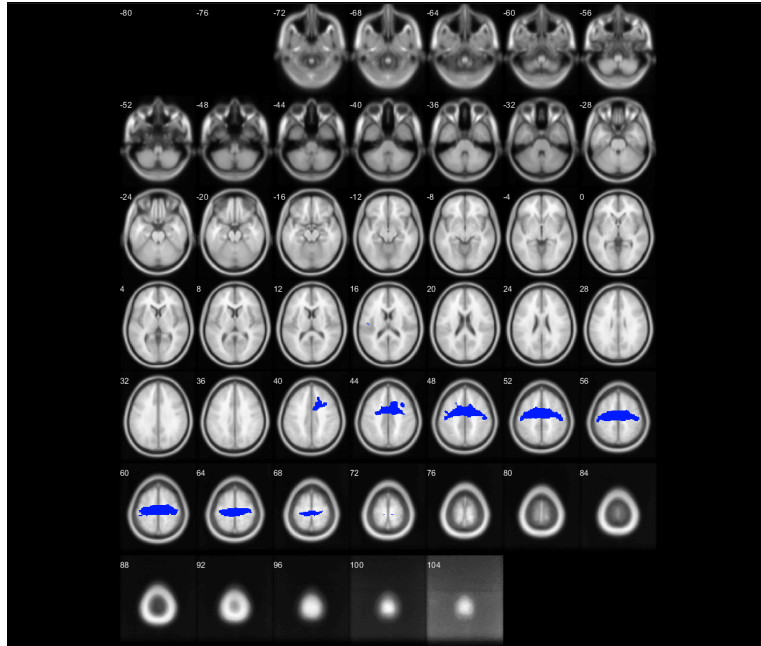


Figure 7.17. Blue areas indicate the voxels which belong to cluster 21 of the control subjects.

18. Cluster 4 consists of 5282 voxels which correspond to 2.337706% of the whole brain (background, soft tissue, bone are excluded).

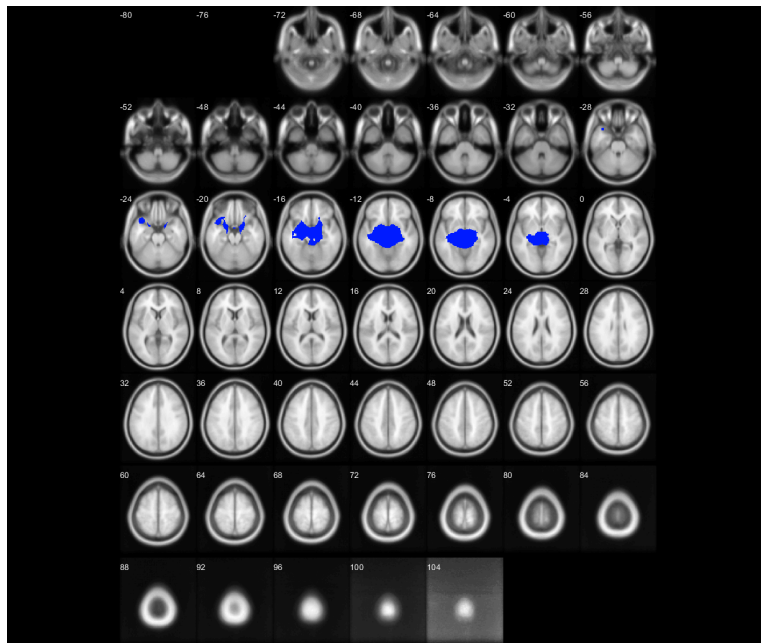


Figure 7.18. Blue areas indicate the voxels which belong to cluster 4 of the control subjects.

19. Cluster 16 consists of 4412 voxels which correspond to 1.9526% of the whole brain (background, soft tissue, bone are excluded).

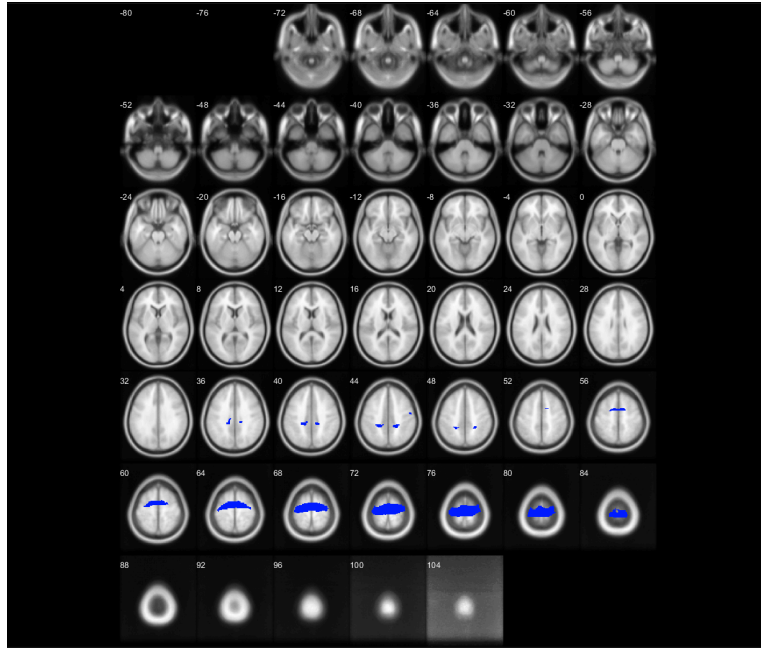


Figure 7.19. Blue areas indicate the voxels which belong to cluster 16 of the control subjects.

20. Cluster 3 consists of 4230 voxels which correspond to 1.8721% of the whole brain (background, soft tissue, bone are excluded).

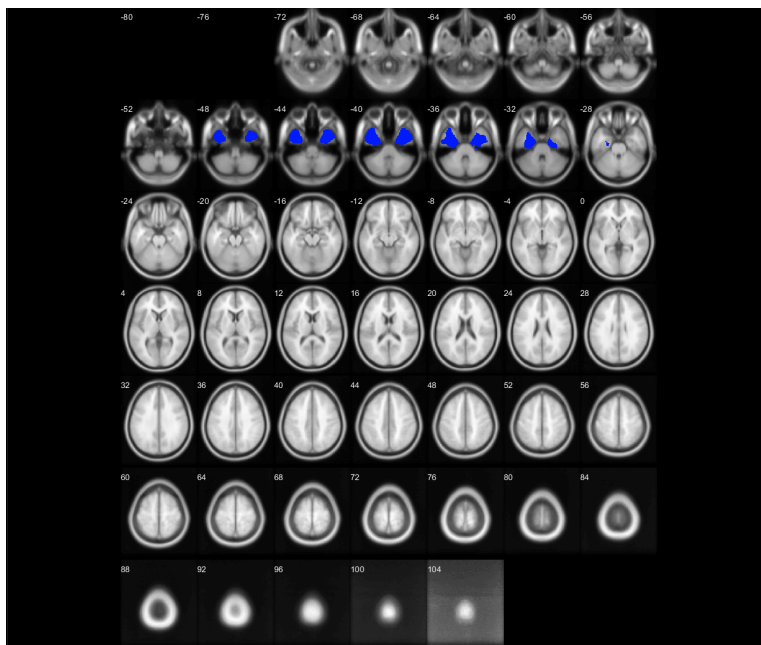


Figure 7.20. Blue areas indicate the voxels which belong to cluster 3 of the control subjects.

21. Cluster 25 consists of 3971 voxels which correspond to 1.7574% of the whole brain (background, soft tissue, bone are excluded).

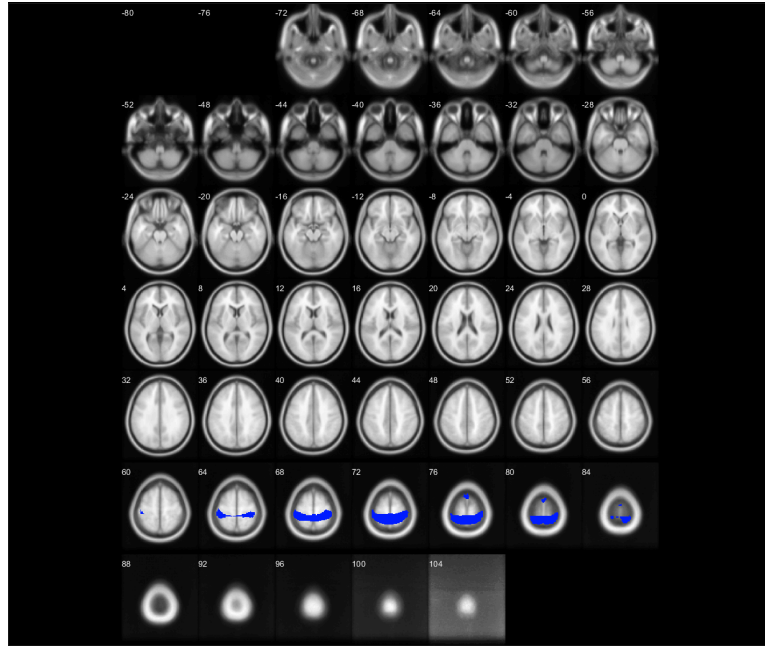


Figure 7.21. Blue areas indicate the voxels which belong to cluster 25 of the control subjects.

22. Cluster 1 consists of 3927 voxels which correspond to 1.7380% of the whole brain (background, soft tissue, bone are excluded).

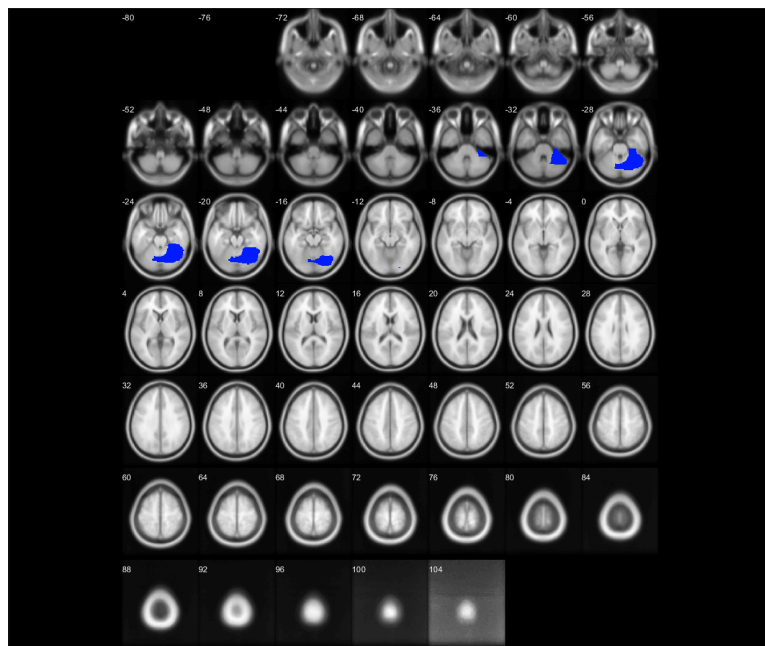


Figure 7.22. Blue areas indicate the voxels which belong to cluster 25 of the control subjects.

23. Cluster 15 consists of 3595 voxels which correspond to 1.5910% of the whole brain (background, soft tissue, bone are excluded).

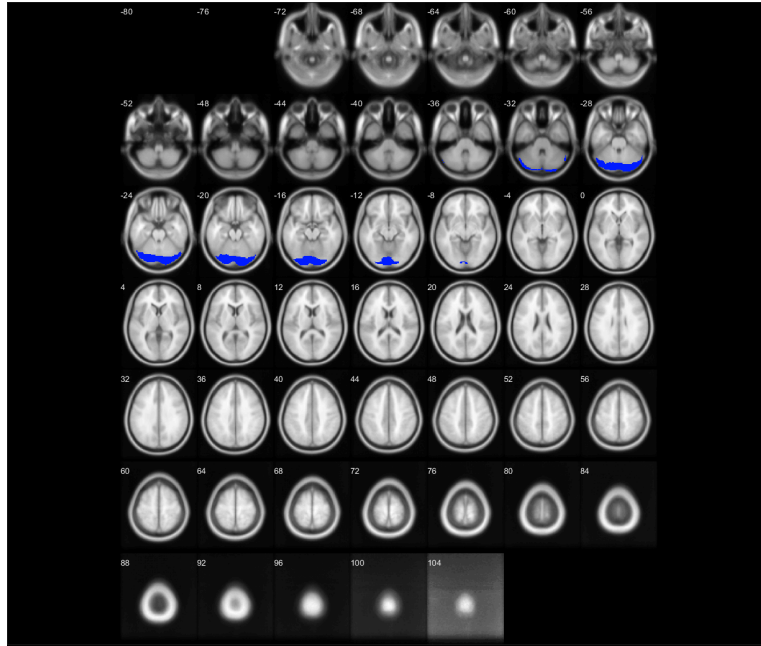


Figure 7.23. Blue areas indicate the voxels which belong to cluster 15 of the control subjects.

24. Cluster 26 consists of 2442 voxels which correspond to 1.0807% of the whole brain (background, soft tissue, bone are excluded).

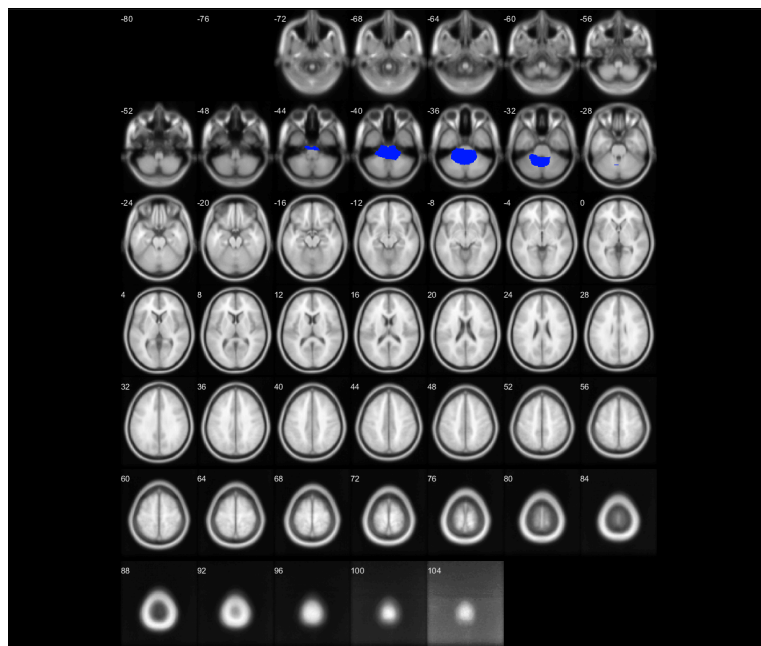


Figure 7.24. Blue areas indicate the voxels which belong to cluster 26 of the control subjects.

25. Cluster 18 consists of 2392 voxels which correspond to 1.0586% of the whole brain (background, soft tissue, bone are excluded).

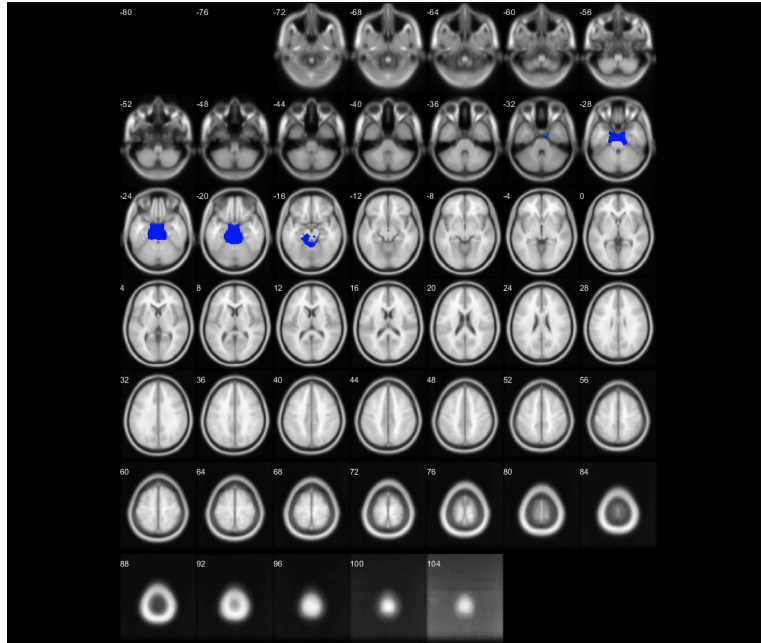


Figure 7.25. Blue areas indicate the voxels which belong to cluster 18 of the control subjects.

26. Cluster 13 consists of 2264 voxels which correspond to 1.0020% of the whole brain (background, soft tissue, bone are excluded).

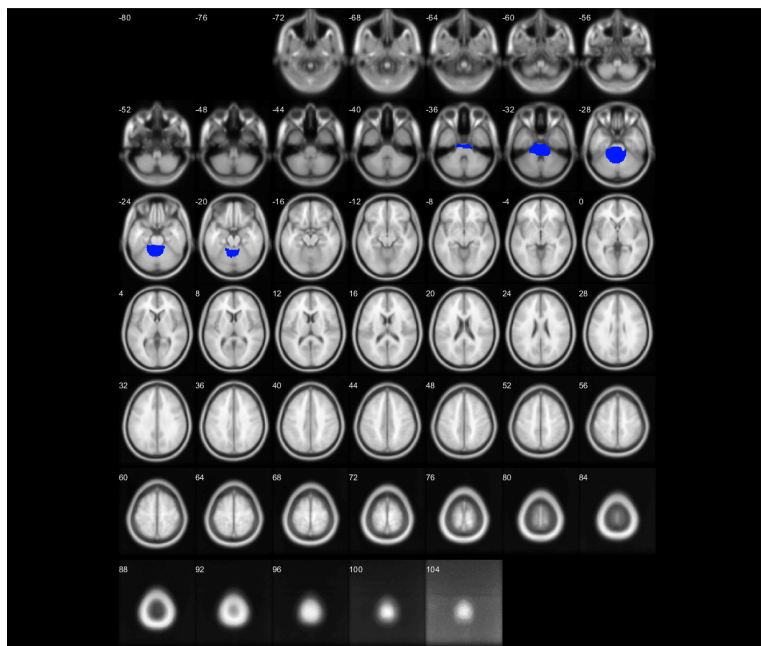


Figure 7.26. Blue areas indicate the voxels which belong to cluster 18 of the control subjects.

27. Cluster 12 consists of 2201 voxels which correspond to 0.9741% of the whole brain (background, soft tissue, bone are excluded).

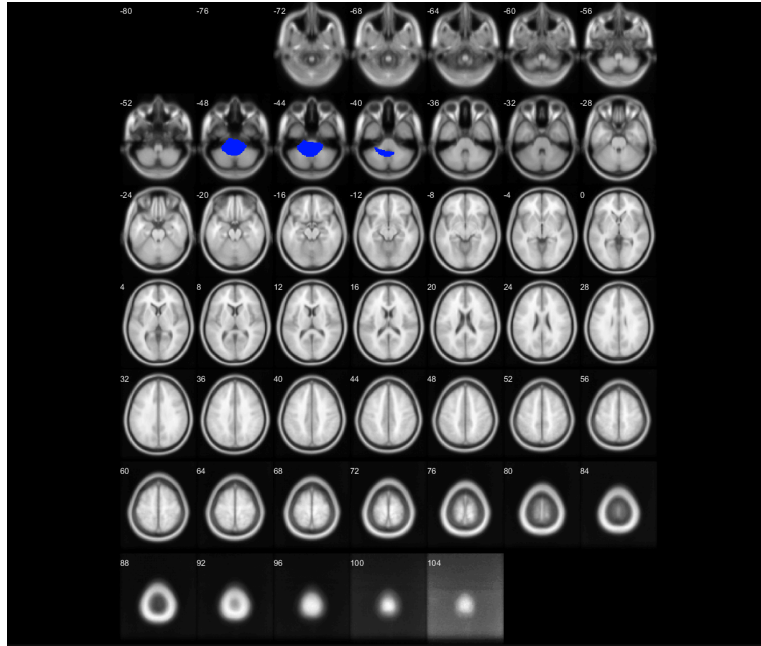


Figure 7.27. Blue areas indicate the voxels which belong to cluster 12 of the control subjects.

7.3 Brain maps for MS subjects

Furthermore the table which is shown below represents the 27 clusters of the non-healthy subjects which has the disease of the multiply sclerosis (MS). The clusters are sorted in descending order by number of voxels.

Cluster MS subjects	Number of voxels
11	25925
17	21273
8	17466
5	12113
1	12094
3	11806
2	10778
20	10663
4	10623
16	10512
7	8983
12	8817
6	8590
24	7206
23	6824
9	6373
15	5443
10	4923
26	4347
25	4063
27	4043
14	3833
22	3433
19	2641
13	2429
18	2170
21	1872

Table 7.2. The clusters of MS subjects having sorted from the largest number of voxels to the smallest (descent).

1. **Cluster 11** consists of 25925 voxels which correspond to 11.3090% of the whole brain (background, soft tissue, bone are excluded).

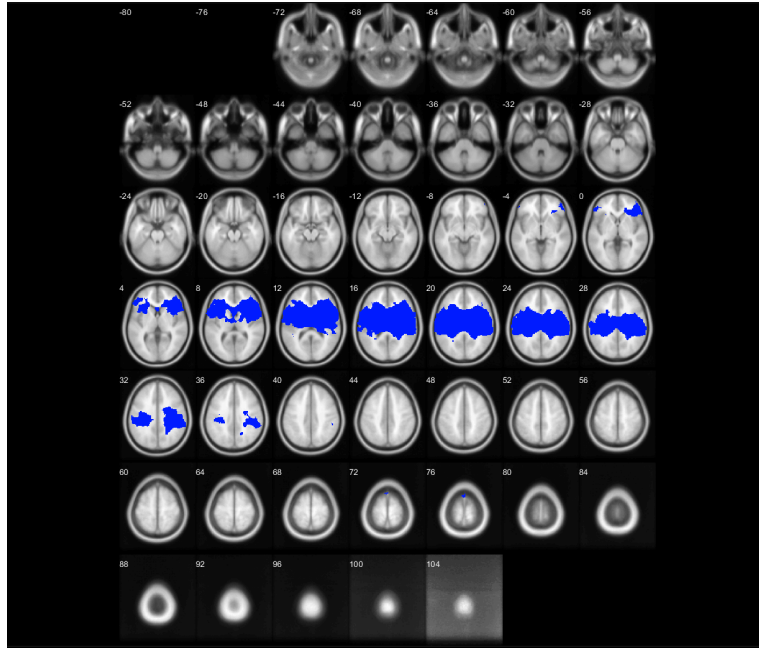


Figure 7.28. Blue areas indicate the voxels which belong to cluster 11 of MS subjects.

2. **Cluster 17** consists of 21273 voxels which correspond to 9.2797% of the whole brain (background, soft tissue, bone are excluded).

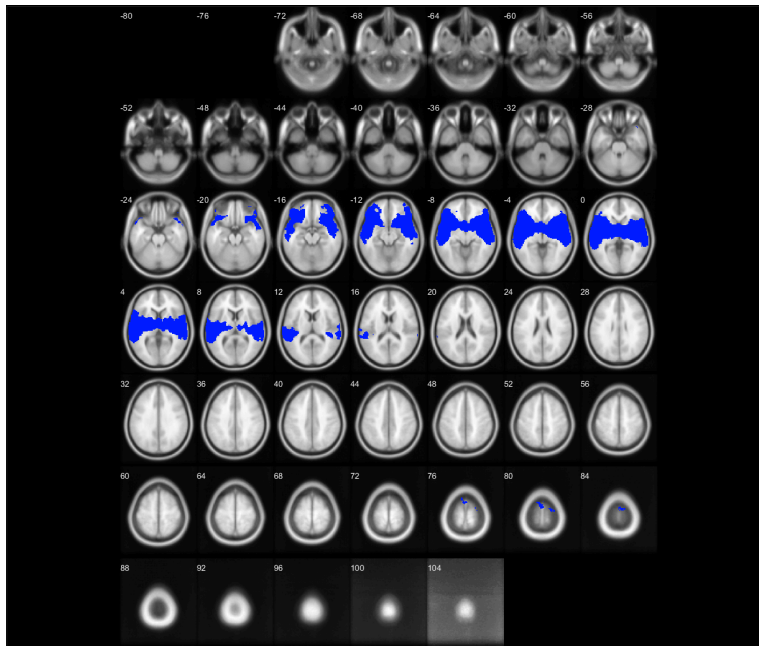


Figure 7.29. Blue areas indicate the voxels which belong to cluster 17 of MS subjects.

3. Cluster 8 consists of 17466 voxels which correspond to 7.6190% of the whole brain (background, soft tissue, bone are excluded).

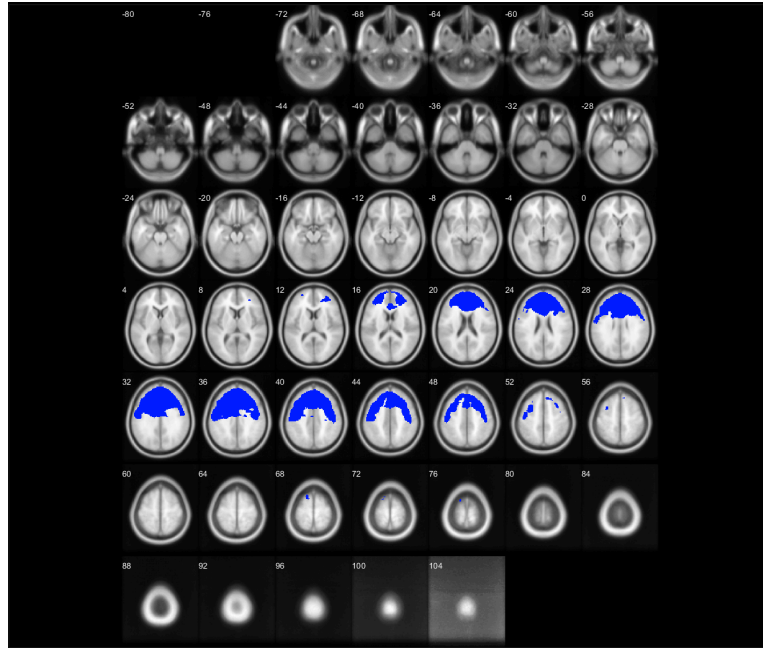


Figure 7.30. Blue areas indicate the voxels which belong to cluster 8 of MS subjects.

4. Cluster 5 consists of 12113 voxels which correspond to 5.2839% of the whole brain (background, soft tissue, bone are excluded).

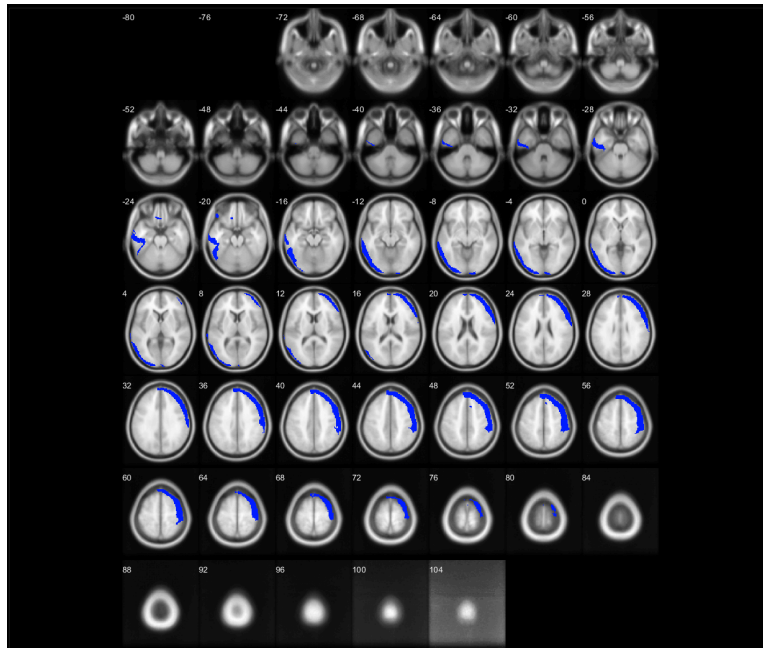


Figure 7.31. Blue areas indicate the voxels which belong to cluster 5 of MS subjects.

5. Cluster 1 consists of 12094 voxels which correspond to 5.2756% of the whole brain (background, soft tissue, bone are excluded).

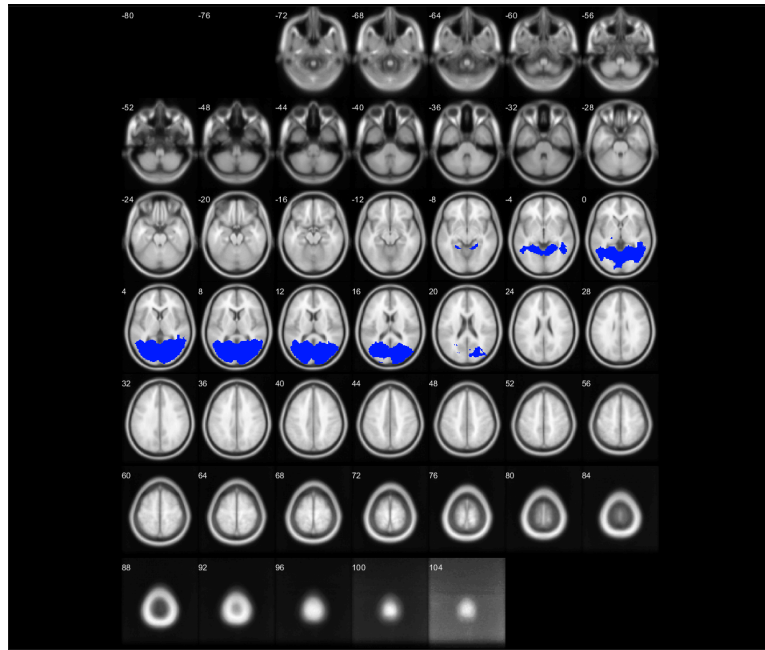


Figure 7.32. Blue areas indicate the voxels which belong to cluster 1 of MS subjects.

6. Cluster 3 consists of 11806 voxels which correspond to 5.1500% of the whole brain (background, soft tissue, bone are excluded).

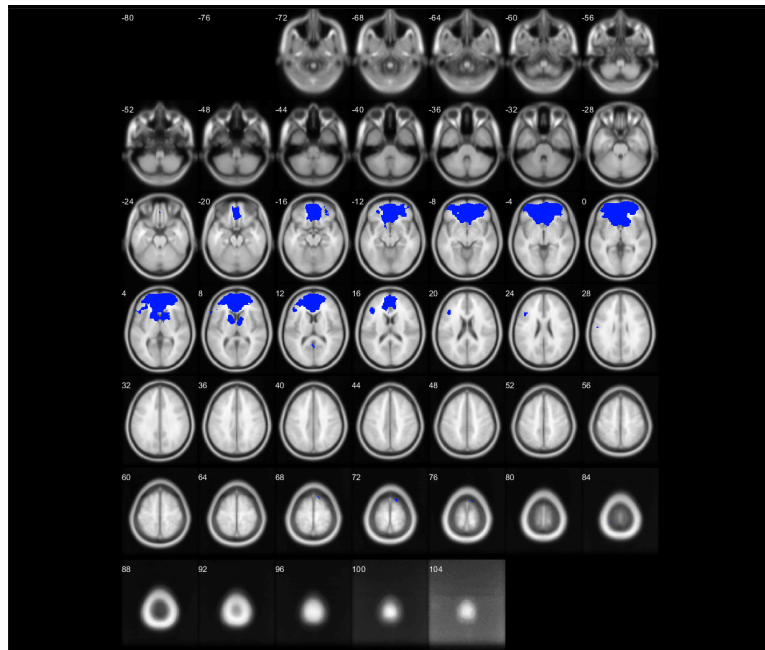


Figure 7.33. Blue areas indicate the voxels which belong to cluster 3 of MS subjects.

7. **Cluster 2** consists of 10778 voxels which correspond to 1.0020% of the whole brain (background, soft tissue, bone are excluded).

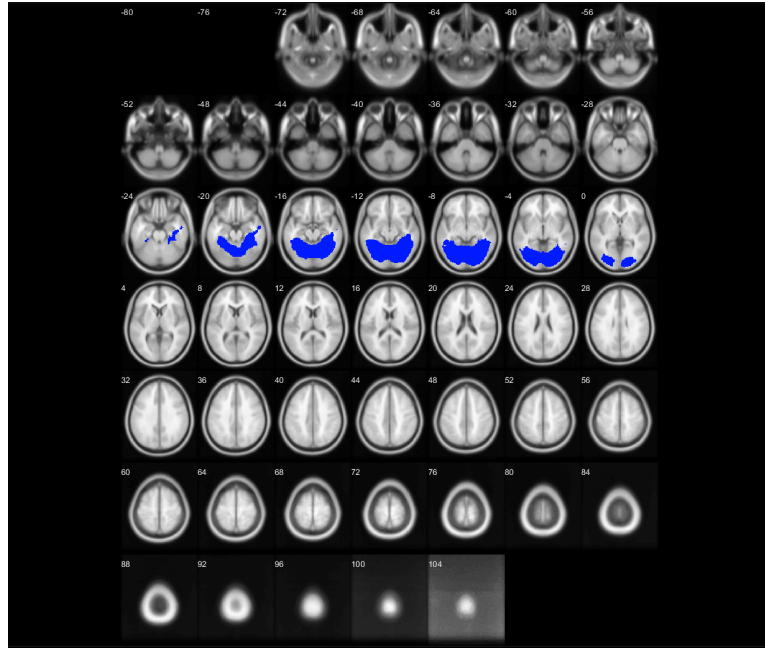


Figure 7.34. Blue areas indicate the voxels which belong to cluster 2 of MS subjects.

8. **Cluster 20** consists of 10663 voxels which correspond to 4.6514% of the whole brain (background, soft tissue, bone are excluded).

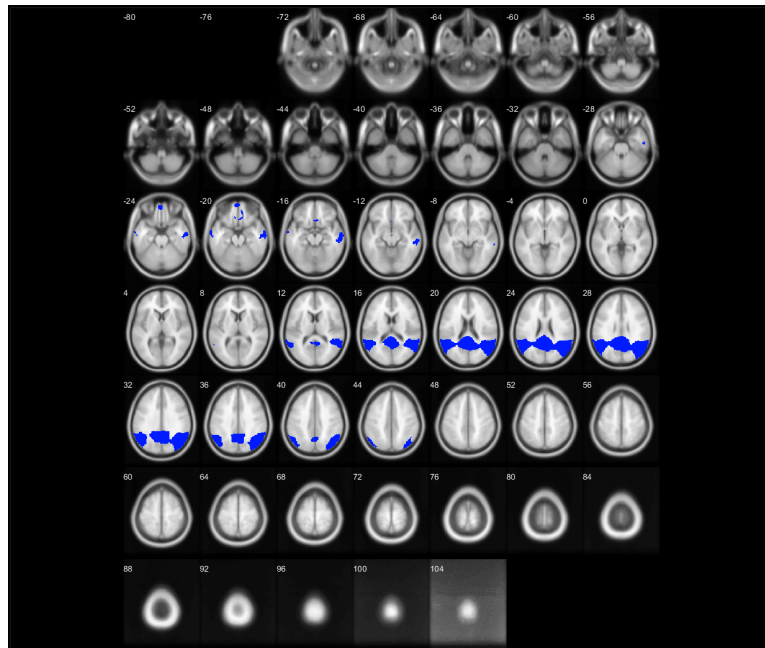


Figure 7.35. Blue areas indicate the voxels which belong to cluster 20 of MS subjects.

9. Cluster 4 consists of 10623 voxels which correspond to 4.6339% of the whole brain (background, soft tissue, bone are excluded).

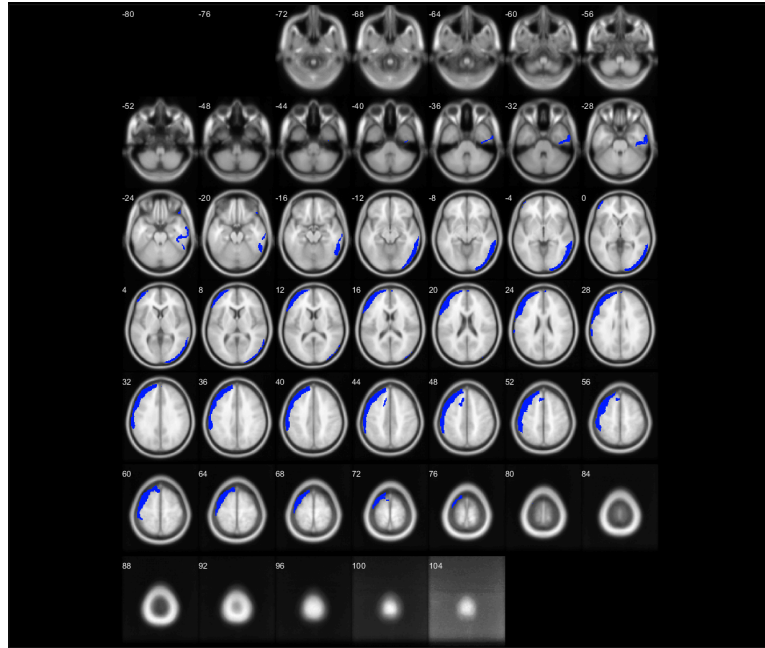


Figure 7.36. Blue areas indicate the voxels which belong to cluster 4 of MS subjects.

10. Cluster 16 consists of 10512 voxels which correspond to 4.5855% of the whole brain (background, soft tissue, bone are excluded).

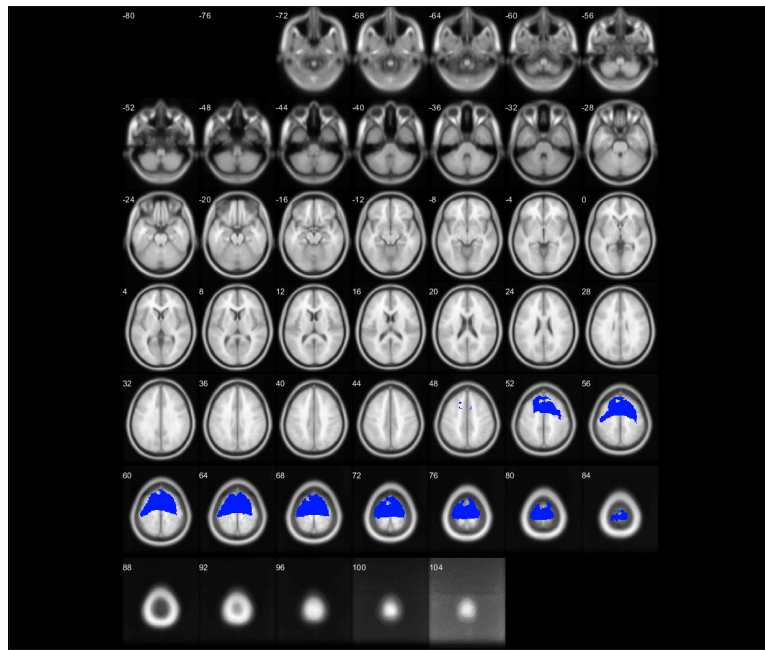


Figure 7.37. Blue areas indicate the voxels which belong to cluster 16 of MS subjects.

11. Cluster 7 consists of 8983 voxels which correspond to 3.9185% of the whole brain (background, soft tissue, bone are excluded).

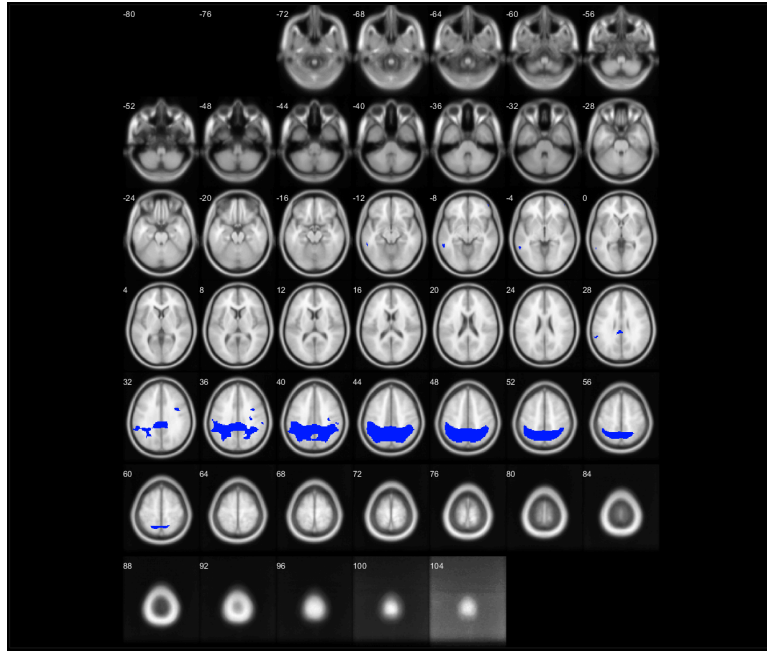


Figure 7.38. Blue areas indicate the voxels which belong to cluster 7 of MS subjects.

12. Cluster 12 consists of 8817 voxels which correspond to 3.8461% of the whole brain (background, soft tissue, bone are excluded).

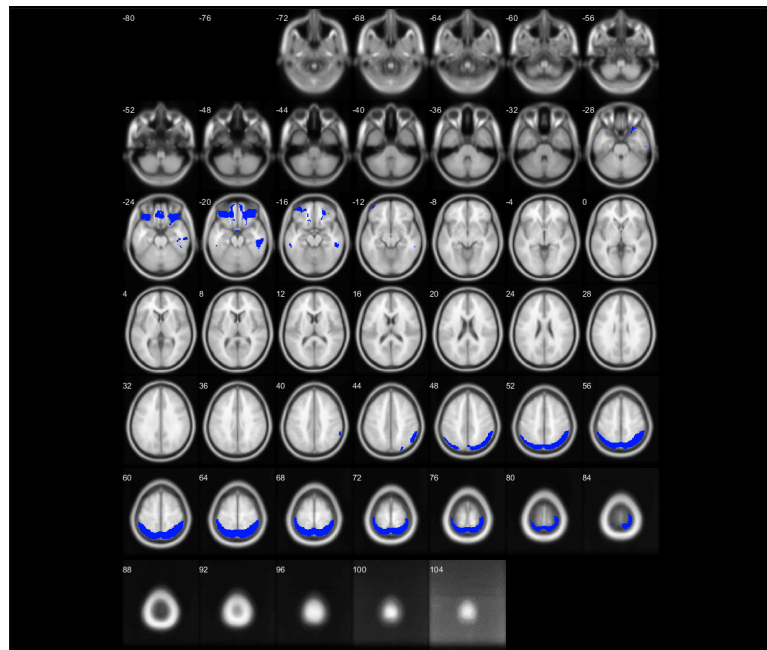


Figure 7.39. Blue areas indicate the voxels which belong to cluster 12 of MS subjects.

13. Cluster 6 consists of 8590 voxels which correspond to 3.7471% of the whole brain (background, soft tissue, bone are excluded).

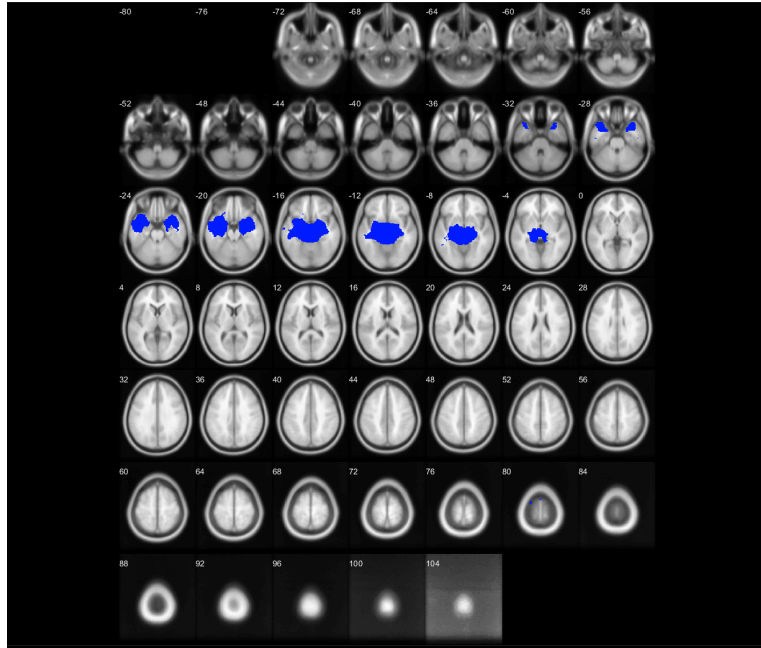


Figure 7.40. Blue areas indicate the voxels which belong to cluster 6 of MS subjects.

14. Cluster 24 consists of 7206 voxels which correspond to 3.1434% of the whole brain (background, soft tissue, bone are excluded).

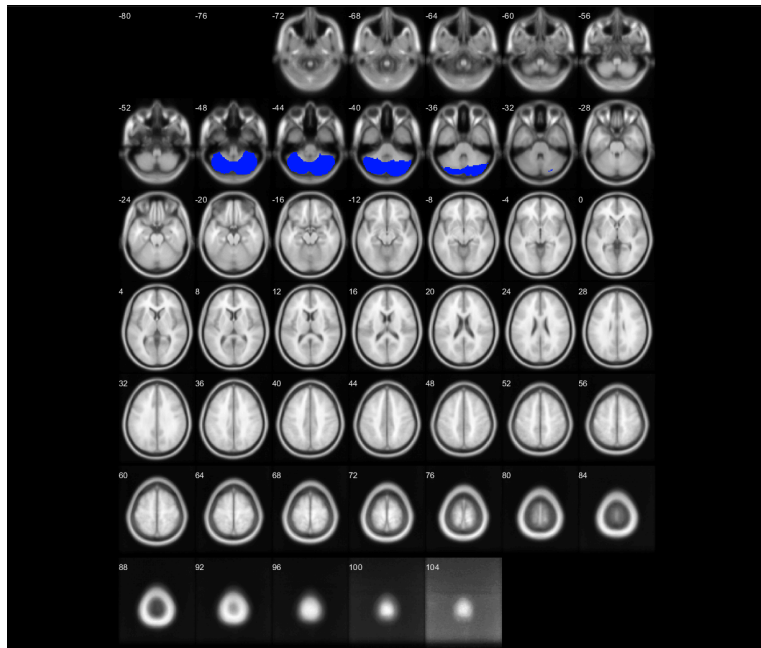


Figure 7.41. Blue areas indicate the voxels which belong to cluster 24 of MS subjects.

15. Cluster 23 consists of 6824 voxels which correspond to 2.9768% of the whole brain (background, soft tissue, bone are excluded).

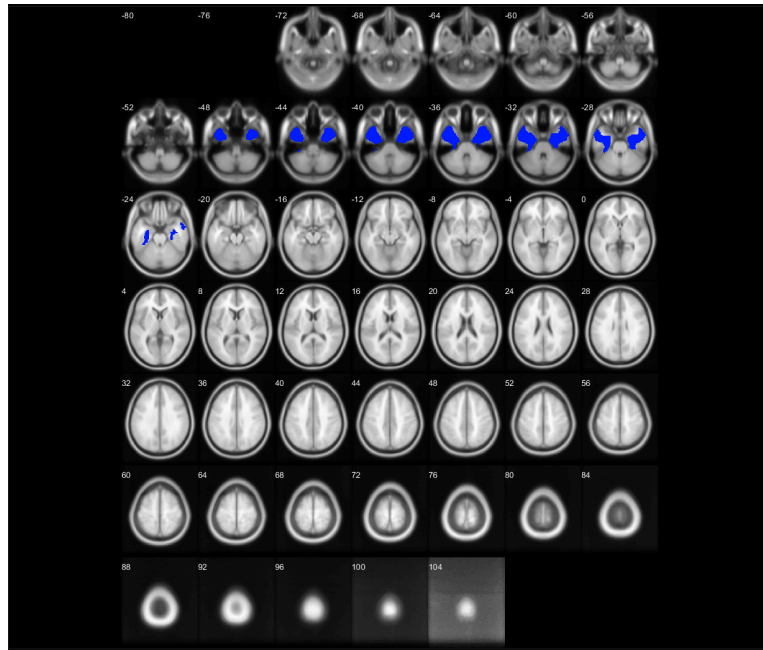


Figure 7.42. Blue areas indicate the voxels which belong to cluster 23 of MS subjects.

16. Cluster 9 consists of 6373 voxels which correspond to 2.7800% of the whole brain (background, soft tissue, bone are excluded).

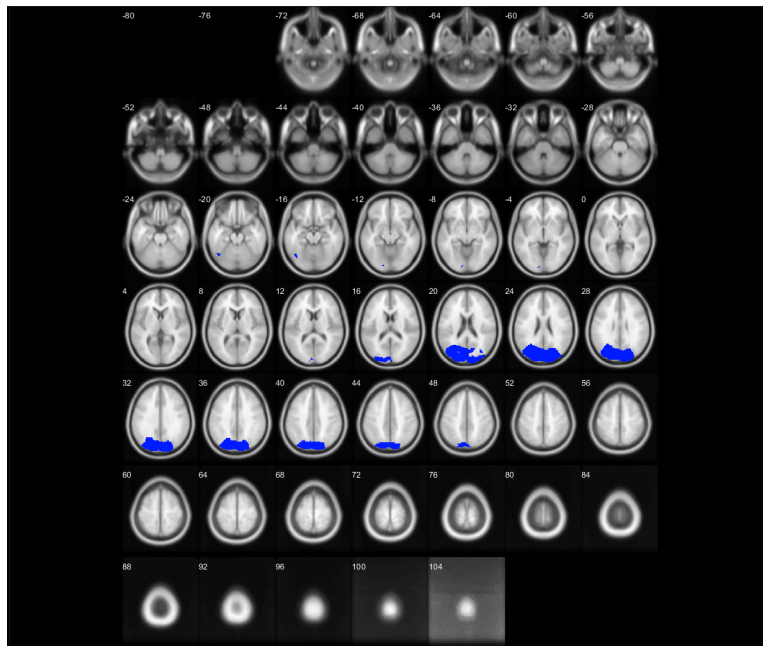


Figure 7.43. Blue areas indicate the voxels which belong to cluster 9 of MS subjects.

17. Cluster 15 consists of 5443 voxels which correspond to 2.3743% of the whole brain (background, soft tissue, bone are excluded).

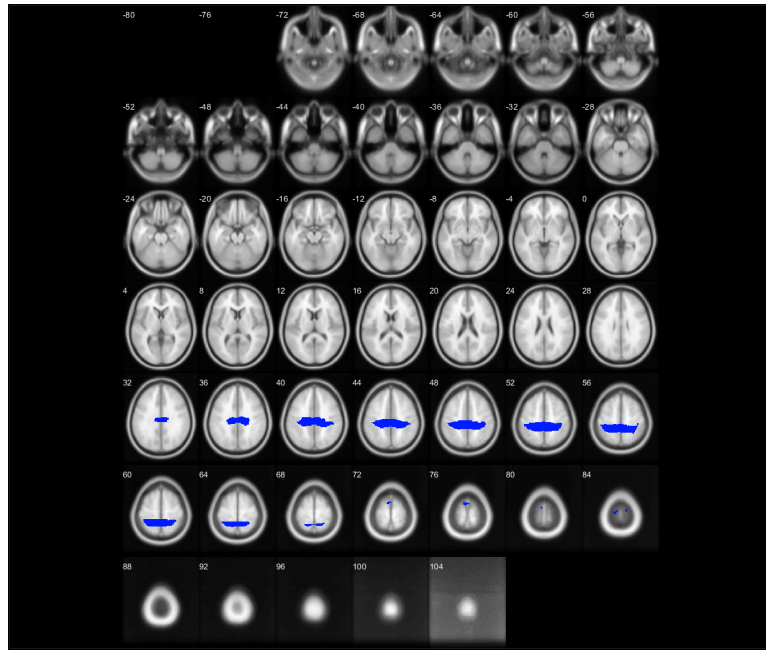


Figure 7.44. Blue areas indicate the voxels which belong to cluster 15 of MS subjects.

18. Cluster 10 consists of 4923 voxels which correspond to 2.1475% of the whole brain (background, soft tissue, bone are excluded).

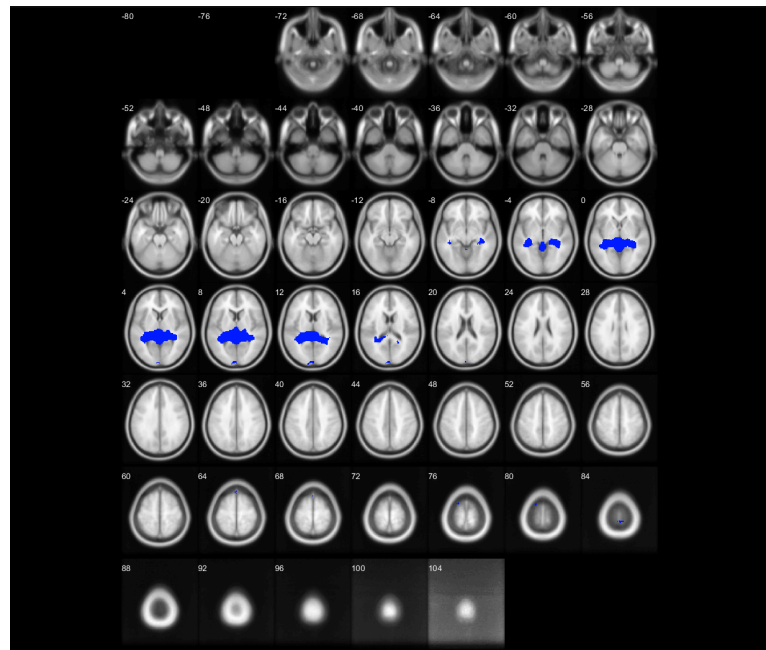


Figure 7.45. Blue areas indicate the voxels which belong to cluster 10 of MS subjects.

19. Cluster 26 consists of 4347 voxels which correspond to 1.8962% of the whole brain (background, soft tissue, bone are excluded).

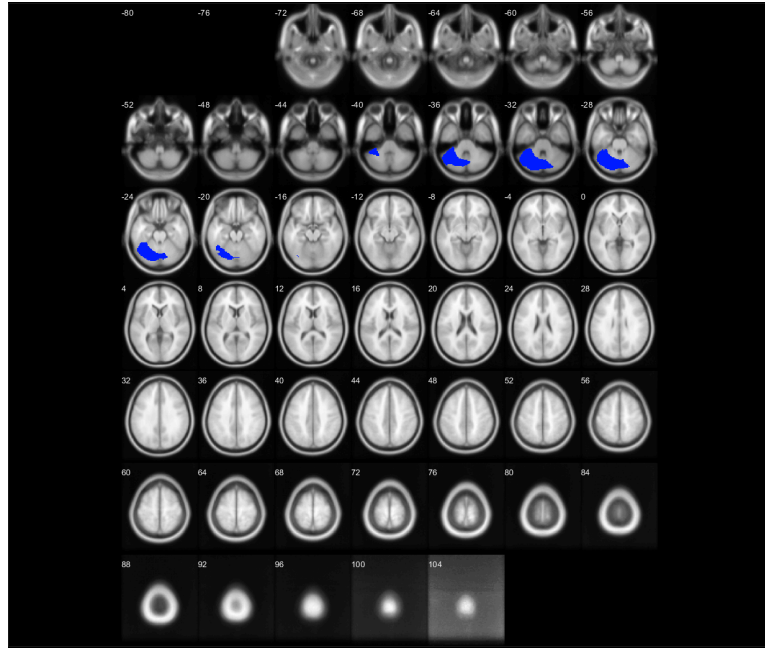


Figure 7.46. Blue areas indicate the voxels which belong to cluster 26 of MS subjects.

20. Cluster 25 consists of 4063 voxels which correspond to 1.7724% of the whole brain (background, soft tissue, bone are excluded).

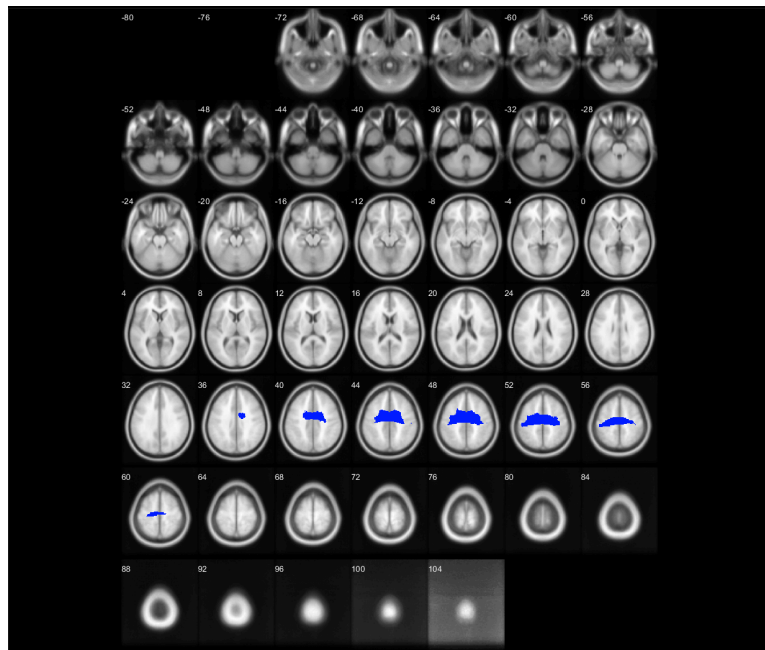


Figure 7.47. Blue areas indicate the voxels which belong to cluster 25 of MS subjects.

21. Cluster 27 consists of 4043 voxels which correspond to 1.7636% of the whole brain (background, soft tissue, bone are excluded).

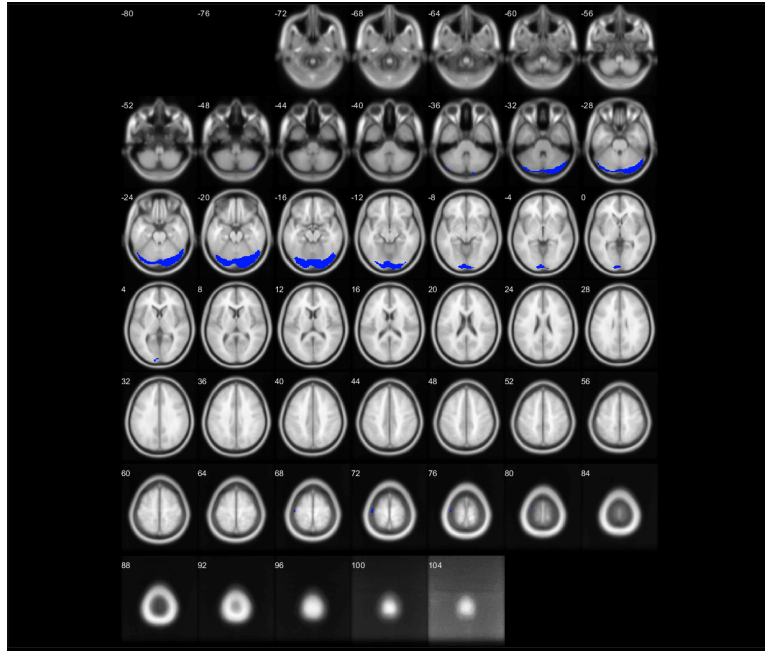


Figure 7.48. Blue areas indicate the voxels which belong to cluster 27 of MS subjects.

22. Cluster 14 consists of 3833 voxels which correspond to 1.6720% of the whole brain (background, soft tissue, bone are excluded).

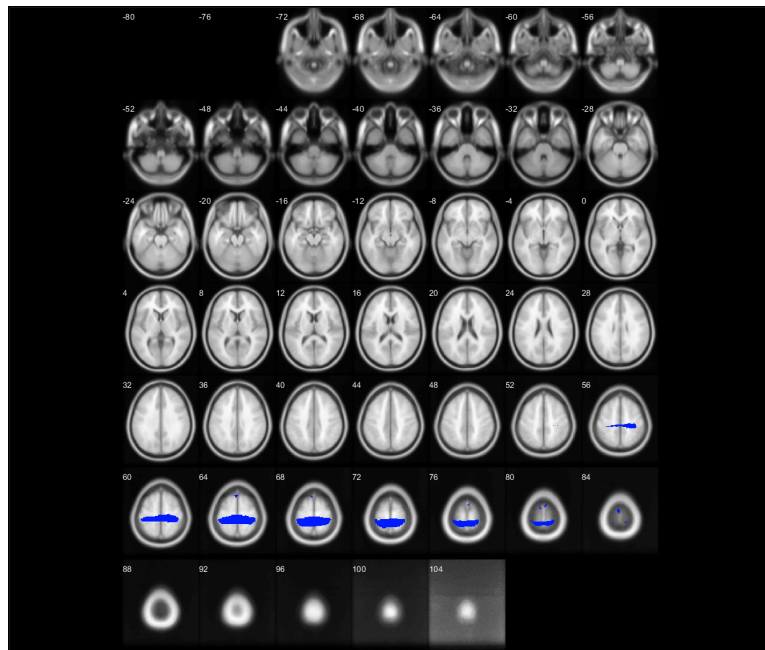


Figure 7.49. Blue areas indicate the voxels which belong to cluster 14 of MS subjects.

23. Cluster 22 consists of 3433 voxels which correspond to 1.4975% of the whole brain (background, soft tissue, bone are excluded).

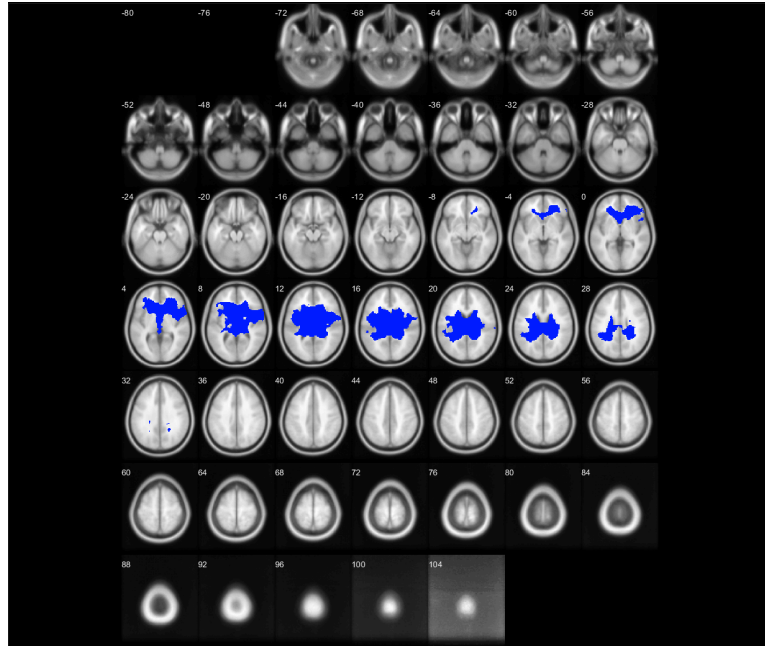


Figure 7.50. Blue areas indicate the voxels which belong to cluster 22 of MS subjects.

24. Cluster 19 consists of 2641 voxels which correspond to 1.1521% of the whole brain (background, soft tissue, bone are excluded).

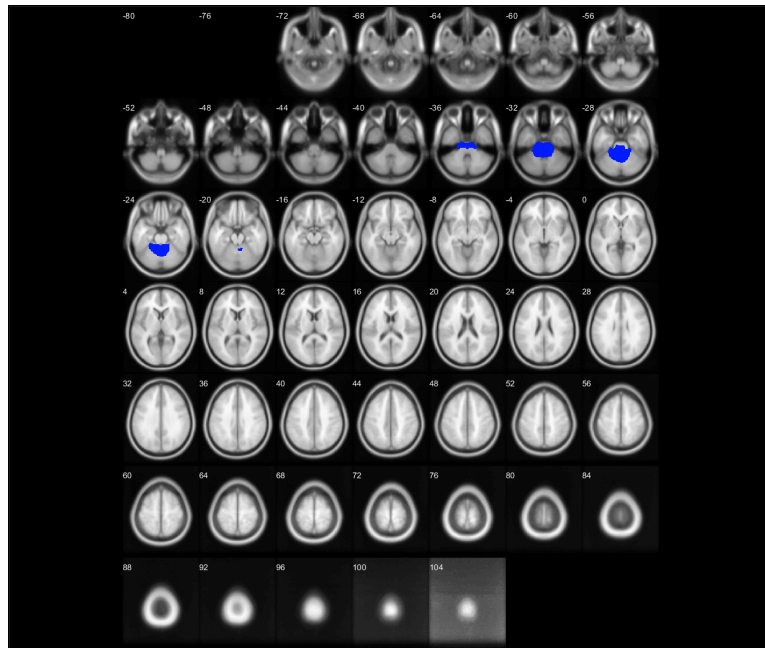


Figure 7.51. Blue areas indicate the voxels which belong to cluster 19 of MS subjects.

25. Cluster 13 consists of 2429 voxels which correspond to 1.0020% of the whole brain (background, soft tissue, bone are excluded).

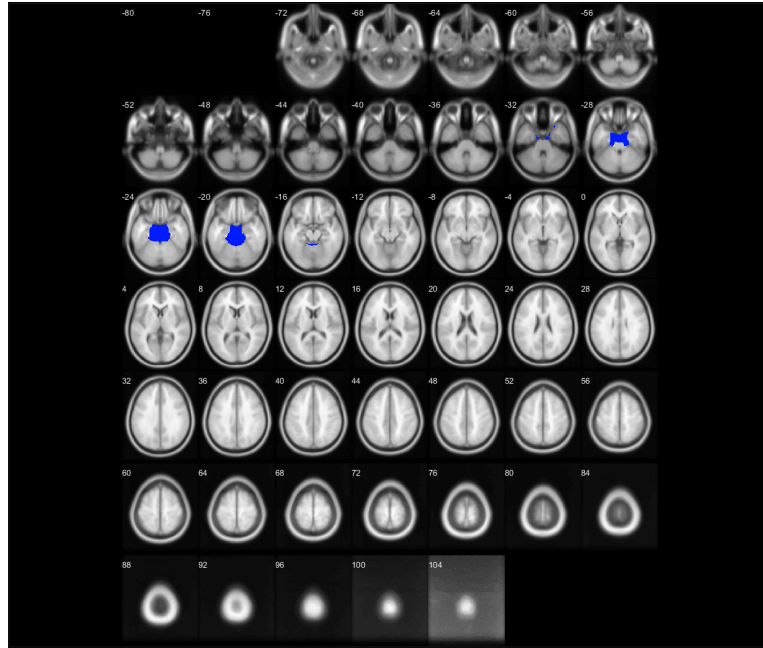


Figure 7.52. Blue areas indicate the voxels which belong to cluster 13 of MS subjects.

26. Cluster 18 consists of 2170 voxels which correspond to 1.0020% of the whole brain (background, soft tissue, bone are excluded).

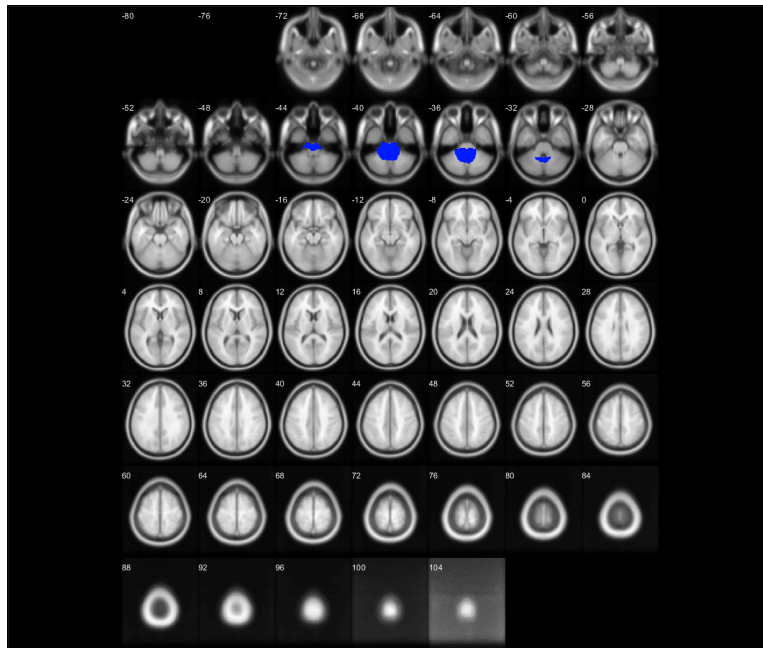


Figure 7.53. Blue areas indicate the voxels which belong to cluster 18 of MS subjects.

27. Cluster 21 consists of 1872 voxels which correspond to 1.0020% of the whole brain (background, soft tissue, bone are excluded).

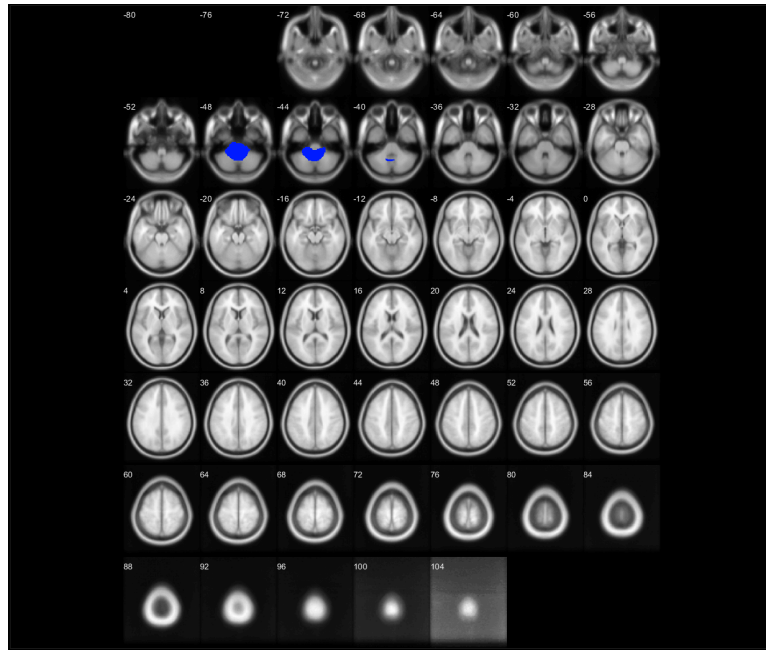


Figure 7.54. Blue areas indicate the voxels which belong to cluster 21 of MS subjects.

7.4 Brain maps for SLE subjects

Cluster SLE subjects	Number of voxels
9	23751
17	19491
6	18925
16	12583
5	11304
13	10398
19	10384
21	9080
12	8725
14	8609
20	8136
18	8042
2	8037
11	7851
7	7475
8	6828
25	6223
1	6034
23	5920
22	5905
10	5877
15	5323
26	4504
3	3268
4	2851
24	1981
27	1738

Table 7.3. The clusters of SLE subjects and the number of voxels on the side according to descent classification.

1. **Cluster 9** consists of 23751 voxels which correspond to 10.3606% of the whole brain (background, soft tissue, bone are excluded).

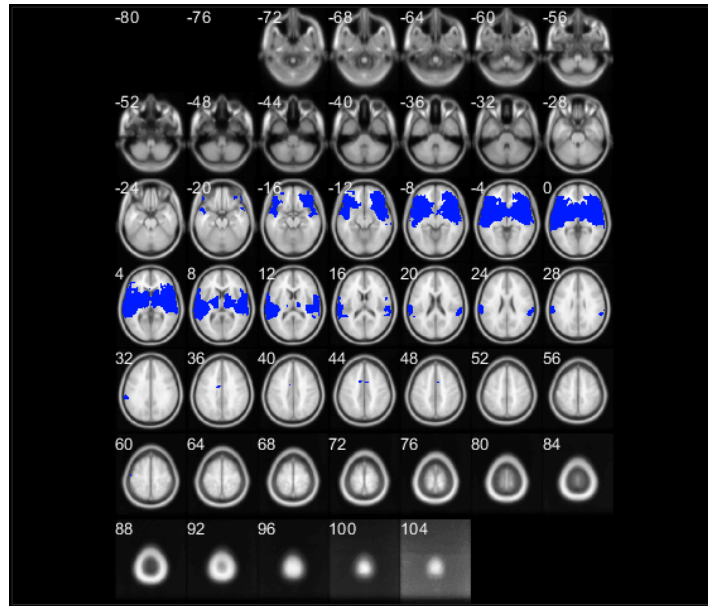


Figure 7.55. Blue areas indicate the voxels which belong to cluster 9 of SLE subjects.

2. **Cluster 17** consists of 23751 voxels which correspond to 10.3606% of the whole brain (background, soft tissue, bone are excluded).

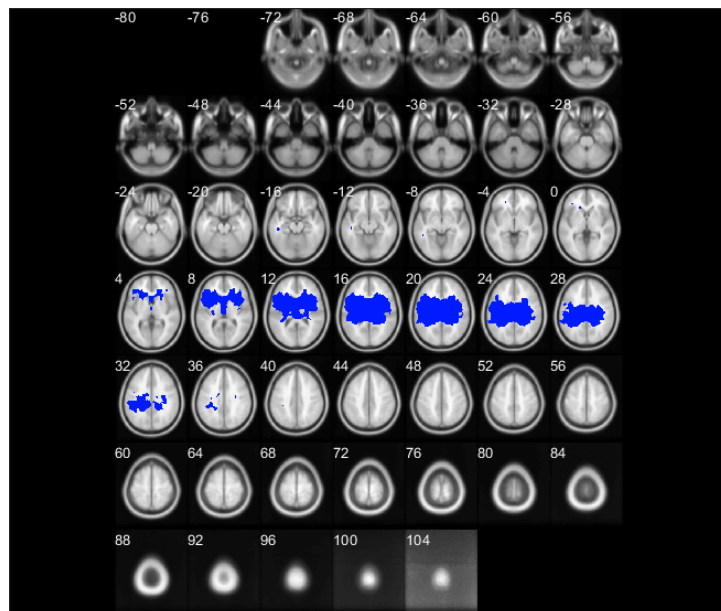


Figure 7.56. Blue areas indicate the voxels which belong to cluster 17 of SLE subjects.

3. Cluster 6 consists of 18925 voxels which correspond to 8.2554% of the whole brain (background, soft tissue, bone are excluded).

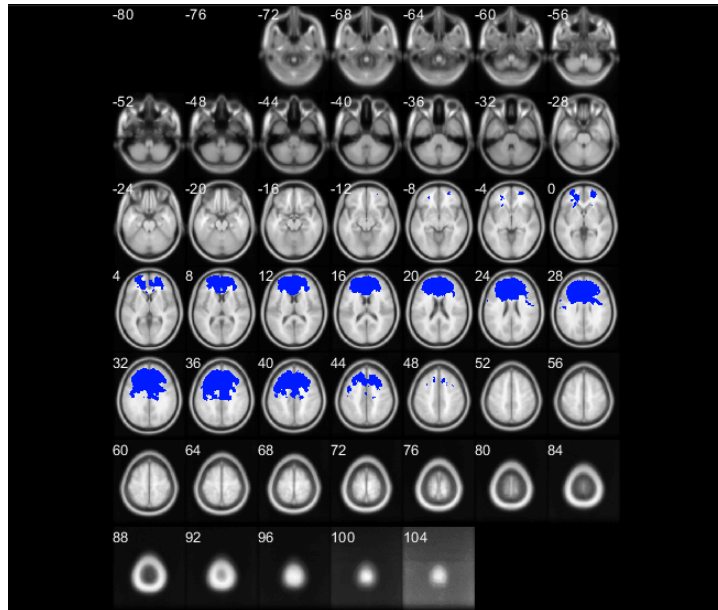


Figure 7.57. Blue areas indicate the voxels which belong to cluster 6 of SLE subjects.

4. Cluster 16 consists of 12583 voxels which correspond to 5.4889% of the whole brain (background, soft tissue, bone are excluded).

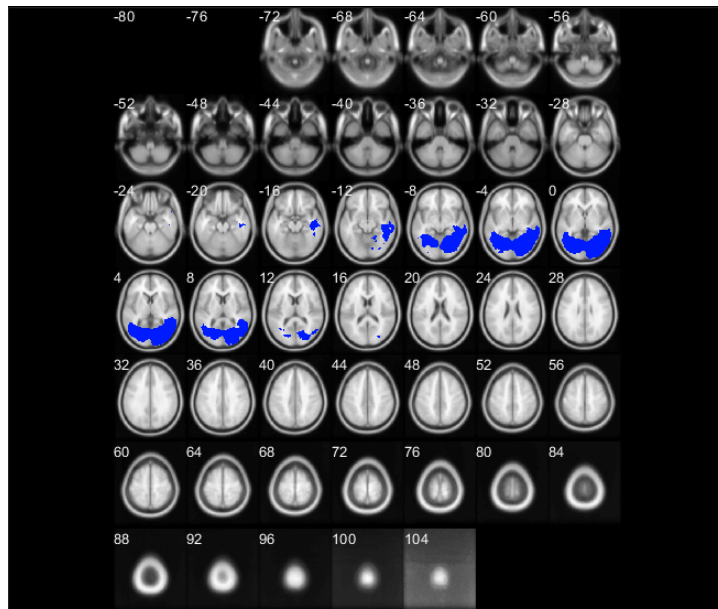


Figure 7.58. Blue areas indicate the voxels which belong to cluster 16 of SLE subjects.

5. Cluster 5 consists of 11304 voxels which correspond to 4.9310% of the whole brain (background, soft tissue, bone are excluded).

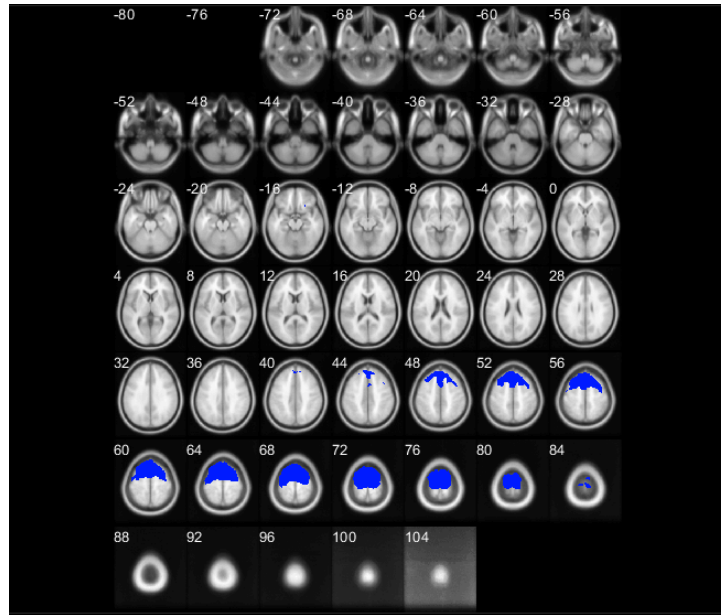


Figure 7.59. Blue areas indicate the voxels which belong to cluster 5 of SLE subjects.

6. Cluster 13 consists of 10398 voxels which correspond to 4.5358% of the whole brain (background, soft tissue, bone are excluded).

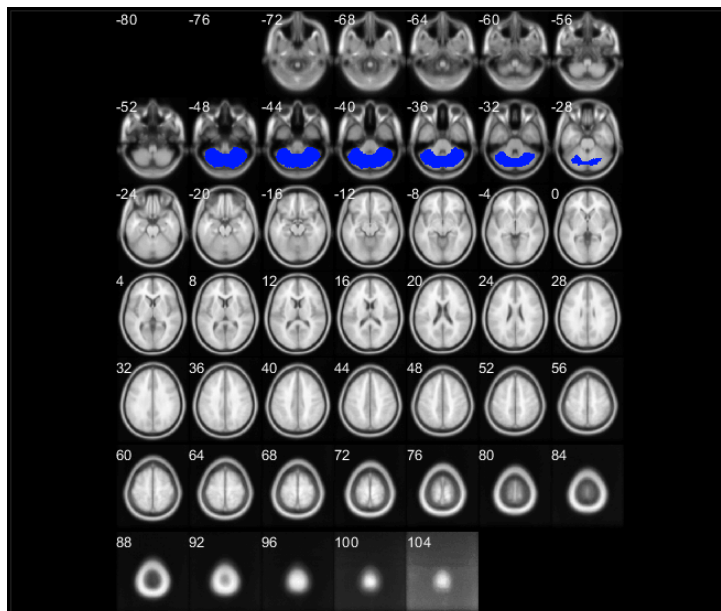


Figure 7.60. Blue areas indicate the voxels which belong to cluster 13 of SLE subjects.

7. Cluster 19 consists of 10384 voxels which correspond to 4.5297% of the whole brain (background, soft tissue, bone are excluded).

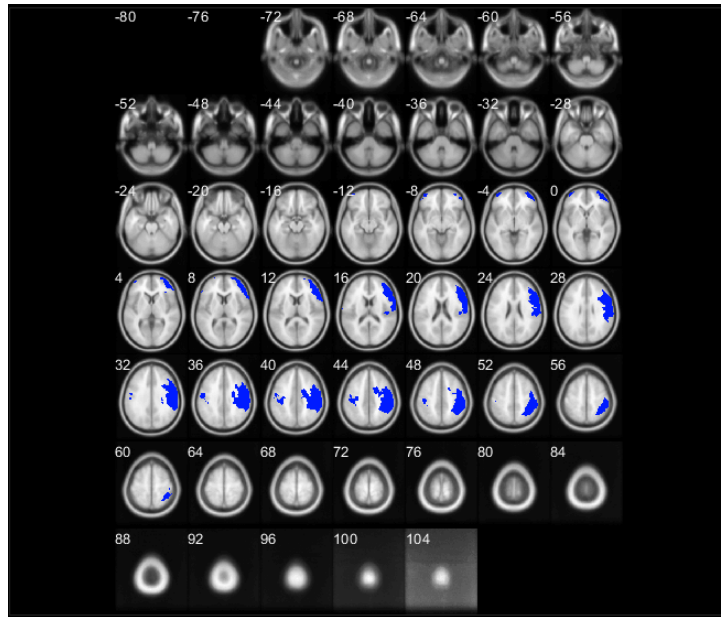


Figure 7.61. Blue areas indicate the voxels which belong to cluster 19 of SLE subjects.

8. Cluster 21 consists of 9080 voxels which correspond to 3.9609% of the whole brain (background, soft tissue, bone are excluded).

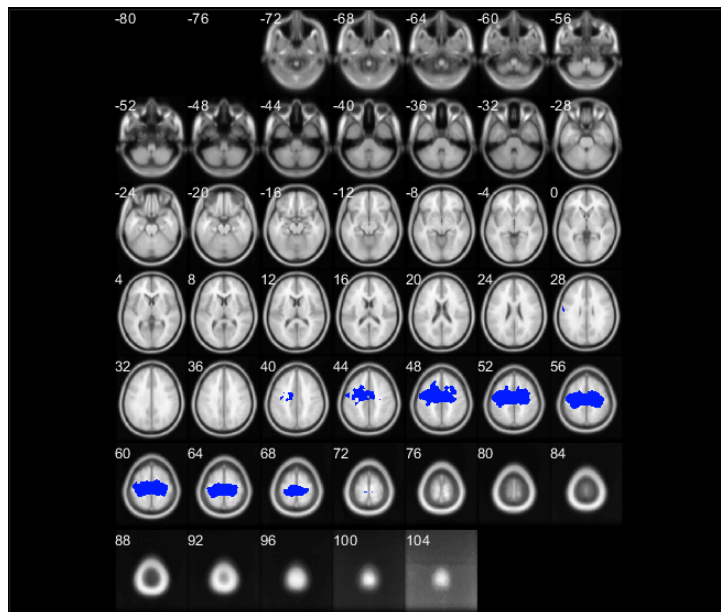


Figure 7.62. Blue areas indicate the voxels which belong to cluster 22 of SLE subjects.

9. Cluster 12 consists of 8725 voxels which correspond to 3.8060% of the whole brain (background, soft tissue, bone are excluded).

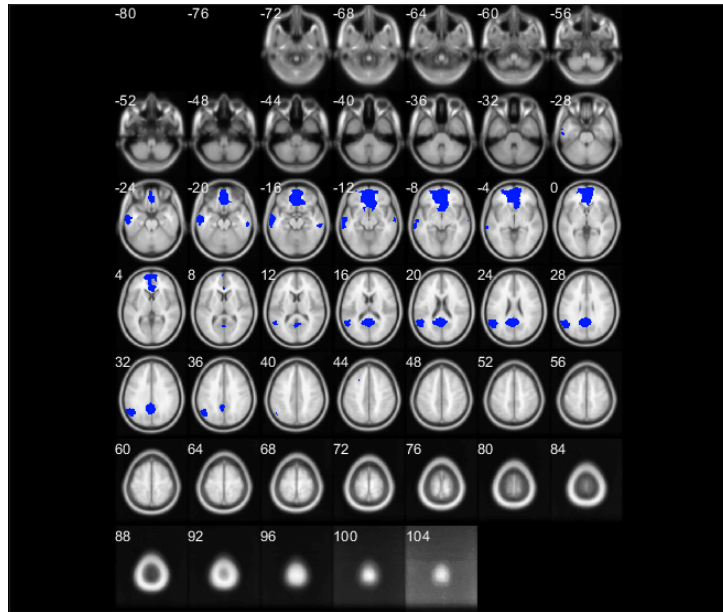


Figure 7.63. Blue areas indicate the voxels which belong to cluster 12 of SLE subjects.

10. Cluster 14 consists of 8609 voxels which correspond to 4.9310% of the whole brain (background, soft tissue, bone are excluded).

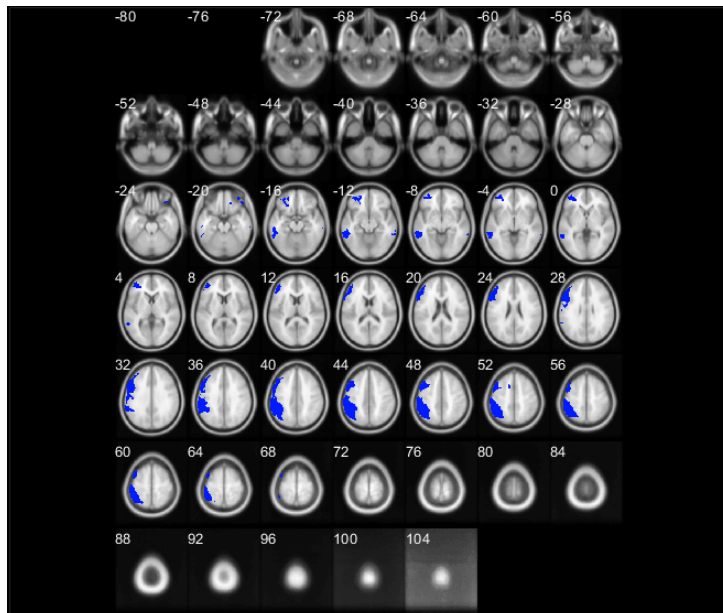


Figure 7.64. Blue areas indicate the voxels which belong to cluster 14 of SLE subjects.

11. Cluster 20 consists of 8136 voxels which correspond to 4.7554% of the whole brain (background, soft tissue, bone are excluded).

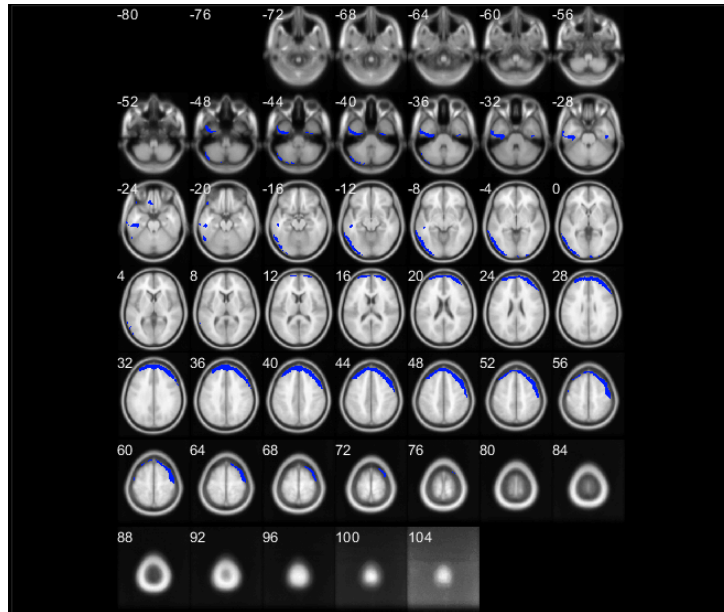


Figure 7.65. Blue areas indicate the voxels which belong to cluster 20 of SLE subjects.

12. Cluster 18 consists of 8042 voxels which correspond to 3.5081% of the whole brain (background, soft tissue, bone are excluded).

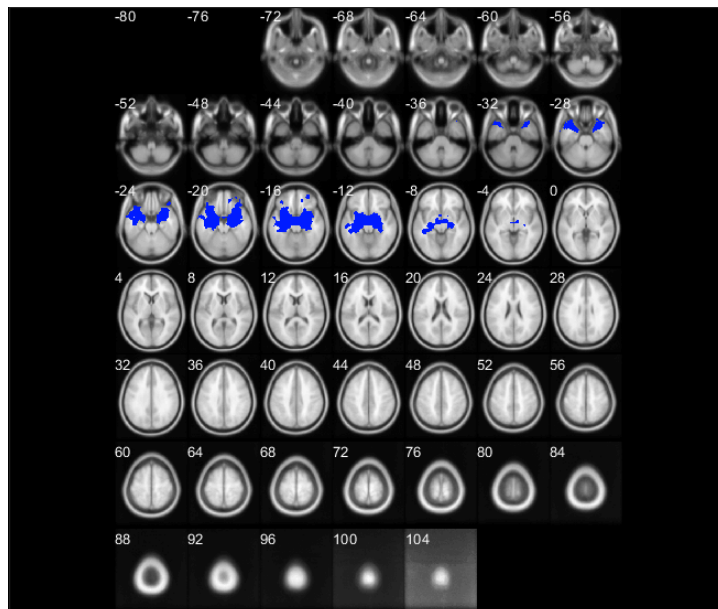


Figure 7.66. Blue areas indicate the voxels which belong to cluster 18 of SLE subjects.

13. Cluster 2 consists of 8037 voxels which correspond to 3.5059% of the whole brain (background, soft tissue, bone are excluded).

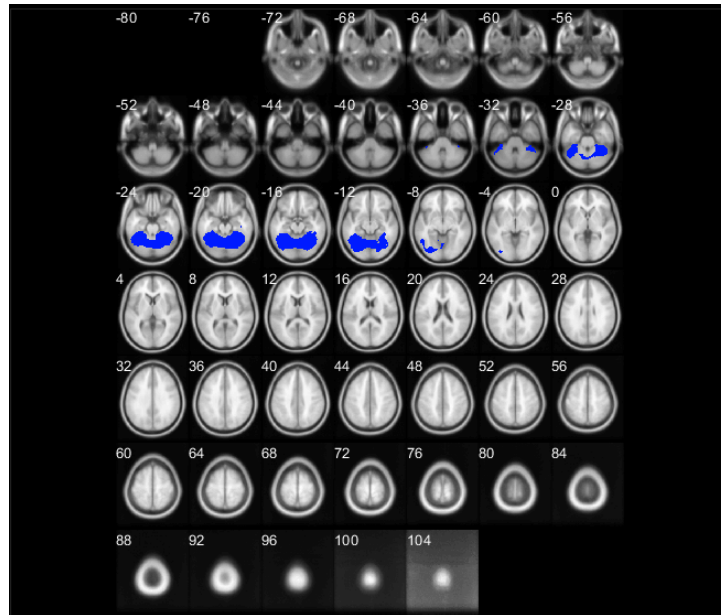


Figure 7.67. Blue areas indicate the voxels which belong to cluster 2 of SLE subjects.

14. Cluster 11 consists of 7851 voxels which correspond to 3.4248% of the whole brain (background, soft tissue, bone are excluded).

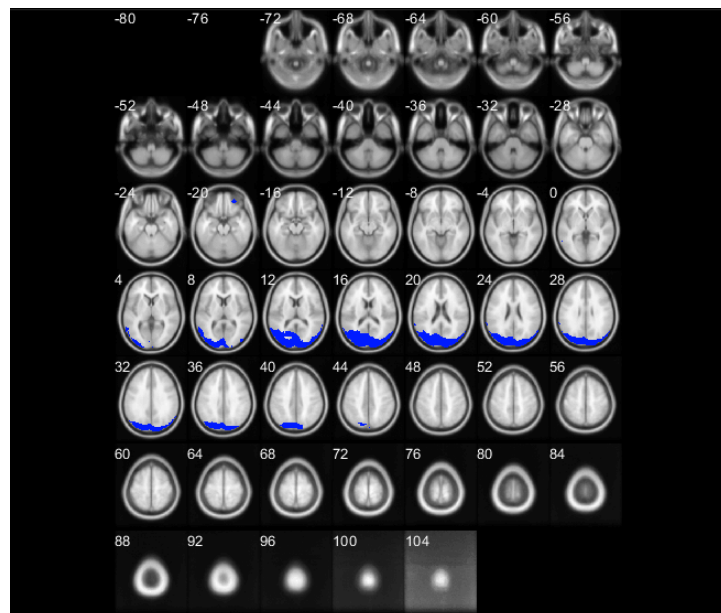


Figure 7.68. Blue areas indicate the voxels which belong to cluster 11 of SLE subjects.

15. Cluster 7 consists of 7475 voxels which correspond to 3.2607% of the whole brain (background, soft tissue, bone are excluded).

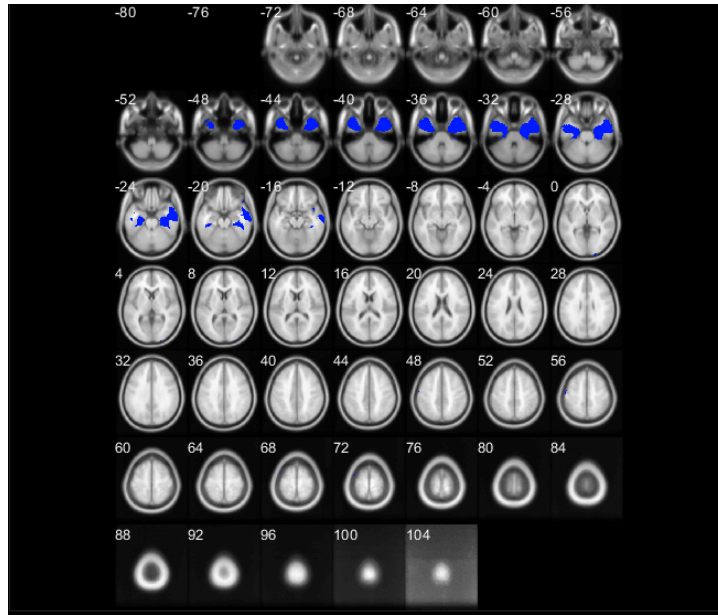


Figure 7.69. Blue areas indicate the voxels which belong to cluster 7 of SLE subjects.

16. Cluster 8 consists of 6828 voxels which correspond to 2.9785% of the whole brain (background, soft tissue, bone are excluded).

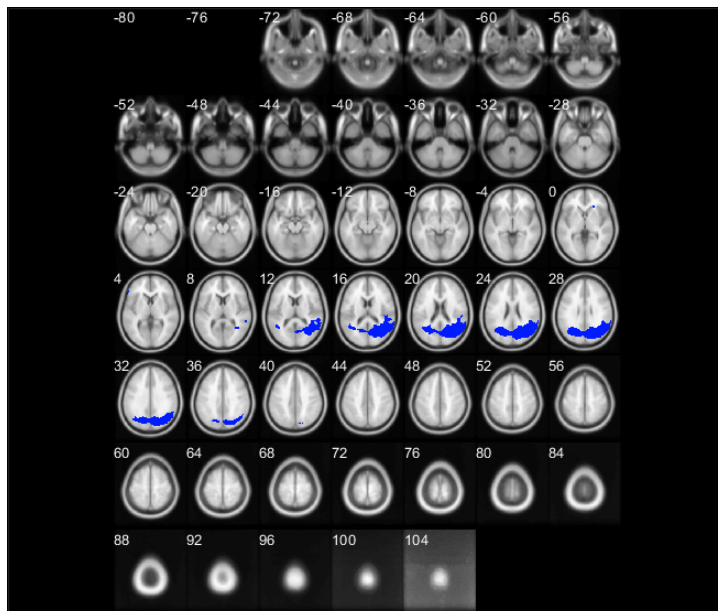


Figure 7.70. Blue areas indicate the voxels which belong to cluster 8 of SLE subjects.

17. Cluster 25 consists of 6223 voxels which correspond to 2.7146% of the whole brain (background, soft tissue, bone are excluded).

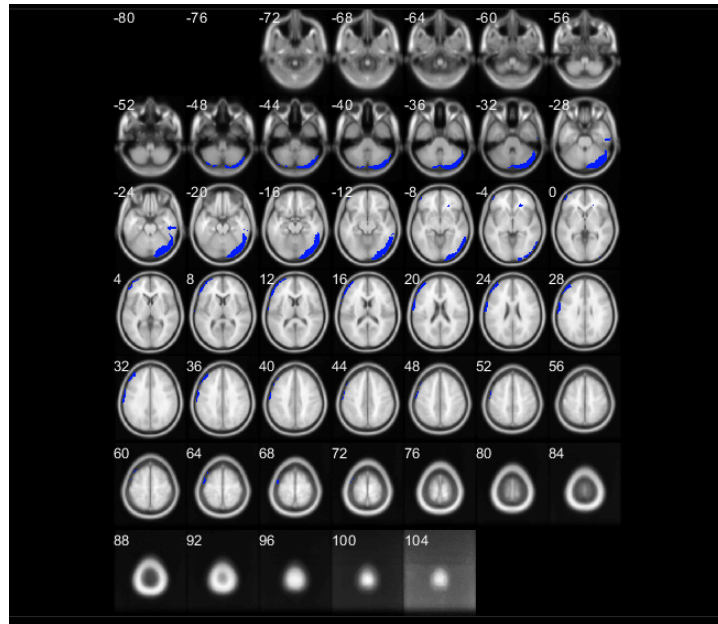


Figure 7.71. Blue areas indicate the voxels which belong to cluster 25 of SLE subjects.

18. Cluster 1 consists of 6034 voxels which correspond 2.6321% of the whole brain (background, soft tissue, bone are excluded).

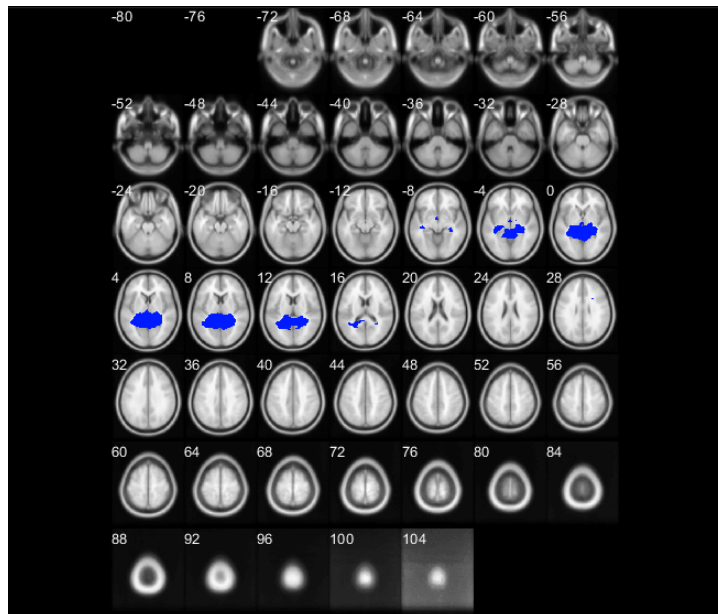


Figure 7.72. Blue areas indicate the voxels which belong to cluster 1 of SLE subjects.

19. Cluster 23 consists of 5920 voxels which correspond to 2.5824% of the whole brain (background, soft tissue, bone are excluded).

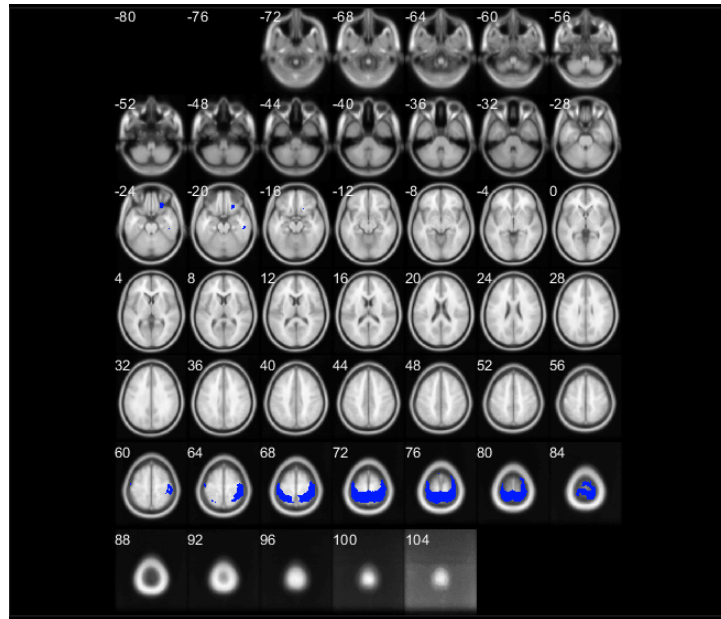


Figure 7.73. Blue areas indicate the voxels which belong to cluster 23 of SLE subjects.

20. Cluster 22 consists of 5905 voxels which correspond to 2.5759% of the whole brain (background, soft tissue, bone are excluded).

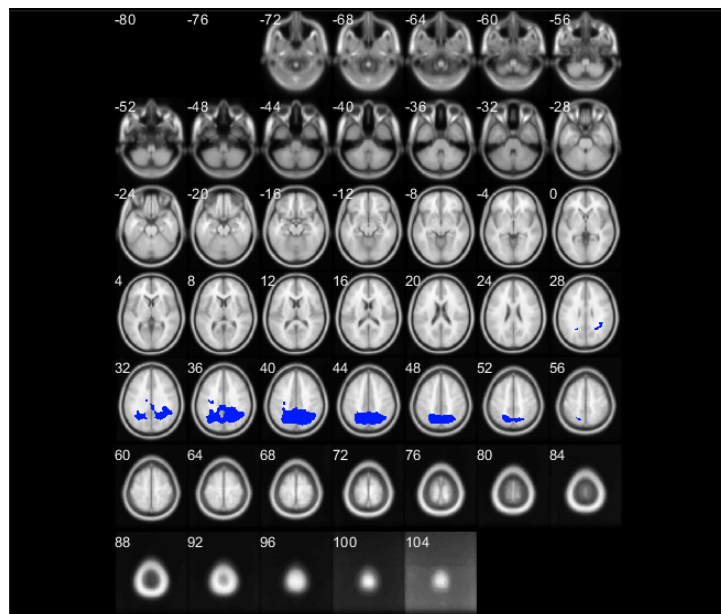


Figure 7.74. Blue areas indicate the voxels which belong to cluster 22 of SLE subjects.

21. Cluster 10 consists of 5877 voxels which correspond to 2.5637% of the whole brain (background, soft tissue, bone are excluded).

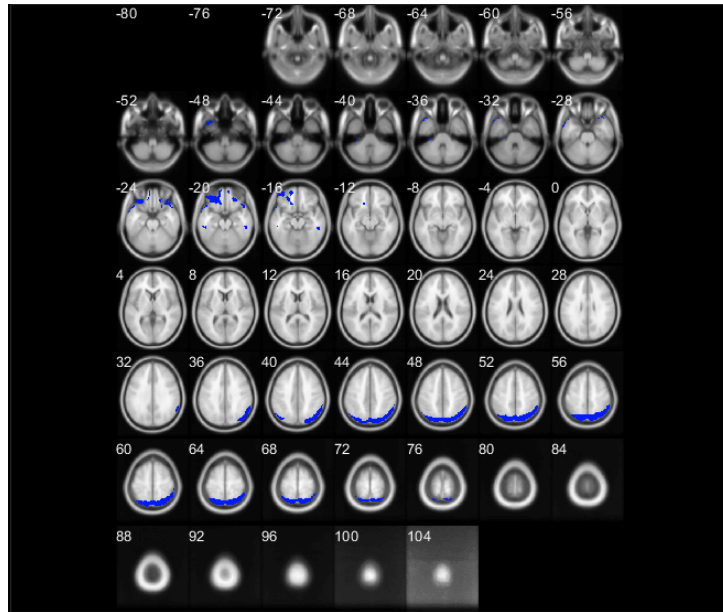


Figure 7.75. Blue areas indicate the voxels which belong to cluster 10 of SLE subjects.

22. Cluster 15 consists of 5323 voxels which correspond to 2.3220% of the whole brain (background, soft tissue, bone are excluded).

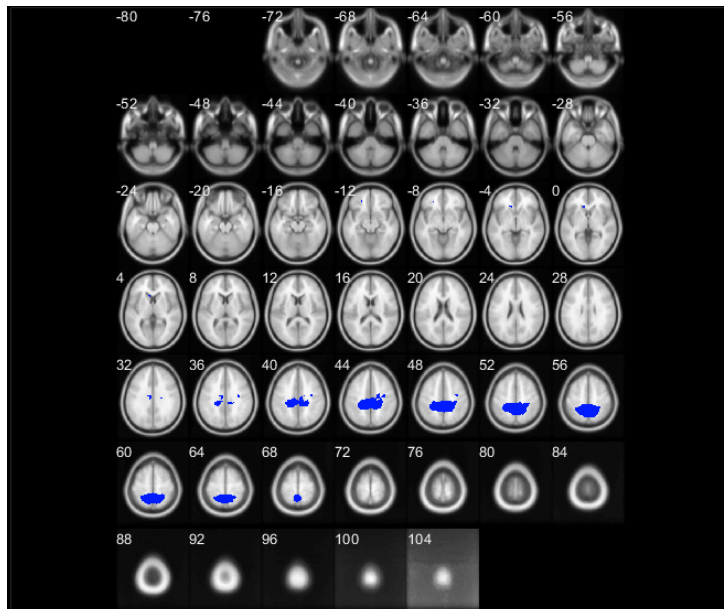


Figure 7.76. Blue areas indicate the voxels which belong to cluster 15 of SLE subjects.

23. Cluster 26 consists of 4504 voxels which correspond to 1.9647% of the whole brain (background, soft tissue, bone are excluded).

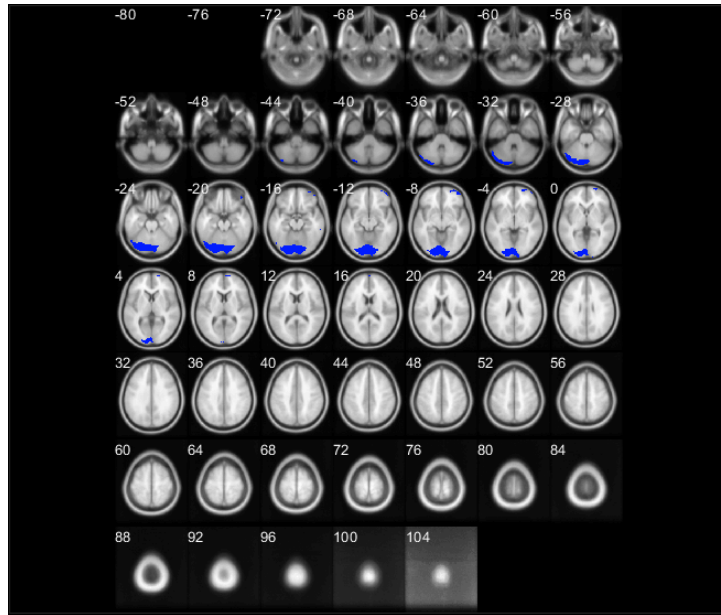


Figure 7.77. Blue areas indicate the voxels which belong to cluster 26 of SLE subjects.

24. Cluster 3 consists of 3268 voxels which correspond to 1.4256% of the whole brain (background, soft tissue, bone are excluded).

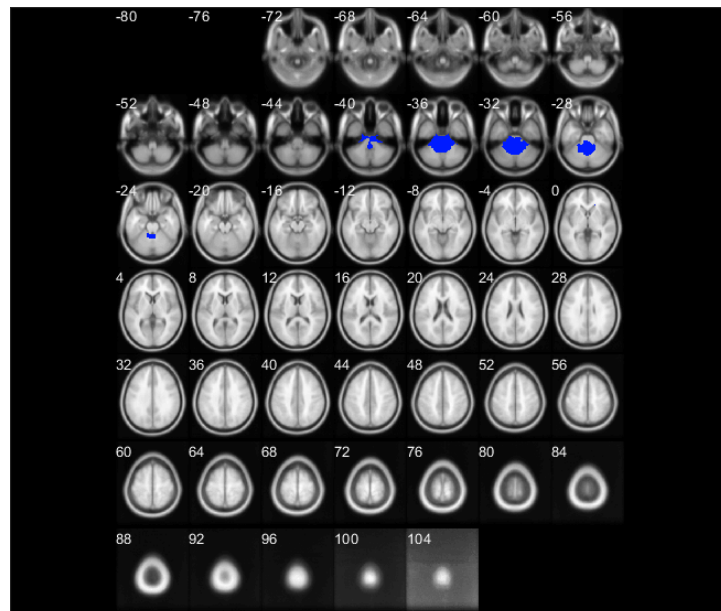


Figure 7.78. Blue areas indicate the voxels which belong to cluster 3 of SLE subjects.

25. Cluster 4 consists of 2851 voxels which correspond to 1.2437% of the whole brain (background, soft tissue, bone are excluded).

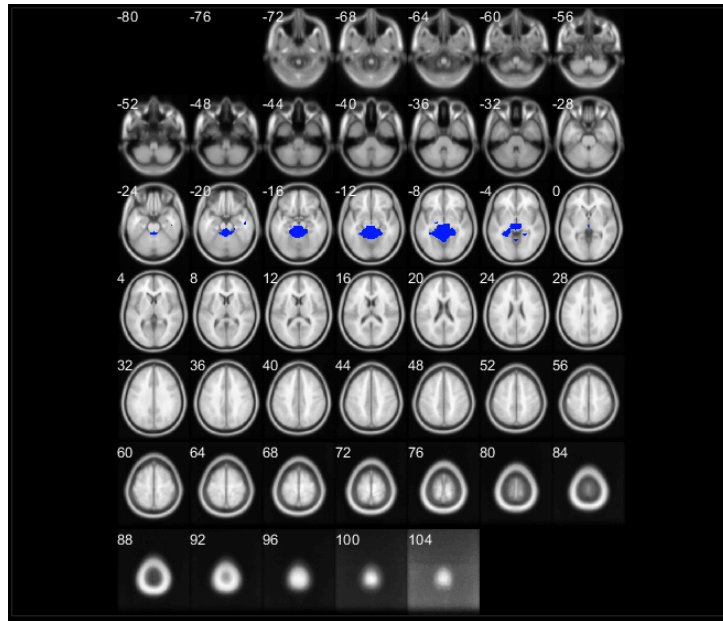


Figure 7.79. Blue areas indicate the voxels which belong to cluster 4 of SLE subjects.

26. Cluster 24 consists of 1981 voxels which correspond to 0.8641% of the whole brain (background, soft tissue, bone are excluded).

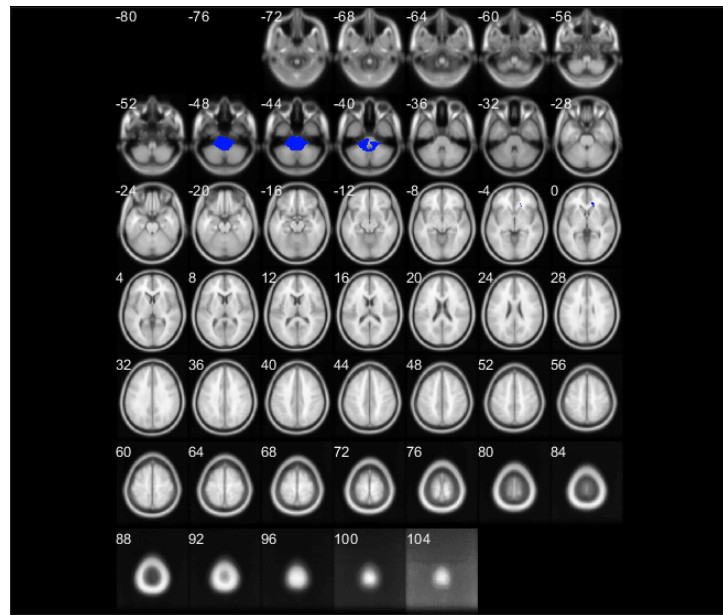


Figure 7.80. Blue areas indicate the voxels which belong to cluster 24 of SLE subjects.

27. Cluster 27 consists of 1738 voxels which correspond to 0.7581% of the whole brain (background, soft tissue, bone are excluded).

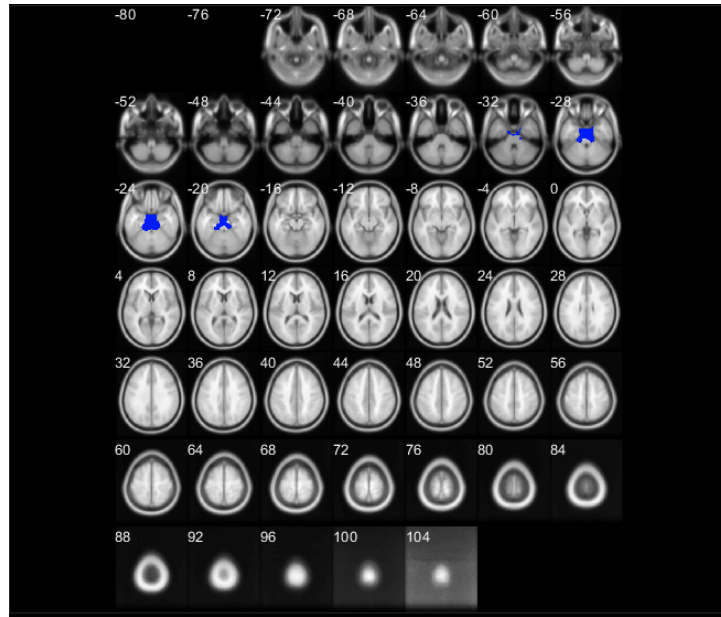


Figure 7.81. Blue areas indicate the voxels which belong to cluster 27 of SLE subjects.

7.5 Number of voxels comparison

In this chapter we try to examine the number of voxels in each illness either in the control subjects as it mention in Table 7.4, or in patients suffering from multiple sclerosis (MS) in Table 7.5 and from systemic lupus erythematosus (SLE) in Table 7.7. The tables which are presented below concern the clusters of both the control and the non-healthy (MS) subjects with the number of voxels that correspond to each cluster. Then, we present an ascent classification as far as the number of voxels is concerned from the smallest to the biggest number of voxels.

Cluster control	Number of voxels
12	2201
13	2264
18	2392
26	2442
15	3595
1	3927
25	3971
3	4230
16	4412
4	5282
21	5530
17	5987
11	6101
20	6614
5	7308
23	7343
6	9826
24	10183
14	10264
9	10302
2	10514
10	10781
8	11279
7	13626
22	17039
27	20290
19	28245

Table 7.4. The clusters of the control subjects having sorted from the smallest number of voxels to the largest (ascent).

Cluster MS	Number of voxels
21	1872
18	2170
13	2429
19	2641
22	3433
14	3833
27	4043
25	4063
26	4347
10	4923
15	5443
9	6373
23	6824
24	7206
6	8590
12	8817
7	8983
16	10512
4	10623
20	10663
2	10778
3	11806
1	12094
5	12113
8	17466
17	21273
11	25925

Table 7.5. The clusters of MS subjects having sorted from the smallest number of voxels to the largest (ascent).

Cluster control	Number of voxels
12	2201
13	2264
18	2392
26	2442
15	3595
1	3927
25	3971
3	4230
16	4412
4	5282
21	5530
17	5987
11	6101
20	6614
5	7308
23	7343
6	9826
24	10183
14	10264
9	10302
2	10514
10	10781
8	11279
7	13626
22	17039
27	20290
19	28245

Table 7.6. The clusters of the control subjects having sorted from the smallest number of voxels to the largest (ascent).

Cluster MS	Number of voxels
27	1738
24	1981
4	2851
3	3268
26	4504
15	5323
10	5877
22	5905
23	5920
1	6034
25	6223
8	6828
7	7475
11	7851
2	8037
18	8042
20	8136
14	8609
12	8725
21	9080
19	10384
13	10398
5	11304
16	12583
6	18925
17	19491
9	23751

Table 7.7. The clusters of SLE subjects having sorted from the smallest number of voxels to the largest (ascent).

Moreover, we illustrate the sorted clusters for the same dimension $R = 27$. We have to notice that the number of clusters is the same for all the types of subjects. Figures 7.82,7.83,7.84 represent the results for different kind of subjects control, (MS) and (SLE). We observe that the size of clusters ranges.

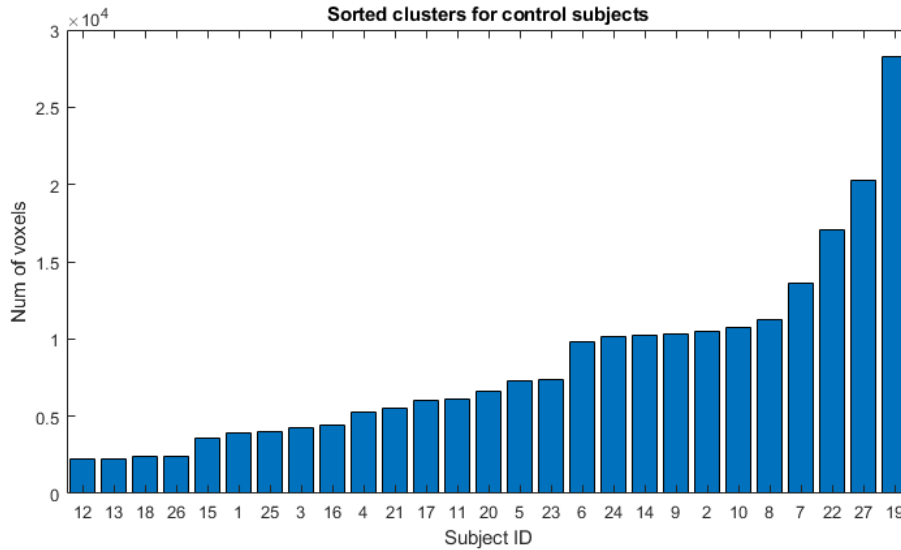


Figure 7.82. The histogram of the number of voxels of the control subjects by applying ascent classification.

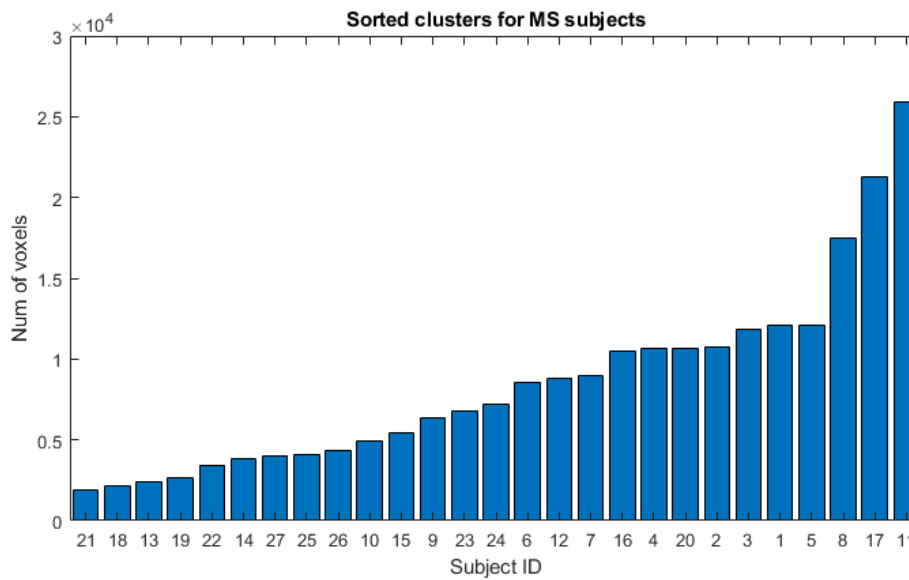


Figure 7.83. The histogram of the number of voxels of the MS subjects by applying ascent classification.

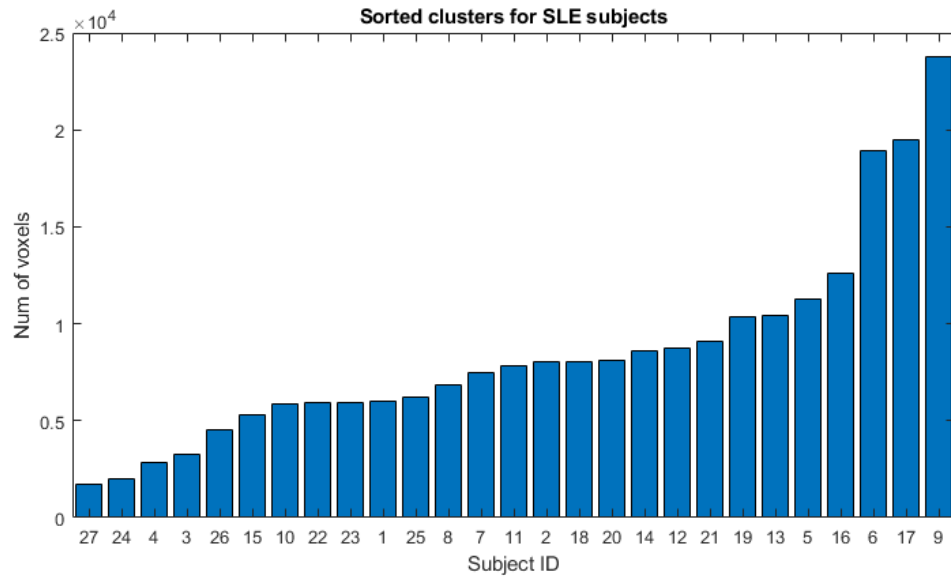


Figure 7.84. The histogram of the number of voxels of the SLE subjects by applying ascent classification.

Finally, we compare the results of clustering for the control subjects for the (MS) and for (SLE) subjects.

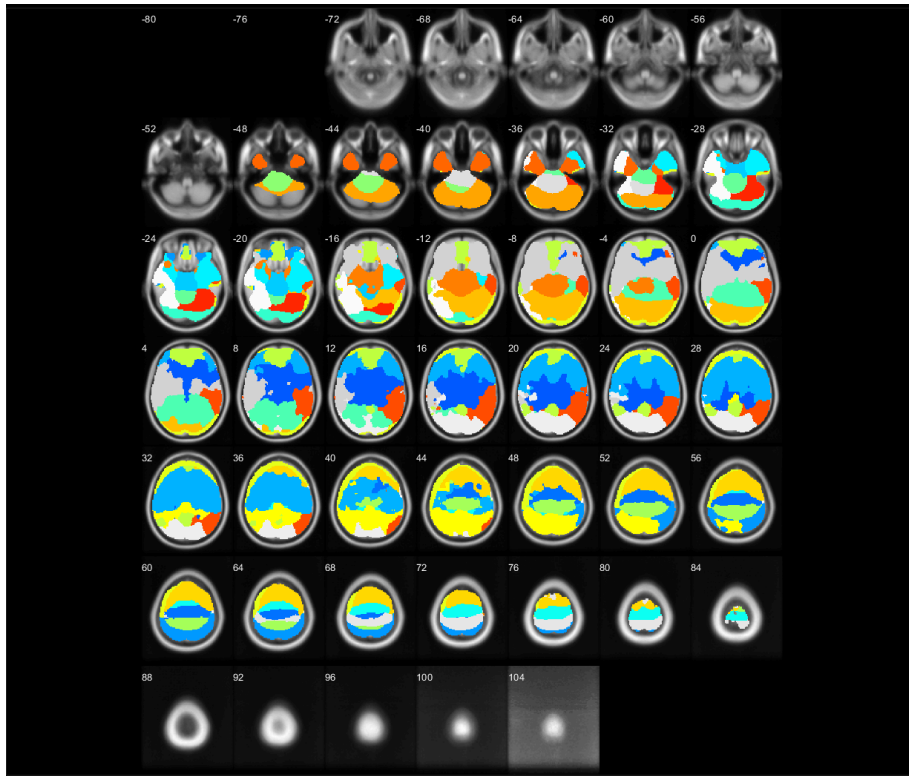


Figure 7.85. The brain map below shows all the clusters $R=27$ of the control subjects. Each colour represents a different cluster.

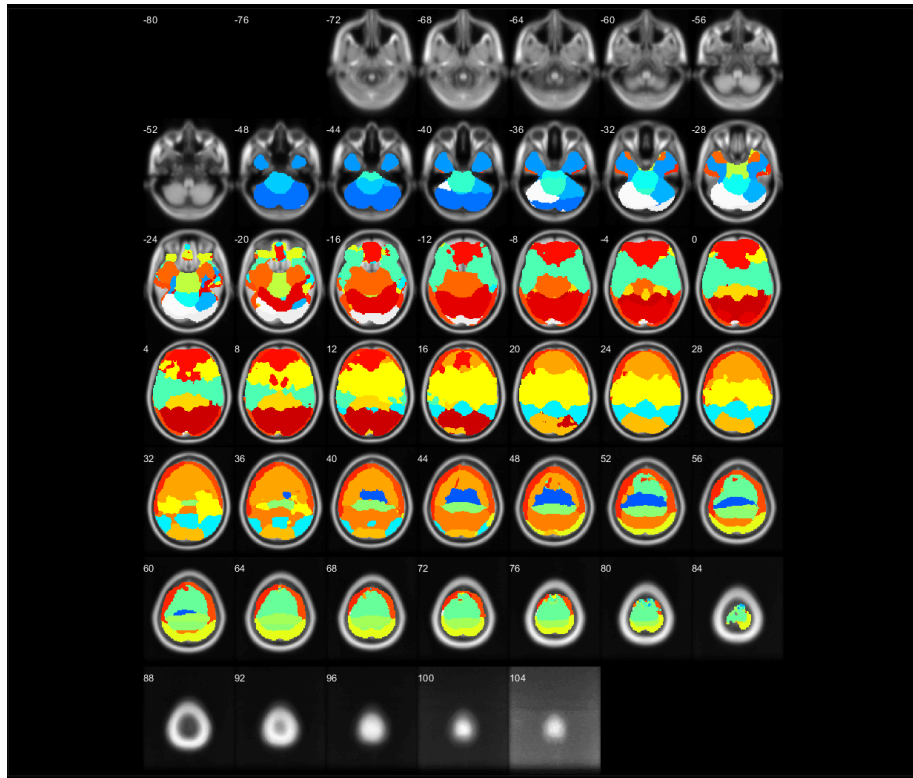


Figure 7.86. The brain map below shows all the clusters $R=27$ of MS subjects. Each colour represents a different cluster.

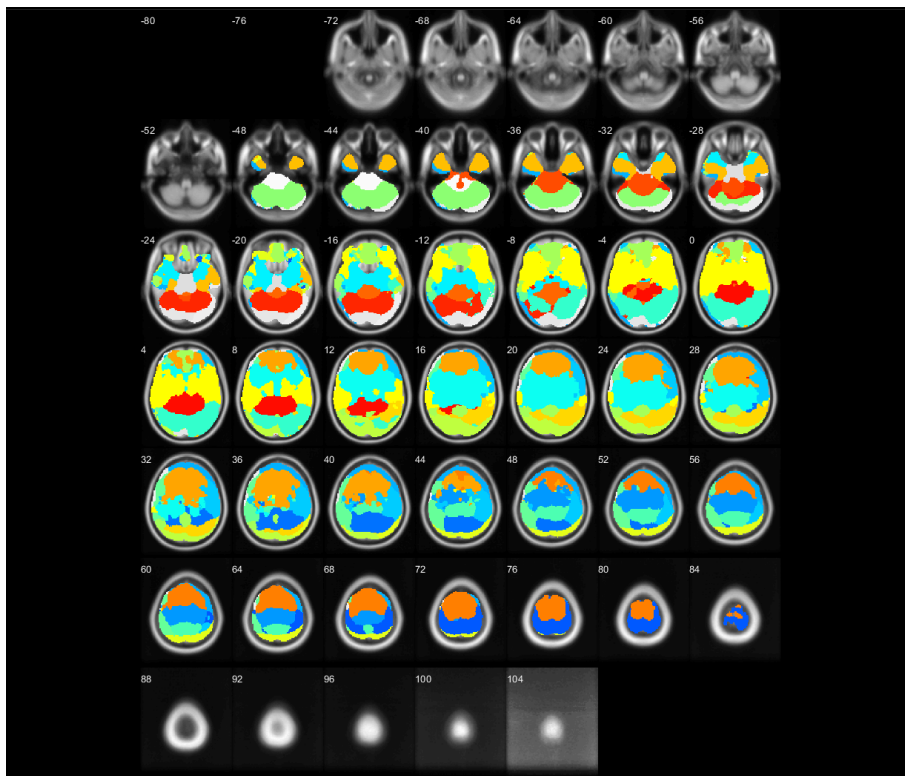


Figure 7.87. The brain map below shows all the clusters $R=27$ of the SLE subjects. Each colour represents a different cluster.

7.6 Comparison clusters of MS with the largest cluster 19 of control subjects.

Furthermore, we calculate the intersection of the largest cluster of the control subjects with the cluster of the non-healthy subjects (MS), namely the shared voxels. Then, we cut out the clusters of which the number of shared voxels is less than 1000 (threshold). The results are shown below. In the Table 7.8 we observe that the largest cluster of the control subjects which is the cluster 19 is matched only with 10 clusters out of 27 that totally are from the non-healthy subjects (MS). We tried to select all the possible ones with value greater than 1000 which is the threshold that we choose because the other price are tiny enough to make a summary and thus the following table is obtained.

Largest cluster of control	Number of clusters (MS)	Number of shared voxels
19	8	11910
19	11	9735
19	5	2047
19	4	1544

Table 7.8. In the table above we matched the number of clusters from MS subjects with the largest cluster of control patients. The limit is that the number of voxels must be greater than 1000.

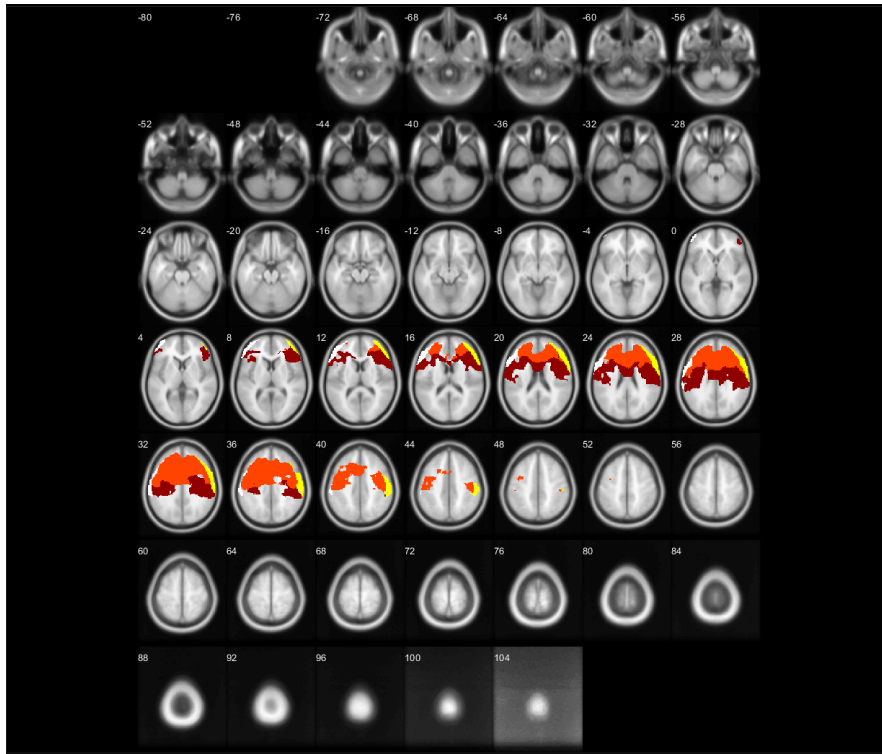
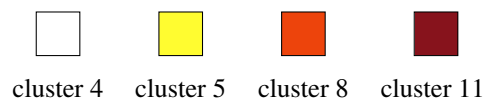


Figure 7.88. The brain map above illustrates the intersection of the 19th cluster of control subjects in terms of the number of shared voxels of the MS subjects.

There exists four different colours one for each cluster. The above colours may differ from the colours of the original image, we just have to mainly show the correspondence of each colour with each cluster. The dark red colour corresponds the cluster 11 the intense red colour the cluster 8, the yellow colour the cluster 5 and finally the white colour the cluster 4.



7.7 Comparison clusters of SLE with the largest cluster 19 of control subjects.

We follow the same procedure for the SLE subjects and the results are shown below in the Table 7.9.

Largest cluster of control	Number of clusters (SLE)	Number of shared voxels
19	6	11914
19	19	6806
19	17	5435
19	14	1903

Table 7.9. In the table above we matched the number of clusters from SLE subjects with the largest cluster of control patients. The limit is that the number of voxels must be greater than 1000 which was the threshold.

There exists four different colours one for each cluster. The above colours may differ from the colours of the original image, we just have to mainly show the correspondence of each colour with each cluster. The red colour corresponds the cluster 6, the orange colour the cluster 14, the yellow colour the cluster 17 and finally the white colour the cluster 19.

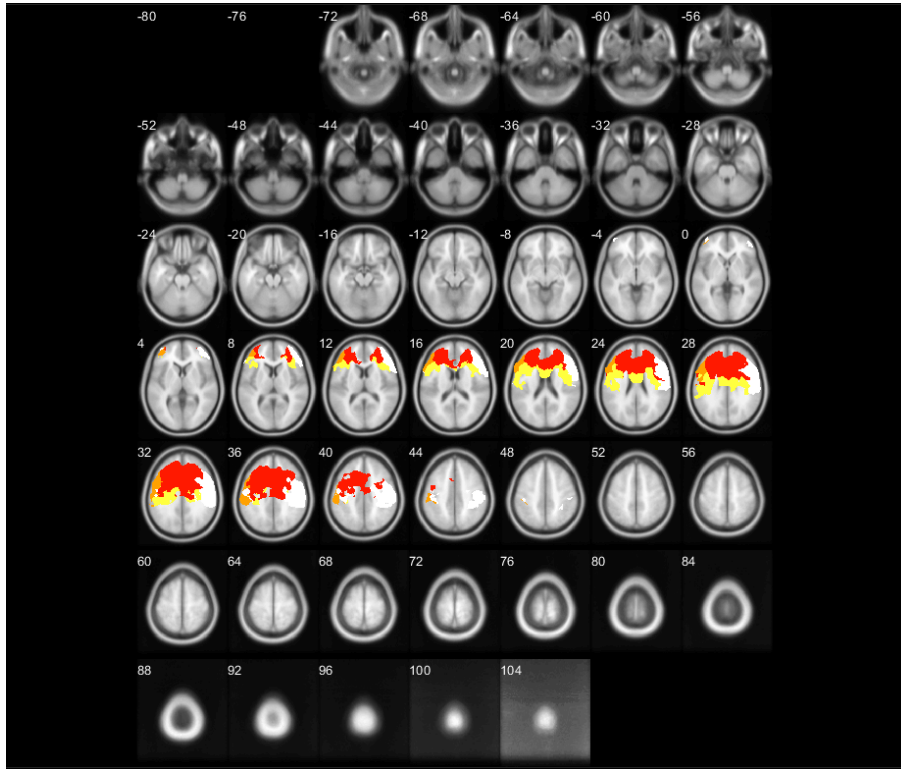
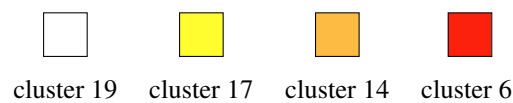


Figure 7.89. The brain map above illustrates the intersection of the 19th cluster of control subjects in terms of the number of shared voxels of the SLE subjects.



7.8 Comparison clusters of SLE with the cluster 27 of control subjects.

We follow the same procedure but we use the next biggest cluster which is the cluster 27 with 20290 number of voxels. We found so only one cluster of (SLE) subjects which corresponds to the one of the control subjects. So because of that we decided to reduce the threshold from 1000 to 700 and so we had the brain maps below.

Largest cluster of control	Number of clusters (SLE)	Number of common voxels
27	9	16290
27	12	952
27	17	784

Table 7.10. In the table above we matched the number of clusters from SLE Subjects with the cluster 27 of control subjects.

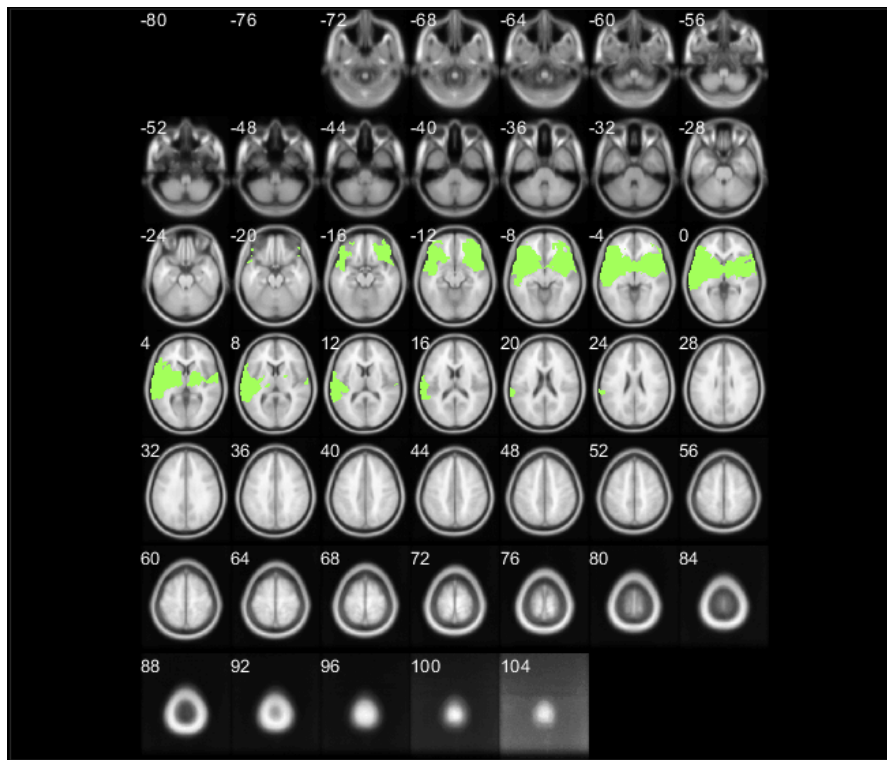


Figure 7.90. The brain map above illustrates the intersection of the 27th cluster of control subjects in terms of the number of shared voxels of the SLE subjects.

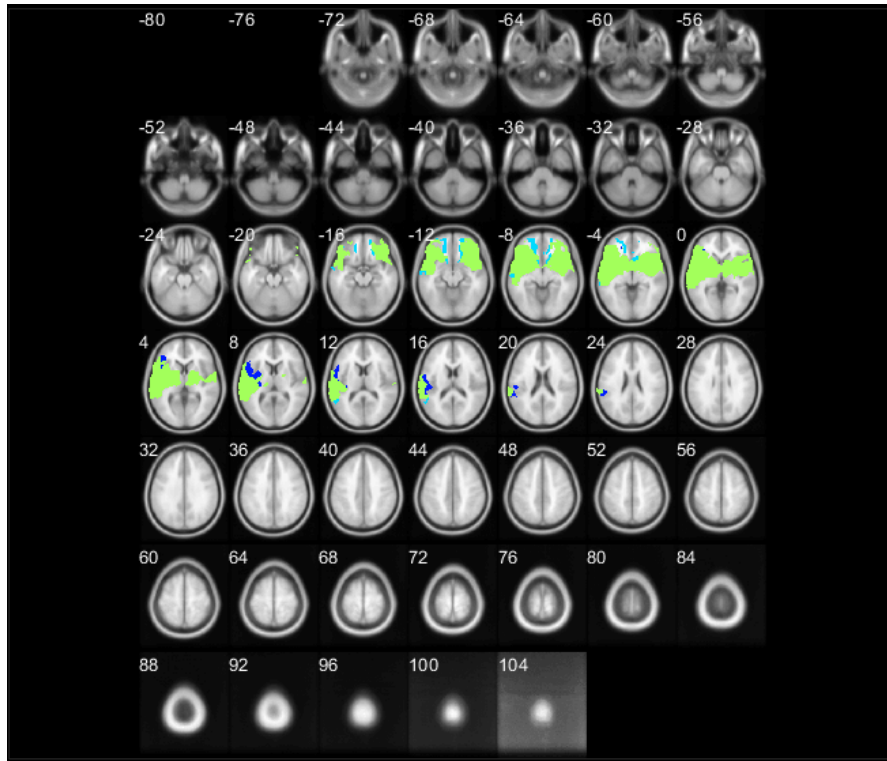
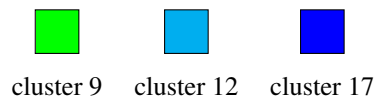


Figure 7.91. The brain map above illustrates the intersection of the 27th cluster of control subjects in terms of the number of shared voxels of the SLE subjects with threshold 700.



7.9 Comparison clusters of SLE with the cluster 22 of control subjects.

We will continue with the next third biggest cluster which is the cluster 22 and so we have.

Largest cluster of control	Number of clusters (SLE)	Number of common voxels
22	17	11518
22	9	3040
22	1	1075

Table 7.11. In the table above we matched the number of clusters from SLE subjects with the cluster 22 of control subjects.

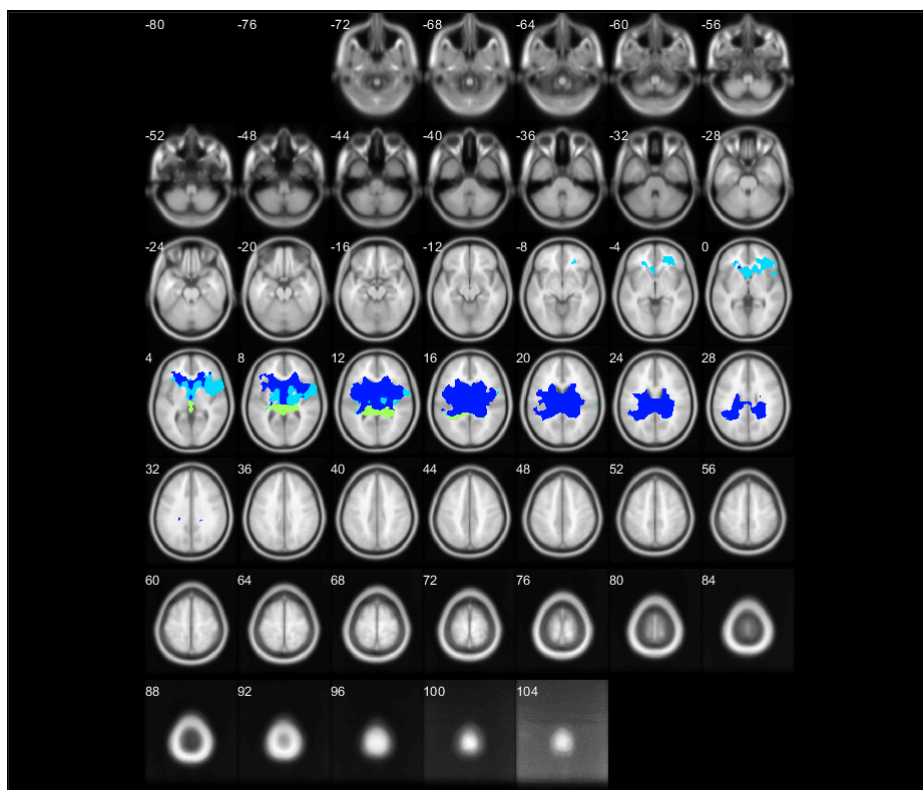
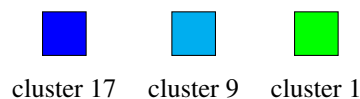


Figure 7.92. The brain map above illustrates the intersection of the 22th cluster of control subjects in terms of the number of shared voxels of the SLE subjects.



7.10 Comparison clusters of SLE with the cluster 7 of control subjects.

And the last one the comparison between the fourth biggest cluster and the SLE subjects.

Largest cluster of control	Number of clusters (SLE)	Number of common voxels
7	5	7810
7	20	2344
7	6	1621

Table 7.12. In the table above we matched the number of clusters from SLE subjects with the cluster 7 of control subjects.

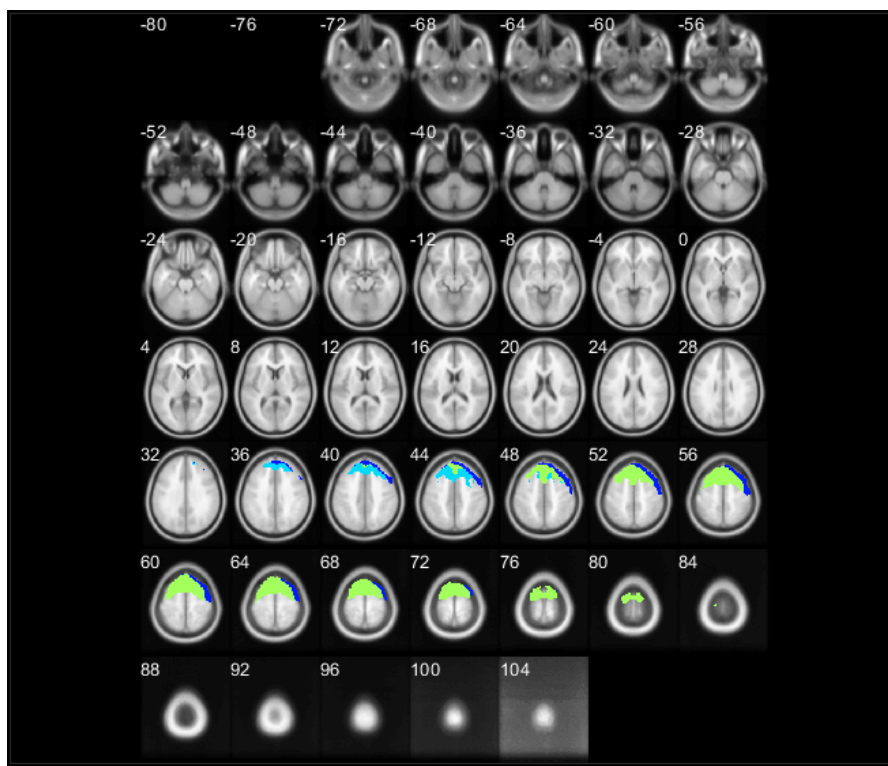
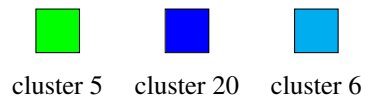


Figure 7.93. The brain map above illustrates the intersection of the 7th cluster of control subjects in terms of the number of shared voxels of the SLE subjects.



Remarks

In conclusion, we compared the largest clusters of healthy subjects and we matched them with the clusters of non-healthy subjects in terms of the number of common voxels. Furthermore, the brain map represents the intersection between the clusters which is decreases as far as the number of shared voxels decrease. we put a threshold of 1000 because the number is small enough that there is no difference in the brain map.

7.11 Comparison the clusters of control and MS subjects.

In the table below indicates four clusters of control patients and four clusters of patients who suffer from multiple sclerosis (MS) and on the side column we observe the number of the common voxels. We performed descent classification according to the biggest number of voxels as far as the cluster of control subjects is concerned. Thus, in the Table 7.13, there is a comparison of clusters of the control subjects in relation to the clusters of the MS subjects in terms of the overlaps that have and the last column shows the number of the shared voxels.

Number of cluster of control	Number of clusters (MS)	Number of common voxels
19	8	11910
27	17	15297
22	11	11908
7	16	4971

Table 7.13. Comparison table of number of clusters of control subjects and (MS) subjects and display of their common voxels.

Number of cluster of control	Number of voxels
19	28245
27	20290
22	17039
7	13626

Table 7.14. Descent classification table of the clusters of control subjects.

Thus, for the brain maps we have three colours. The first one is the yellow colour which refers to the (MS) subjects. The second one is the red colour which refers to the control subjects and the last one the blue refers to the number of common voxels between them.

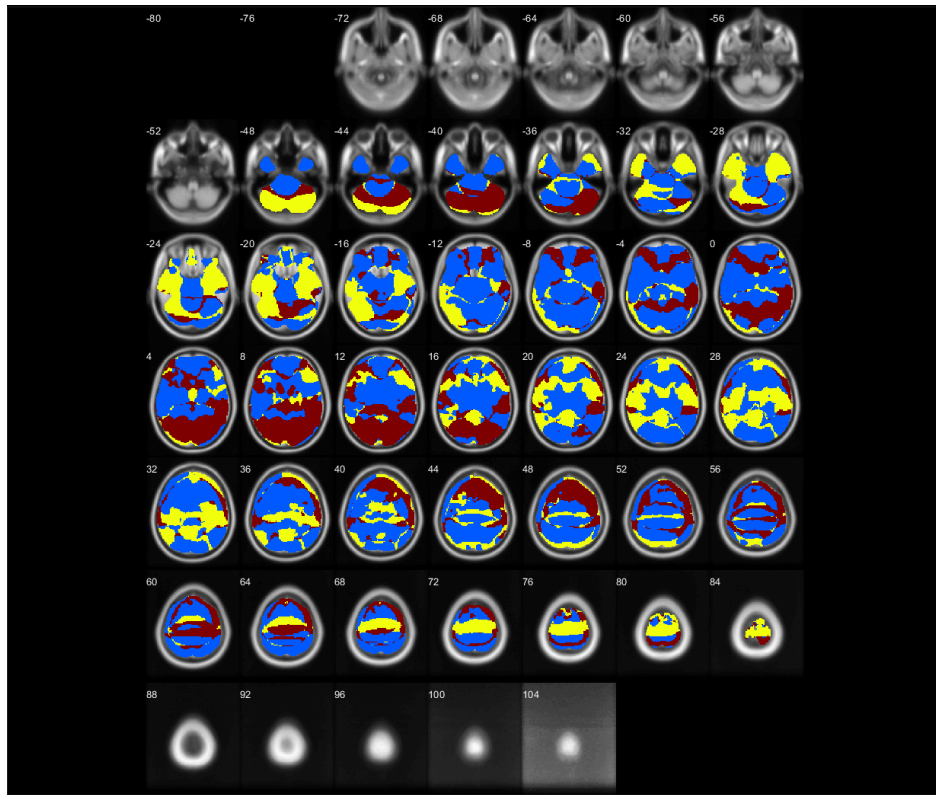
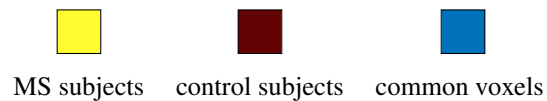


Figure 7.94. The brain map below shows the cluster of control, MS subjects and the number of common voxels.



7.12 Comparison the clusters of control and SLE subjects.

We follow the same procedure for the (SLE) subjects so as a result we have the Table 7.15.

Number of cluster of control	Number of clusters (SLE)	Number of common voxels
19	6	11914
27	9	16290
22	17	11518
7	5	7810

Table 7.15. Comparison table of number of clusters of control subjects and (SLE) subjects and display of their common voxels.

Number of cluster of control	Number of voxels
19	28245
27	20290
22	17039
7	13626

Table 7.16. Descent classification table of the clusters of control subjects.

We follow the same procedure for the (SLE) subjects and we have the brain map below.

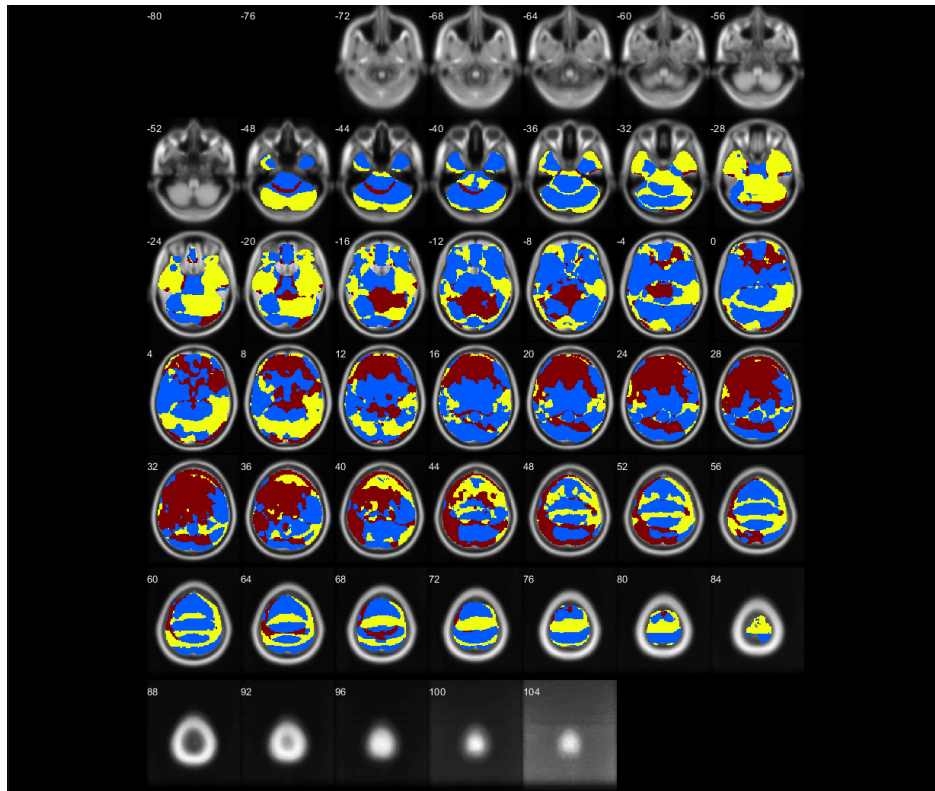


Figure 7.95. The brain below shows the cluster of control, SLE subjects and the number of common voxels.



Remarks

As it is shown above, we have two brain maps which represent the occupied area by healthy subjects, non-healthy subjects and the number of common voxels. So comparing the two brain maps we can conclude that the majority of the brain is occupied by common voxels between healthy and non-healthy subjects. Furthermore, the rest of the brain map area consists of the healthy and non-healthy subjects which is either (SLE) or (MS). In conclusion we observe that the healthy subjects in the first brain map (MS) occupies the 64% of the rest area whereas in the second map the percentage for the (SLE) subjects is smaller near to 60%.

Appendices

8.1 Histograms of energy of each material

In this section we studied the energy of healthy and non-healthy people for each material. Our aim was to find a contrast between the patients analyzing only the energy of each material. To implement the histograms we initially calculated the energy of each material of the patients as well as the mean energy of each material. Then we subtracted the mean energy of each material and calculated the histograms with the subtracted mean of the control, MS (multiple sclerosis) and SLE (systemic lupus erythematosus) patients for all materials. In the histograms below, we display the results for the control, MS and SLE patients.

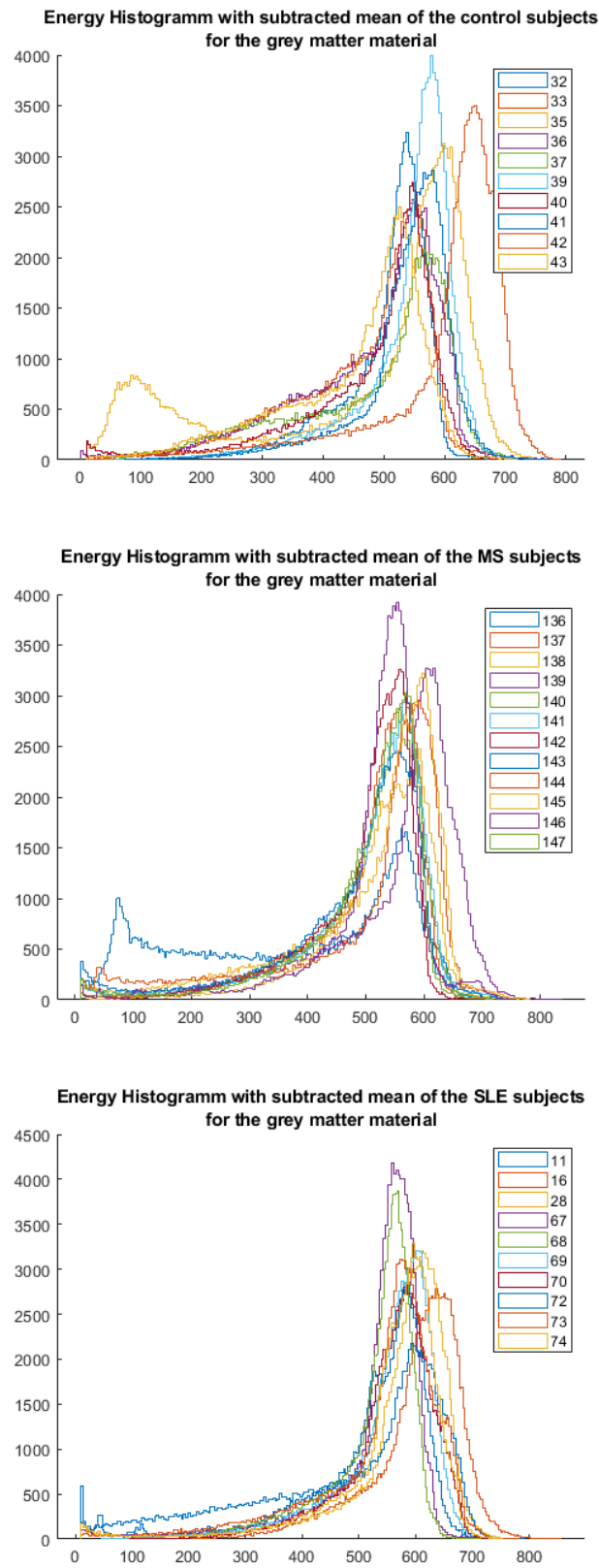


Figure 8.1. Histogramms of the material grey matter for the control, MS and SLE subjects.

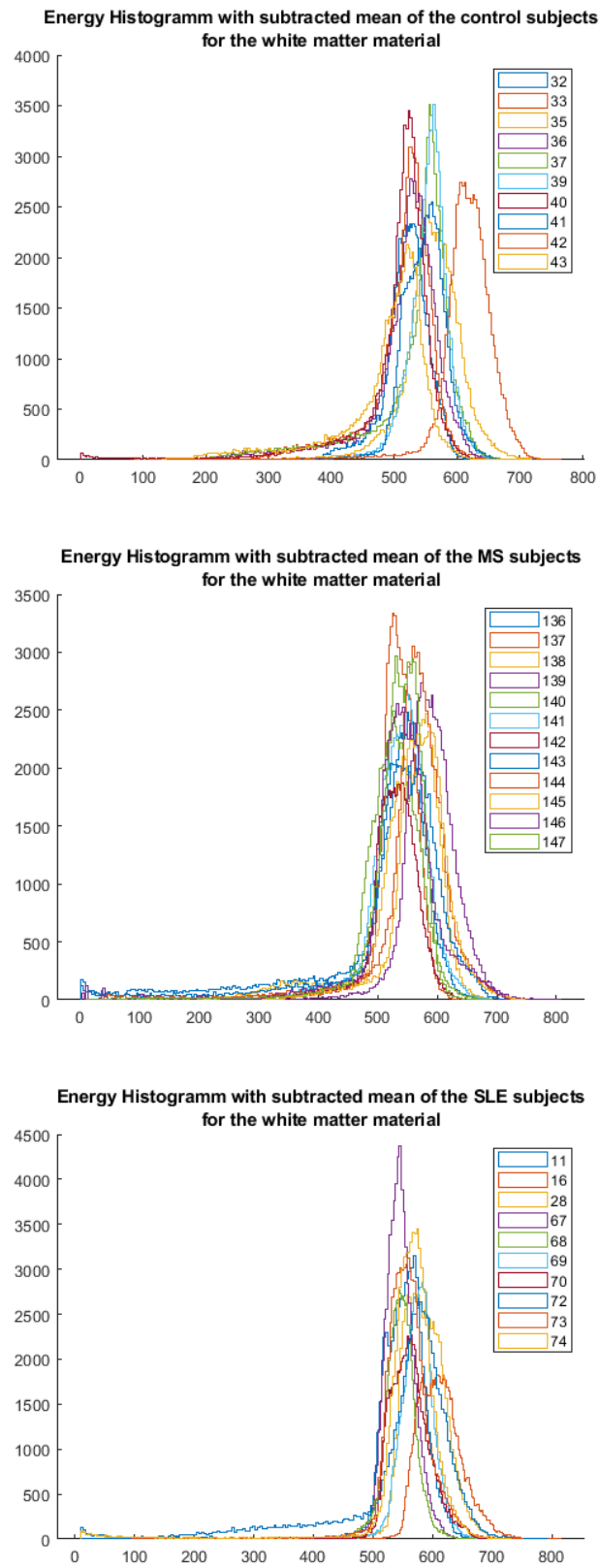


Figure 8.2. Histogramms of the material white matter for the control, MS and SLE subjects.

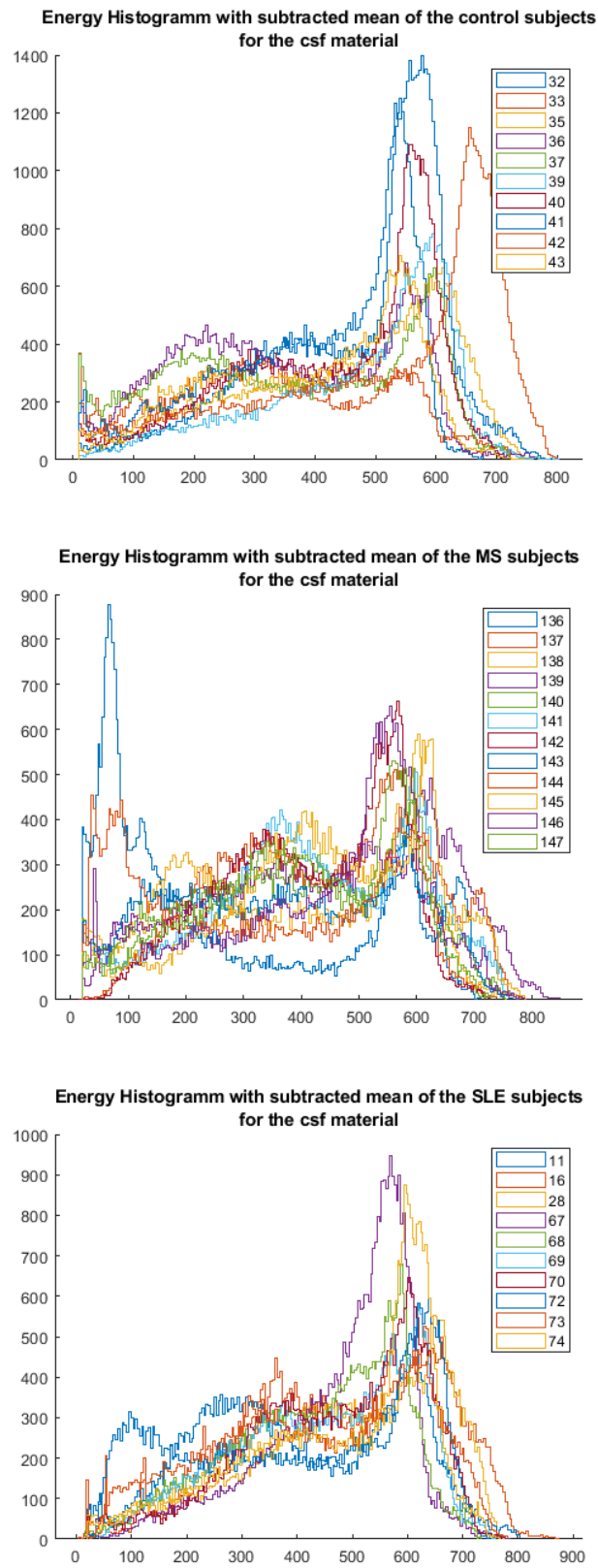


Figure 8.3. Histogramms of the material csf for the control, MS and SLE subjects.

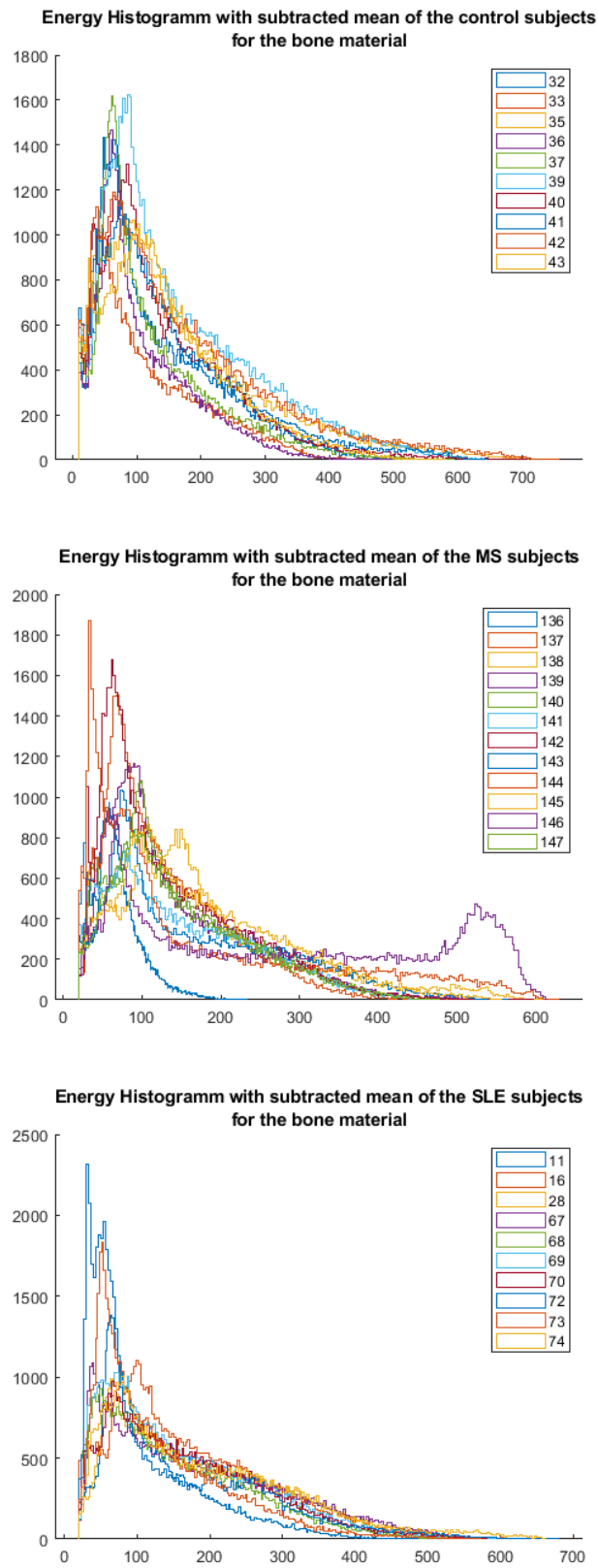


Figure 8.4. Histogramms of the material bone for the control, MS and SLE subjects.

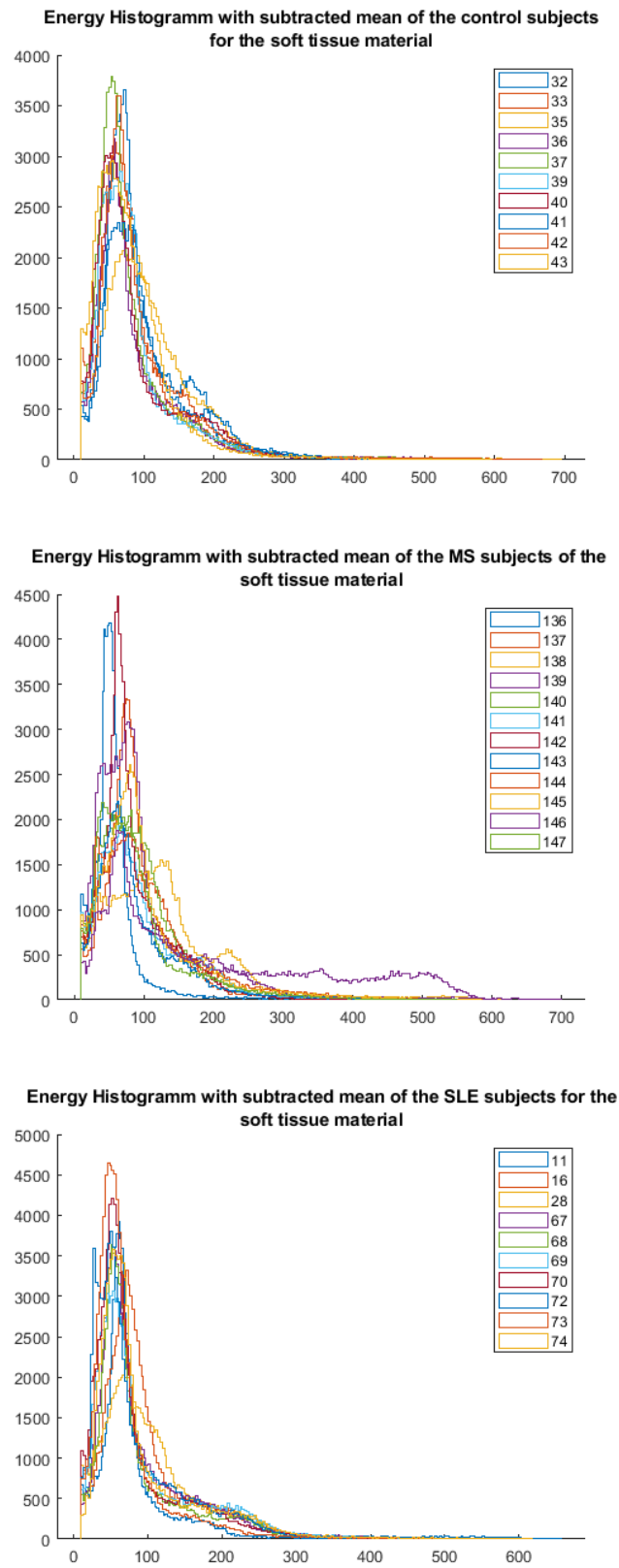


Figure 8.5. Histogramms of the material soft tissue for the control, MS and SLE subjects.

Remarks

As displayed above, energies have similar distributions for healthy and MS patients for all materials. The differences between the energies which concern the patients and the energies which concern the control patients are very small. For the soft tissue material we can see that the value for the patients (MS) has a small difference only for two subjects so we cannot verdict about all materials. Also a small difference can be seen in bone material for one subject and in csf material for two subjects. In white matter there exists one subject which is quite bigger, whereas in gray matter the energies are almost identical for all subjects of healthy, (SLE) and (MS) patients. Therefore, in this case, using only the energy histograms, we cannot predict the disease.

List of Abbreviations

fMRI	Functional Magnetic Resonance Imaging
MRI	Magnetic Resonance Imaging
HRF	Hemodynamic Response Function
SLE	Systemic Lupus Erythematosus
CIS	Clinically Isolated Syndrome
RRMS	Relapsing-Remitting Multiple Sclerosis
PPMS	Primary Progressive Multiple Sclerosis
SPMS	Secondary Progressive Multiple Sclerosis
gCCA	Generalized Canonical Correlation Algorithm
MS	Multiple Sclerosis
TR	Repetition time
TE	Echo time
CSF	Cerebrospinal Fluid

Bibliography

- [1] N. D. Sidiropoulos P. G. Simos P. A. Karakasis A. P. Liavas and E. Papadaki. “Multi-subject resting-state fmri data analysis via generalized canonical correlation”. In: *28th European Signal Processing Conference (EUSIPCO)* (2021), pp. 1040–1044.
- [2] E. Dohmatob B. Thirion G. Varoquaux and J.-B. Poline. “Which fmri clustering gives good brain parcellations?” In: *Frontiers in Neuroscience* 8 (2014), p. 167. DOI: <https://www.frontiersin.org/article/10.3389/fnins.201400167>.
- [3] J. Sepulcre M. Sabuncu D. Lashkari M. Hollinshead J. Roffman J. Smoller L. Zilei J. Polimeno B. Fischl H. Liu B. Yeo F. Krienen and R. Buckner. “The organization of the human cerebral cortex estimated by intrinsic functional connectivity”. In: *J Neurophysiol* (2011).
- [4] F. G. Ashby. “An introduction to fmri”. In: *An introduction to model-based cognitive neuroscience* (Springer, 2015).
- [5] Dr. Patrick J. Rock. “T1 relaxation time”. In: *Radiopaedia* (28 Feb 2021).
- [6] Dr. Miriam Scadeng. “What is fMRI?” In: *UC San Diego Center for Functional MRI* (2018).
- [7] M.D Larissa Hirsch. “Your Brain & Nervous System”. In: *KidsHealth* (May 2019).
- [8] M.D. By Yvetter Brazier Nancy Hammond. “Multiple Sclerosis: What you need to know”. In: *MedicalNewsToday* (August 22, 2022).
- [9] “MS Classifications Revised”. In: *National Multiple Sclerosis Society* (2000).
- [10] MPH FACP Brenda B. Springs M.D. “Systemic Lupus Erythematosus (SLE)”. In: *healthline* (May 29, 2020).
- [11] Dall’Era M. “Systemic lupus erythematosus. In: Imboden JB, Hellman DB, Stone JH. (Eds)”. In: *Current Rheumatology Diagnosis and Treatment* (3rd ed. New York, NY:McGraw-Hill 2013).
- [12] Mikolaitis RA Rodby RA Sequeira W Block JA. Jolly M Pickard SA. “Lupus QoL-US benchmarks for US patients with systemic lupus erythematosus. *J Rheumatol*”. In: (2010).

- [13] Stephen C. Strother Babak Afshin-Pour Gholam-ALi Hossein Zadeh. “Enhancing reproducibility if fMRI statistical maps using generalized canonical correlation analysis”. In: (1 May 2012).
- [14] J. R. KETTENRING. “Caninical analysis of several sets of variables”. In: *Biometrika* (12 1971). DOI: <https://dio.org/10.1093/biomet/58.3.433>.
- [15] G. Zhou B. Li and A. Cichocki. “Two efficient algorithms for approximately orthogonal nonnegative matrix factorization”. In: *IEEE Signal Processing Letters* (2015), pp. 843–846.